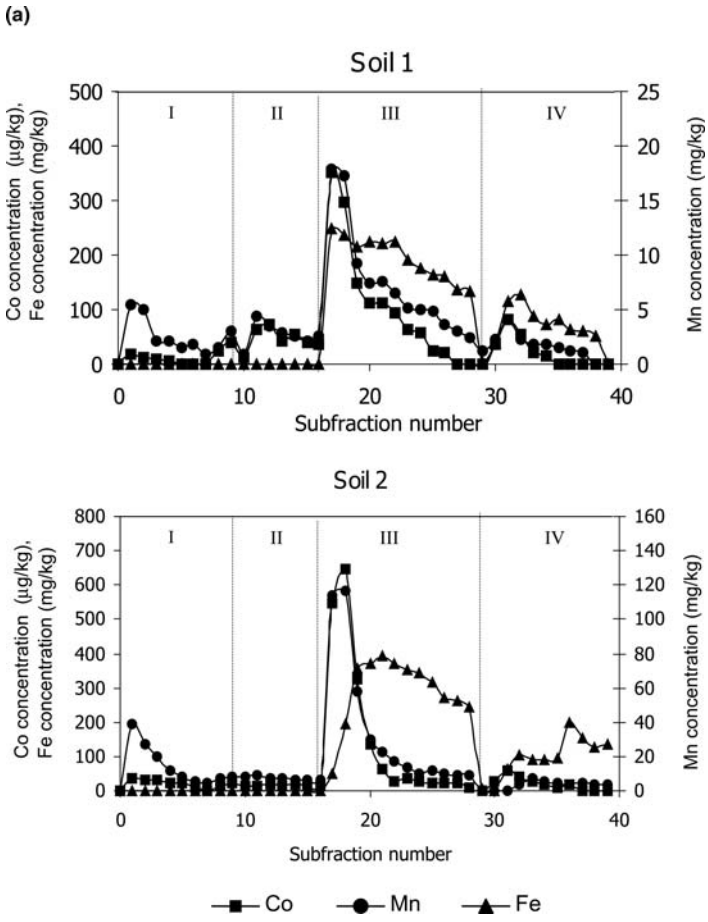

Figure 3a. Extractograms obtained using the continuous-flow method for Soil 1 and Soil 2. (Sample/chamber volume ratio 0.75 g/10 mL; subfraction volumes of 10, 15, 30, and 30 mL in fractions I, II, III, and IV, respectively.)

simultaneous dissolution of the two elements, providing clear evidence of their elemental association in all four samples. However, Fe (which was also extracted in the same phase) gave a much broader peak throughout the extraction step and therefore did not appear to be closely associated with either Mn or Co. In Soil 4, the Co peak appeared simultaneously with the first Mn peak, but not associate with the second Mn peak.

The extractograms obtained from the continuous-flow extraction system show that, apart from the large amounts in the residue (Table 4), Fe was found predominantly in the reducible and oxidizable (organic-bound) phases. In all cases, there was significant dissolution of both Co and Fe in those two phases. However, the extraction peak shapes of Co and Fe in the

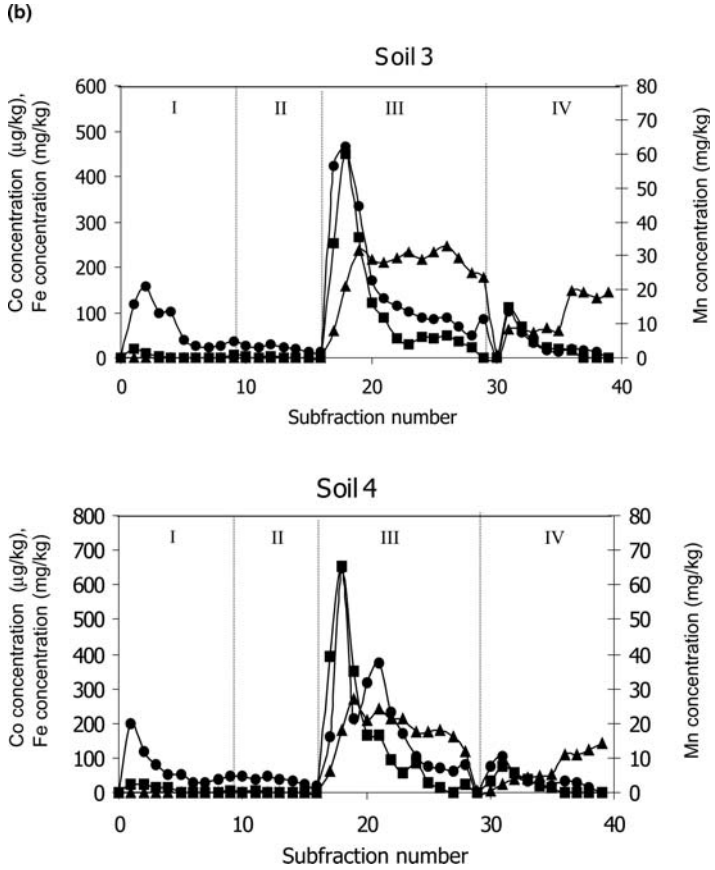

Figure 3b. Extractograms obtained using the continuous-flow method for Soil 3 and Soil 4. (Conditions as in Fig. 3a)

reducible fraction (III) were distinctly different from each other. As can be seen in the extractogram of Soil 1 (Fig. 3a), Co does appear to dissolve at the same time as Fe in the early stages of the reducible fraction. This might indicates some association between Co and Fe; however the divergence between the Co and Fe extractograms later in the fraction would mean that the distribution of Co within Fe oxides is not uniform. The coincidence of an early Fe peak with the main Co and Mn peaks could possibly be due to the dissolution of amorphous Fe oxides; however for Soils 2, 3, and 4, the initial Fe peak clearly lagged behind those of Co and Mn. It would therefore appear that there was no simultaneous dissolution of Co and Fe in the subfractions of the reducible phase.

The close relationship between Co and Mn, but not with Fe, was also observed in the oxidizable (organic-bound) phase (Figs. 3a and 3b).

The extraction profiles of Co and Mn showed up as a peaks decreasing to the baseline by the end of the fraction, whereas for Fe, for three of the soils, concentrations remained well above baseline when the extraction (Step IV) was discontinued.

Evaluation of Association between Elements Using Statistical Correlations

In previous studies (Li et al., 2001a) batch sequential extraction data has been used to evaluate the chemical association between Co and Mn in the soil. Chemical associations are examined by the calculation of correlation coefficients (r) between the amounts (or proportions) of Co and Mn determined in the same extraction step. Highly significant correlations have been interpreted as the two elements having close associations. Nevertheless, results from such studies have demonstrated that the amounts of Co and Mn extracted in the reducible phase are strongly correlated (Jarvis, 1984), and it has been suggested that the association is due to the strong sorption of Co by Mn oxides. More recently, Li et al. (1999, 2001a, 2001b) have reported chemical relationships and associations between Co, Mn, and Fe for batch extraction data, based on linear correlation analysis. However, since the batch system provides only a single metal concentration value for each extraction step, correlations as found using the batch technique may not always indicate a true elemental association. Elements may be dissolved at different times during the same extraction step.

To further investigate possible relationships between Co, Mn, and Fe in soil, Li et al. (2001b) also used multiple regression modeling based on batch fractionation data. Their multiple regression models suggested that the Fe content of the soils strongly influences the proportions of both Co and Mn present in exchangeable, reducible, and organic-bound fractions.

In this current work, linear correlation (r) was used to evaluate the relationships between Co and Mn and between Co and Fe, using the flow extraction data. For each phase of each sample, the r value was calculated for the linear correlations between extractable Co and extractable Mn concentrations in the subfractions of that phase. The r values between Co and Mn, and between Co and Fe, calculated in this way from the flow extraction data, are summarized in the first four columns of Tables 5 and 6. For comparison purposes, correlations calculated using the batch extraction data for all four samples are shown in the last columns of Tables 5 and 6.

It was found that, in the flow system, concentrations of Co and Mn in the reducible phase were highly and significantly correlated for three of the soils ($r > 0.95$). For Soil 4, the correlation was not as high ($r = 0.80$) and as noted previously, the extractogram for this soil showed a second Mn peak that was not accompanied by a corresponding peak for Co. In comparison to the correlations between Co and Mn in the reducible phase, those between Co and Fe

Table 5. Correlations (r) between Co and Mn concentrations in fractions obtained from flow and batch extractions

Fraction	Flow extraction[a]				Batch extraction (all soils)[b]
	Soil 1	Soil 2	Soil 3	Soil 4	
Exchangeable	0.91*** (9)	0.86** (9)	0.68* (9)	0.90*** (9)	0.66
Acid-soluble	0.88** (8)	0.34 (8)	0.81* (8)	0.44 (8)	0.71
Reducible	0.99*** (12)	0.99*** (12)	0.96*** (12)	0.80** (12)	0.90
Oxidizable	0.88*** (11)	0.20 (11)	0.69* (11)	0.85*** (11)	0.67

*$P < 0.05$; ** $P < 0.01$; ***$P < 0.001$.

[a]r values calculated from concentrations in individual subfractions; number of subfractions for each soil/fraction shown in parenthesis.

[b]r values calculated from metal concentrations in particular fractions of the four soils.

were not significant for three of the soils and only significant at $P > 0.05$ for the fourth soil (Table 6). It is interesting to note that for the batch extraction data, equally high r values were calculated for the reducible fraction, between Co and Mn, and between Co and Fe. However, because of the small number of samples neither r value was statistically significant.

Apart from the reducible fraction, correlations between Co and Mn for the flow extraction data were also generally high for the exchangeable fraction (Table 5). However, correlations for the acid-soluble and oxidizable fractions were much more variable, ranging from highly significant for some soils to nonsignificant for others. Correlations between Co and Fe in the oxidizable fraction were much poorer than between Co and Mn in the same fraction. Correlations were not calculated between Co and Fe in the

Table 6. Correlations (r) between Co and Fe concentrations in fractions obtained from flow and batch extractions

Fraction	Flow extraction[a]				Batch extraction[b] (all soils)
	Soil 1	Soil 2	Soil 3	Soil 4	
Exchangeable	ND	ND	ND	ND	0.89
Acid-soluble	ND	ND	ND	ND	0.11
Reducible	0.69* (12)	0.32 (12)	0.46 (12)	0.14 (12)	0.86
Oxidizable	0.66* (11)	0.24 (11)	0.42 (11)	0.58 (11)	0.37

*$P < 0.05$.

[a]r values calculated from concentrations in individual subfractions; number of subfractions for each soil/fraction shown in parenthesis.

[b]r values calculated from metal concentrations in particular fractions of the four soils.

ND = not determined since Fe concentrations at or below detection limit.

exchangeable and acid-soluble fractions because of the negligible concentrations of Fe extracted.

In the case of the batch extraction data, in addition to the high (but nonsignificant) r values between Co and Mn or Fe in the reducible fraction, relatively high r values were obtained for some of the other fractions (Tables 5 and 6). However, unlike the flow extraction data, these did not generally agree with the trends between elements observed in the extractograms.

CONCLUSIONS

This study has demonstrated that a continuous-flow extraction system can be used to fractionate Co, Mn, and Fe in soils with similar precision and accuracy to those obtained using a traditional batch fractionation procedure. In addition, the continuous-flow system reduces some tedious procedures, such as centrifugation and manual filtration that are required for the batch method. A four-step continuous-flow extraction can be completed within 5–7 h, compared with 5 days for a batch method. Although clearly requiring a greater number of chemical analyses than the batch system, an additional advantage of the flow system is the detailed information obtained from the extractogram. This appears to be a very useful tool for evaluating a true chemical association between elements. The visual interpretation of elemental associations using the extractograms is strongly supported by examination of the flow extraction data using a statistical correlation technique. In contrast, there are clearly limitations in using the data obtained from batch extractions to examine the association between elements.

For the soils in this study, results from the flow extraction system suggest a clear association between Co and Mn but little direct evidence of a strong Co interaction with Fe. This contrasts with some previous studies using batch fractionations, in which statistical correlations between Co and Fe have been taken as evidence for an association between these elements.

ACKNOWLEDGMENTS

The authors would like to gratefully thank the Royal Golden Jubilee Grant and the Thailand Research Fund for funding this project, and the Postgraduate Education and Research Program in Chemistry (PERCH) for partial support.

REFERENCES

Adams, S.N., Honeysett, J.L., Tiller, K.G., and Norrish, K. (1969) Factors controlling the increase of cobalt in plants following the addition of a cobalt fertilizer. *Australian Journal of Soil Research*, 7: 29–42.

Chomchoei, R., Shiowatana, J., and Pongsakul, P. (2002) Continuous-flow system for reduction of metal readsorption during sequential extraction of soil. *Analytical Chimica Acta*, 472: 147–159.

Hewitt, A.E. (1993) *New Zealand Soil Classification: Landcare Research Science Series No. 1*; Manaaki Whenua Press: Lincoln, New Zealand.

Hinsin, D., Pdungsap, L., and Shiowatana, J. (2002) Continuous-flow extraction system for elemental association study: a case of synthetic metal doped iron hydroxide. *Talanta*, 58: 1365–1373.

Jarvis, S.C. (1984) The association of cobalt with easily reducible manganese in some acidic permanent grassland soils. *Journal of Soil Science*, 35: 431–438.

Li, Z., McLaren, R.G., and Metherell, A.K. (1999) The effect of soil manganese status on the bioavailability of soil cobalt for pasture uptake in New Zealand soils. *Proceeding of the New Zealand Grassland Association*, 61: 133–137.

Li, Z., McLaren, R.G., and Metherell, A.K. (2001a) Cobalt and manganese relationship in New Zealand soils. *New Zealand Journal of Agriculture Research*, 44: 191–200.

Li, Z., McLaren, R.G., and Metherell, A.K. (2001b) Fractionation of cobalt and manganese in New Zealand soils. *Australian Journal of Soil Research*, 39: 951–967.

McKenzie, R.M. (1969) The reaction of cobalt with manganese dioxide minerals. *Australian Journal of Soil Research*, 8: 97–106.

McLaren, R.G. (2002) Cobalt and iodine. In *Encyclopedia of Soil Science*; Lal, R., ed.; Marcel Dekker Inc. New York.

McLaren, R.G. and Cameron, K.C. (1996) *Soil Science: Sustainable Production and Environmental Protection*; Oxford University Press: Auckland, New Zealand.

Shiowatana, J., Tantidanai, N., Nookabkaew, S., and Nacapricha, D. (2001a) A flow system for the determination of metal speciation in soil by sequential extraction. *Environment International*, 26: 381–387.

Shiowatana, J., Tantidanai, N., Nookabkaew, S., and Nacapricha, D. (2001b) A novel continuous-flow sequential extraction procedure for metal speciation in solids. *Journal of Environmental Quality*, 30: 1195–1205.

Shiowatana, J., McLaren, R.G., Chanmekha, N., and Samphao, A. (2001c) Fractionation of arsenic in soil by a continuous-flow sequential extraction method. *Journal of Environmental Quality*, 30: 1940–1949.

Taylor, R.M., McKenzie, R.M., and Norrish, K. (1964) The mineralogy and chemistry of manganese in some Australian soils. *Australian Journal of Soil Research*, 2: 235–48.

Taylor, R.M. and McKenzie, R.M. (1966) The association of trace elements with manganese minerals in Australian soils. *Australian Journal of Soil Research*, 4: 29–39.

Tessier, A., Campbell, P.G.C., and Bisson, M. (1979) Sequential extraction procedure for the speciation of particulate trace metal. *Analytical Chemistry*, 66: 3562–3565.

Tiller, K.G., Honeysette, J.L., and Hallsworth, E.G. (1969) The isotopically exchangeable form of native and applied cobalt in soils. *Australian Journal of Soil Research*, 7: 43–56.

Anal Bioanal Chem (2007) 389:733–742
DOI 10.1007/s00216-007-1308-x

ORIGINAL PAPER

Flow field–flow fractionation–inductively coupled optical emission spectrometric investigation of the size-based distribution of iron complexed to phytic and tannic acids in a food suspension: implications for iron availability

Sopon Purawatt · Atitaya Siripinyanond · Juwadee Shiowatana

Received: 31 January 2007 / Revised: 11 April 2007 / Accepted: 12 April 2007 / Published online: 30 May 2007

Abstract Flow field–flow fractionation–inductively coupled plasma optical emission spectrometry (FlFFF–ICP–OES) was applied to achieve the size-based fractionation of iron in a food suspension in order to gain insights into iron availability. The binding of iron with phytic and tannic acids, employed as model inhibitors of iron availability in foods, was investigated at pH 2.0 (representing stomach fluid), pH 5.0 (the transition stage in the upper part of the duodenum), and pH 7.0 (the small intestine). In the presence of phytic acid, iron was found as a free ion or it was associated with molecules smaller than 1 kDa at pH 2.0. Iron associated with molecules larger than 1 kDa when the pH of the mixture was raised to 5.0 and 7.0. In the presence of tannic acid, iron was again mostly associated with molecules smaller than 1 kDa at pH 2.0. However, at pH 5.0, iron and tannic acid associated in large molecules (~25 kDa), while at pH 7.0, most of the iron was associated with macromolecules larger than 500 kDa. Iron size-based distributions of kale extract and tea infusion containing phytic and tannic acids, respectively, were also examined at the three pH values, with and without enzymatic digestion. Without enzymatic digestion of the kale extract and the tea infusion at pH 2.0, most of the iron was released as free ions or associated with molecules smaller than 1 kDa. At other pH values, most of the iron in the kale extract and the tea infusion was found to bind with ~2 kDa and >500 kDa macromolecules, respectively. Upon enzymatic gastrointestinal digestion, the iron was not observed to bind to macromolecules >1 kDa but <500 kDa, due to the enzymatic breakdown of large molecules to smaller ones (<1 kDa).

Keywords Iron · FlFFF · ICP–OES · Size-based elemental fractionation

S. Purawatt · A. Siripinyanond · J. Shiowatana (✉)
Department of Chemistry, Faculty of Science, Mahidol University, Rama VI Rd.,
Bangkok 10400, Thailand
e-mail: scysw@mahidol.ac.th

Introduction

Iron deficiency is one of the commonest nutritional problems worldwide, affecting ~20% of the world's population. Various iron fortification and dietary strategies have been proposed to maximize the intake and the bioavailability of iron [1]. Non-heme Fe, which comprises most of the Fe taken in, is absorbed in ionic form by receptors on the mucosa cells, and its bioavailability varies depending on the Fe status of the subjects and different dietary factors. Some food components show a marked inhibitory effect on the absorption of non-heme Fe in humans [2]. The strong inhibitory effects of phytic acid (PA) and tannic acid (TA) on iron absorption have been documented previously [3, 4]. Phytic acid (myo-inositol-1,2,3,4,5,6-hexakisphosphate) is the most abundant myo-inositol compound. It is reported to occur as highly phosphorylated molecules that are present in cereal grains and seeds, and it is an excellent chelator of metal ions [5–7]. Owing to the presence of six phosphate groups in very close proximity in the molecule, it strongly binds practically any metal ion. According to its pK_a of ~1.1 [8], phytic acid is present in ionic form under slightly acidic conditions and is thus able to bind with free metal ions. Most research suggests that the formation of

phytate–metal complexes in the intestinal tract prevents metal absorption [2–4, 9, 10].

TA is a hydrolyzable tannin that was reported to have a high capacity to bind iron to form a stable complex [11]. TA is a polyphenolic compound found, along with other condensed tannins, in beverages such as red wine, beer, coffee, black tea, green tea, as well as many foodstuffs such as grapes, pears, bananas, sorghum, black-eyed peas, lentils, and chocolate [12, 13]. TA is hydrolyzed by acid to form glucose and gallic acid. The latter contains a galloyl group, which has been implicated in the inhibition of iron absorption through the binding of iron [14].

As food compositions are very complex, iron and other minerals may be associated with molecules or particles of different sizes. Therefore, knowledge of the size-based distribution of iron in food suspensions during gastrointestinal digestion should lead to a better understanding of iron absorption. To study size-based elemental distribution, it is necessary to couple a separation unit with elemental detection. Gel chromatography with flame atomic absorption and polarographic detection was used to study the distributions of free and bound cadmium, zinc, copper, and silver in lobster digestive gland extract [15]. Size-based metal distributions (of free ion, low molecular weight bound, and medium molecular weight bound forms) provide information about metal–protein binding and release behavior under different conditions. Size exclusion chromatography (SEC) hyphenated with inductively coupled plasma mass spectrometry (ICP–MS) was found to be useful for exploring metal binding and association behavior, as reviewed by Sadi [16]. Wuilloud et al. employed SEC–UV–ICP–MS to determine the molecular weight distributions of associations of metal with various compounds in edible mushroom [17]. A Superdex-75 column was used to examine the association of metals with molecules of different molecular weights in fungi porcini mushroom. In chromatographic techniques, organic solvents are often used as the carrier liquid, and a sample pretreatment step is necessary to clean up the sample prior to sample introduction. The organic solvent can cause carbon overloading in the plasma of the ICP-MS.

The non-chromatographic technique flow field–flow fractionation (FlFFF), when coupled with a highly sensitive elemental detection unit such as an inductively coupled plasma optical emission spectrophotometer (ICP–OES) or ICP–MS, has been exploited to investigate the binding and association of elements with various kinds of molecules, such as proteins [18], macromolecules [19–22], and bacteria [23]. Barnes and Siripinyanond performed a feasibility study of the applicability of FlFFF–ICP–MS to metal fractionation in a protein standard including metallothionein, carbonic anhydrase, ceruloplasmin, alcohol dehydrogenase, and thyroglobulin [18]. The simple interface between the FlFFF and ICP–MS, resulting from their compatible flow rates, makes this a potentially promising and versatile technique for elemental fractionation in proteins. Jackson et al. successfully used FlFFF–ICP–MS to investigate uranium sorption behavior on bacterial cells [23]. Recent reports have suggested that FlFFF–ICP–MS and FlFFF–ICP–OES are highly capable techniques for investigating metal binding and association behavior via size-based metal distributions.

In this work, the binding of iron with phytic acid and tannic acid in food suspensions was investigated using FlFFF–ICP–OES. The size-based distribution of iron in kale extract and tea infusion with and without enzymatic digestion was also examined. Non-enzymatic incubation of the sample at pH 2.0, 5.0 and 7.0 was performed in order to mimic the pH conditions of the gastrointestinal digestion processes in the stomach, the upper part of the duodenum, and the small intestine, respectively. To obtain enzymatic incubations, pepsin and pancreatic bile extract, which are predominantly found and known to be active in the respective stages of gastrointestinal digestion, were added. To our knowledge, this is the first attempt to use hyphenated FlFFF–ICP–OES to investigate the size-based distribution of an element in a food suspension at various pHs during simulated gastrointestinal digestion.

Experimental

Chemicals and samples

Deionized water (MilliQ plus, 18.2 MΩ cm^{-1}) was used throughout the experiments. All glassware was washed with liquid detergent, rinsed with water, soaked overnight in 10% HNO_3, and rinsed again before use. All chemicals were of analytical grade. All standard working solutions of iron were prepared by diluting a 1000 mg L^{-1} standard solution of iron (prepared from Fe(III) nitrate by Merck, Darmstadt, Germany) with deionized water. Phytic acid (FW=660.04 Da; Fluka, Milan, Italy) and tannic acid (FW= 1700.79 Da; Fluka, were weighed and dissolved in deionized water to create stock solutions for the iron-inhibitor binding study. The enzymes pepsin (P-7000, from porcine stomach mucosa), pancreatin (P-1750, from porcine pancreas), and bile extract (B-6831, porcine) were from Sigma (St. Louis, MO, USA). A pepsin solution was prepared by dissolving 0.16 g of pepsin in 1 mL of 0.1 M hydrochloric acid, and a pancreatin bile extract (PBE) mixture was made by dissolving 0.004 g of pancreatin and 0.025 g of bile extract in 5 mL of 0.001 M $NaHCO_3$.

Fresh Chinese kale was washed with deionized water. It was then dried at 65 °C to constant weight and ground up before being stored in a desiccator until required. To prepare

the tea infusion, instant tea was bought from a local market and prepared by following the recommended instructions. A tea bag was dipped in 120 mL of deionized water and heated at 80 °C for 10 min. To obtain kale extract, 1 g of dried, ground Chinese kale was added to 10 mL of deionized water and heated at 80 °C for 10 min. The suspension was then centrifuged at 3000 rpm for 20 min in order to separate out the precipitated residue. The tea infusion and the Chinese kale extract was stored at 4 °C until use.

The carrier liquid for FlFFF operating at pH 2.0, 0.01 M HCl, was prepared by diluting 0.8 mL of 37% HCl (Merck) in 1000 mL of deionized water. Carrier liquids at pH 5.0 and 7.0 were prepared by adding 0.8 mL of HCl to 800 mL of deionized water and then adjusting to the required pH using $NaHCO_3$ and NaOH solutions. The solution volume was finally made up to 1000 mL. Monodisperse polystyrene sulfonates (PSS) (Fluka), which were used as FlFFF molecular weight calibrating standards (4.3, 17, and 49 kDa), were individually prepared by diluting in deionized water to obtain 10 mg mL^{-1}. All samples were centrifuged at 3000 rpm for 20 min to eliminate large particles before the FlFFF investigation.

Iron-inhibitor binding study

A flow chart for this sample preparation process is shown in Fig. 1. According to the literature, an iron:phytic acid weight ratio in excess of 1:10 (~1:1 mole ratio) clearly inhibits iron availability [24]. To demonstrate the degree of iron binding that causes the inhibition of iron absorption, 1:10, 1:50, and 1:100 weight ratios were therefore selected. Phytic and tannic acids were individually mixed with 300 mg L^{-1} iron at weight ratios (iron:phytic acid/tannic acid) of 1:10, 1:50 and 1:100. The pH was adjusted with dilute HCl or $NaHCO_3$ or NaOH solutions in order to investigate iron binding at pH values of 2.0, 5.0, and 7.0.

Non-enzymatic incubation

For the unspiked kale extract, the pH of 2.5 mL of the kale extract was adjusted to either 2.0, 5.0, or 7.0. The final volume was adjusted to 5.0 mL. For the iron-spiked kale extract or tea infusion, 1.5 mL of the 1000 mg L^{-1} standard solution of iron was added to 2.5 mL of the kale extract or tea infusion before pH adjustment. The solution volume was finally made up to 5.0 mL. The flow chart for this sample preparation process is shown in Fig. 1.

Gastrointestinal digestion

Simulated gastrointestinal digestion of food samples was carried out starting with peptic digestion with pepsin, and then pancreatic digestion with PBE (see Fig. 2). In the simulated peptic digestion step, a portion of the sample (0.5 g for a solid sample or 2.0 mL for a liquid sample) was added to 10.0 mL of purified water and adjusted to pH 2.0 with 6 M hydrochloric acid. The volume of the sample suspension was finally adjusted to 12.5 mL with purified water, and 375 μL of pepsin solution was added. This digestion step was performed in an incubator shaker at 37± 1 °C for 2 h. After that, the suspension pH was adjusted to 5.0 and incubated for 30 min to simulate the digestion in the upper part of the duodenum, at the juncture between the stomach and the intestine. An aliquot of 2.5 mL of the digestate at pH 5.0 was taken, adjusted to pH 7.0, and diluted to 5.0 mL. The freshly prepared PBE mixture (625 μL) was then added, and the incubation was continued for 2 h.

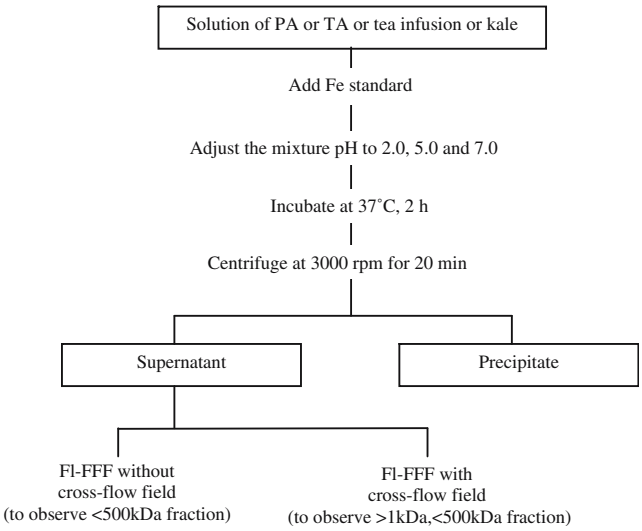

Fig. 1 Non-enzymatic mixing of test samples (kale extract and tea infusion) containing phytic acid (PA) or tannic acid (TA) with iron solution, at various pH values, to investigate the size-based iron distribution

Instrumentation

A pH meter (model 215, Denver Instrument, Denver, CO, USA) with a glass combination electrode was used for all pH measurements. Commercial standard buffers (Merck) of pH 4.00 and 7.00 were employed for the pH calibration. An incubator shaker, model SS40-D2 from Grant Instruments (Cambridge, UK), was used to incubate the samples at 37± 1 °C. A FlFFF system (model PN-1021-FO, Postnova Analytics, Landsberg, Germany) equipped with a 1000-Da molecular weight cut-off poly(cellulose acetate) membrane (Postnova Analytics) was used. The FlFFF channel was 27 cm long, 2.0 cm wide and 0.0254 cm thick. A high-pressure liquid chromatography (HPLC) pump (model PN 2101, Postnova Analytics) was employed to deliver the channel flow. Another HPLC pump of the same model was employed to regulate the cross-flow. The FlFFF can be

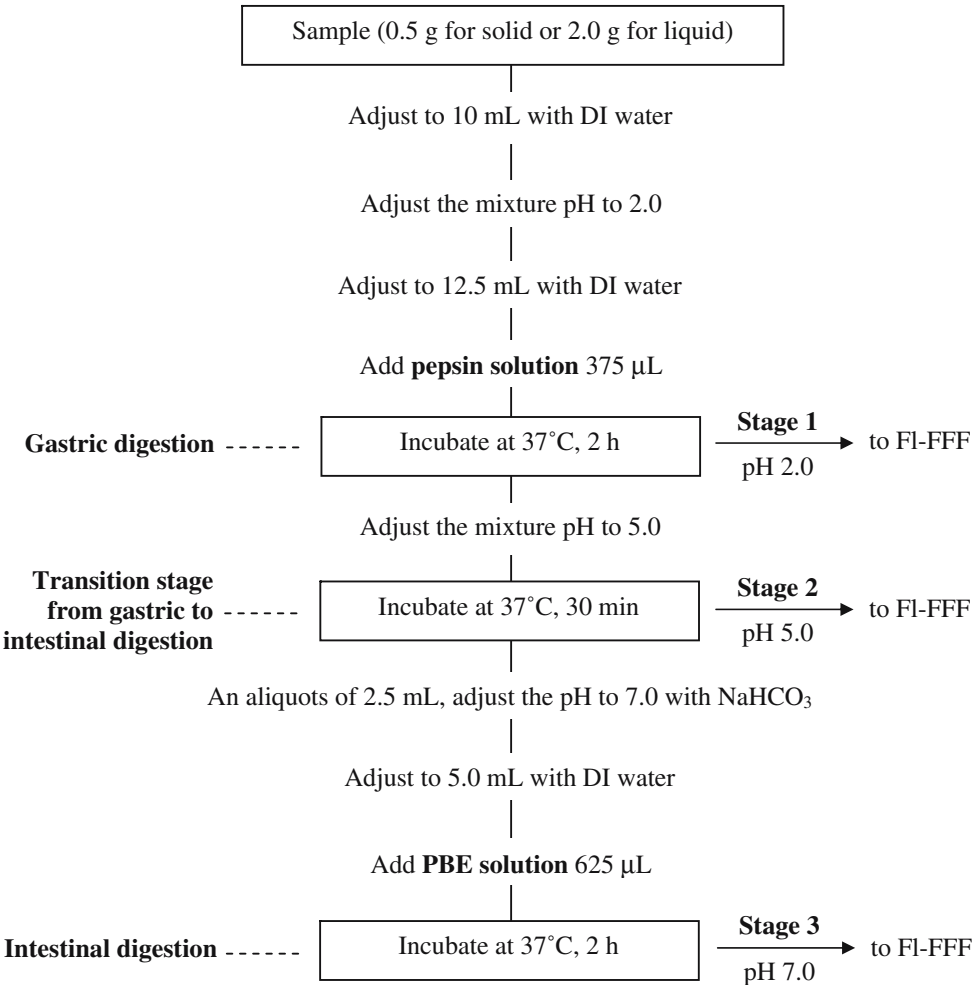

Fig. 2 Enzymatic digestion procedure used to simulate gastrointestinal digestion

operated in two modes; with and without cross-flow. In the presence of cross-flow, sample components that are smaller than the membrane cutoff (1 kDa) are forced through a membrane and leave the channel, whereas the remaining components are separated under cross-flow field. Without using cross-flow, all sample components are retained in the channel and leave the channel through the outlet connected to the detectors. UV absorption of the eluted molecules was monitored at 254 nm by a UV-visible spectrophotometer (model S 3210, Postnova Analytics). An end-on view Spectro CirosCCD ICP–OES system (Spectro Analytical Instruments, Kleve, Germany) was used as an elemental detector. The outlet of the spectrophotometer flow cell was connected directly to the modified Lichte nebulizer of the ICP–OES system with poly(tetrafluoroethylene) tubing. The operating conditions employed when taking FlFFF and ICP-OES measurements are summarized in Table 1. The iron emission was monitored at 238.20(II), 259.94(II) and 239.56(II) nm.

Calculating the iron distribution

To gauge the total iron concentrations in the phytic and tannic acid experiments, including those involving the iron-spiked and unspiked kale extracts and the tea infusion, their wet acid digestates were measured by ICP–OES using external calibration. After enzymatic and non-enzymatic incubation, the sample suspension was separated into supernatant (assumed to be the <500 kDa fraction) and precipitation phases (assumed to be the >500 kDa fraction). The total iron in the supernatant was calculated from the area of the iron fractogram obtained without cross-flow field of the supernatant. The iron in the precipitation phase (>1 kDa but <500 kDa) was calculated from the area of the iron fractogram obtained with cross-flow field of the supernatant.

The iron associated with the supernatant was calculated by subtracting the iron in the precipitation phase from the total iron in the supernatant. The >500 kDa fraction was

Table 1 Instrumental operating conditions

FlFFF condition	
Carrier liquid	
pH 2.0	0.01 M HCl
pH 5.0	0.01 M HCl adjusted to pH 5.0 by $NaHCO_3$
pH 7.0	0.01 M HCl adjusted to pH 7.0 by NaOH
Membrane	1000 Da MWCO, poly(cellulose acetate)
Channel flow rate (mL min^{-1})	0.75
Cross flow rate (mL min^{-1})	2
ICP–OES condition	
RF generator frequency (MHz)	27.2
RF power / W	1350
Nebulizer gas flow rate (L min^{-1})	1
Coolant gas flow rate (L min^{-1})	12
Auxiliary gas flow rate (L min^{-1})	1

obtained by subtracting the total iron concentration in the supernatant from the total iron concentration in the samples. The percentage distributions were calculated by dividing the iron concentration in each fraction by the total iron concentration and multiplying by 100.

Results and discussion

I. FlFFF channel calibration

To calibrate the FlFFF channel effectively, the type of molecular weight standard used should be selected carefully. In this study, poly(styrene sulfonate) standards were selected for two reasons. The first reason is the similar secondary structure (a random coil) of the phytic and tannic acids and the poly(styrene sulfonate). Second, in contrast to protein standards, poly(styrene sulfonate) maintains its structural integrity at the pH values examined in this work. As FlFFF has rarely been performed at pH 2, we carefully evaluated the feasibility of performing size characterization at this acidic pH, and found that satisfactory results were obtained.

By calibrating the FlFFF channel with known molecular weight poly(styrene sulfonate) standards (4.3, 17.0, and 49 kDa), calibration functions were obtained for each pH value, as follows:

$$\log t_r = 0.572 \log M - 0.556, R^2 = 0.984 \text{ for pH } 2.0$$
$$\log t_r = 0.437 \log M - 0.065, R^2 = 0.999 \text{ for pH } 5.0$$
$$\log t_r = 0.526 \log M - 0.100, R^2 = 0.994 \text{ for pH } 7.0$$

The parameters t_r and M represent retention time (min) and molecular weight (kDa), respectively. The retention time (t_r) was measured at the peak maximum of the fractogram. These equations were used to translate the retention time into molecular weight information. The slightly different calibration equation at each pH may be due to changes in the properties of the FlFFF membrane at different pH values, which could lead to a slight shift in retention. Therefore, channel calibration must be performed at all pH values studied.

II. The size-based distribution of iron in the presence of inhibitors

FlFFF–ICP–OES fractograms were obtained in order to study the binding behavior of iron to phytic and tannic acids at pH 2.0, 5.0, and 7.0 (Fig. 3a–d, right, and Fig. 4), considering the pH change from ~2.0 to ~7.0 in the gastrointestinal pathway where iron and other minerals are absorbed. The amount of phytic acid was varied by employing weight ratios (Fe:PA) of 1:10, 1:50 and 1:100, and size-based distribution profiles of iron at pH 2.0, 5.0, and 7.0 were obtained. The molecular weight at the peak was calculated from the molecular weight calibration equation obtained at each pH value. Initially, fractograms of iron solution with phytic and tannic acids were examined. Without any phytic or tannic acids, iron in its free form is not retained in the FlFFF channel, and it is thus forced to pass through the channel membrane and leave the channel. Therefore, no iron distribution is seen in the fractogram, as shown in Fig. 3d, right. However, upon binding with an inhibitor with a large molecular weight, the iron phytate chelation results in larger molecules which are retained above the channel membrane, gaving an iron signal at 1–1.5 min, equivalent to a molecular weight of ~1 kDa. The UV fractograms of the retained molecules showed similar profiles to those of the iron distribution profiles, suggesting that iron was highly associated with the phytic acid molecules (Fig. 3a–d, left). The UV fractograms and iron distributions gave peak maxima at the same retention time for every phytic acid iron ratio. The peak areas of UV absorption and iron distribution increased when the phytic acid to iron ratio was increased.

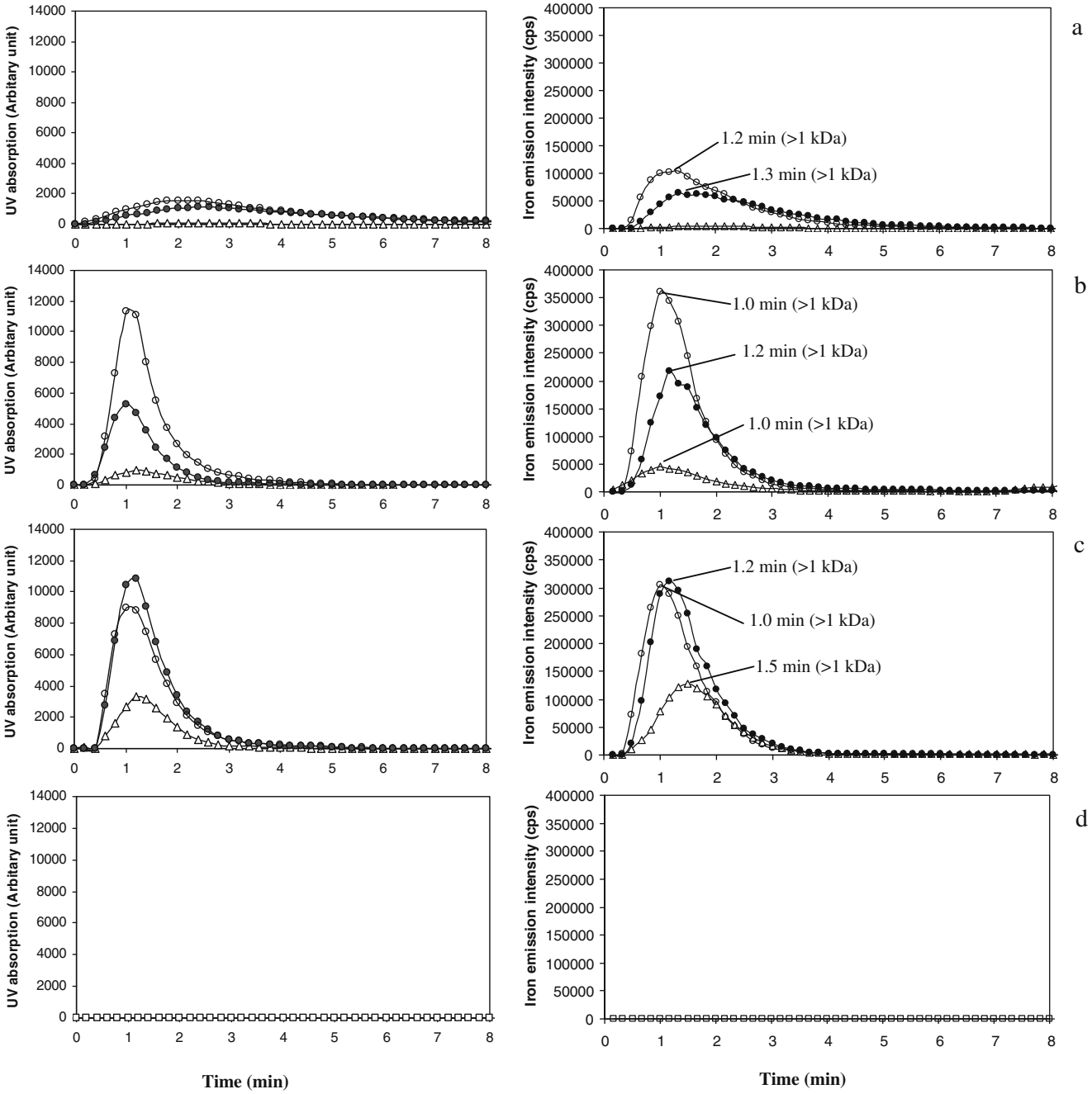

Fig. 3a–d Fractograms (UV detection on the *left* and ICP–OES detection on the *right*) for iron in the presence of varying amounts of phytic acid at pH 2.0 (**a**), 5.0 (**b**), and 7.0 (**c**). **d** shows fractograms of iron without phytic acid. Fe:PA was 1:10 (*triangles*), 1:50 (*filled circles*), and 1:100 (*unfilled circles*)

At all pH values studied, the iron association in the FlFFF-observable range of >1 kDa but <500 kDa was found to increase when more phytic acid was added. The highest association, as observed from the peak areas in Fig. 3, right), was found for weight ratios of 1:50 and 1:100 at pH 7.0. For a fixed amount of phytic acid, the binding of iron and phytic acid increased when the pH was increased.

Three molecular weight ranges were then classified: (a) <1 kDa; (b) >1 kDa but <500 kDa; and (c) >500 kDa. The size-distributions of the iron associations for all three weight ranges are summarized in Table 2. Fraction (b) was calculated from area under the fractogram, as observed using FlFFF–ICP–OES. The iron associated with molecules smaller than 1 kDa (a) was obtained from the area of the

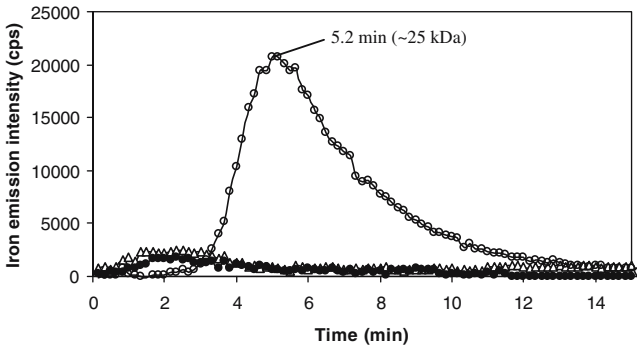

Fig. 4 Iron fractograms of iron in tannic acid (weight ratio 1:100) at pH 2.0 (*triangles*), 5.0 (*unfilled circles*) and 7.0 (*filled circles*)

fractogram yielded by FlFFF–ICP–OES without the application of cross-flow field minus the same value for (b). The equivalent value for the fraction larger than 500 kDa (c) was calculated by subtracting the values for (a) and (b) from the total iron value.

High associations between iron and phytic acid were observed for every pH and every iron:phytic acid ratio. For an iron:phytic acid ratio of 1:10, the iron was largely distributed in the >500 kDa fraction at all pH values tested. For the other iron:phytic acid ratio, the amount of iron in this fraction was less significant. This phenomenon was in agreement with the results reported by Evan and Martin [25], who found that iron phytate precipitated at ratios of approx. 1:10 and 1:40. Free iron or iron associated with molecules smaller than 1 kDa was clearly predominant at pH 2.0. The amount of iron in this fraction decreased when solution pH was increased to 5.0 and 7.0. At pH 5.0 and 7.0, the iron was concentrated in the fraction associated with phytic acid (>1 kDa), as observed in the FlFFF fractogram. Most of the iron was associated with phytic acid.

In the presence of tannic acid, iron was associated with small molecules (<1 kDa) at pH 2.0 (Table 2). At pH 5.0 and 7.0, however, iron only appeared in the >500 kDa fraction, except for an iron:tannic acid ratio of 1:100 at pH 5.0, as illustrated in Fig. 4. The association of iron with macromolecules (~25 kDa) was observed at t_r = 5.2 min. At high levels of tannic acid and for slightly acidic conditions, the iron that formed macromolecules with tannic acid did not precipitate completely. For other ratios and at pH 5.0 and 7.0, precipitation readily occurred when the iron and tannic acid solutions were mixed. The amount of free iron or iron associated with molecules smaller than 1 kDa was extremely low. It can therefore be concluded that iron was completely bound to tannic acid when the pH was higher than 5.0.

At pH 5.0 and 7.0, most of the iron was associated with the phytic acid or tannic acid. The phytic and tannic acids

Table 2 Size-based distributions of iron in the presence of various concentrations of phytic acid (PA) and tannic acid (TA) at pH 2.0, 5.0, and 7.0

Sample	pH	Proportions of iron (%)		
		<1 kDa[(a)]	>1 kDa, <500 kDa[(b)]	>500 kDa[(c)]
Fe + PA (1:10)	2.0	16.0	2.0	81.9
	5.0	3.9	25.5	70.7
	7.0	6.0	45.5	48.4
Fe + PA (1:50)	2.0	49.6	50.4	0.0
	5.0	19.8	66.0	14.2
	7.0	0.0	93.8	6.2
Fe + PA (1:100)	2.0	45.2	54.8	0.0
	5.0	17.2	82.8	0.0
	7.0	4.5	95.5	0.0
Fe + TA (1:10)	2.0	98.9	1.1	n.d.
	5.0	0.5	0.4	99.1
	7.0	0.1	0.6	99.3
Fe + TA (1:50)	2.0	98.9	1.2	0.0
	5.0	0.9	0.7	98.4
	7.0	1.1	0.6	98.2
Fe + TA (1:100)	2.0	98.9	1.1	n.d.
	5.0	2.5	16.1	81.5
	7.0	1.7	1.7	96.6

[(a)] Obtained from the area of the iron profile yielded by FlFFF–ICP–OES without the cross-flow field minus the value for (b)
[(b)] Obtained from the area of the iron profile yielded by FlFFF–ICP–OES with the cross-flow field
[(c)] Obtained from the total iron minus the values for (a) and (b)
n.d., not determined, as the concentration in this fraction was lower than the detection limit of 0.2 mg L^{-1}
Total iron concentration was 300 mg L^{-1}.

showed high potential to produce iron complexes which are reportedly not absorbable by the intestine [2–4, 9, 10].

III. Size-based distributions of iron in kale extract and tea infusion

Kale and tea contain inhibitor molecules—phytic acid and tannic acid, respectively. The inhibitors in kale and tea can bind with the iron to form iron complexes, and so they exhibit an inhibition effect. Therefore, the size-based distribution of iron in kale extract and tea infusion was investigated at pH 2.0, 5.0, and 7.0 under both non-enzymatic and enzymatic conditions. Due to the low iron content in tea itself, free iron was spiked into the tea infusion to a level of 300 mg L^{-1} prior to investigation.

Table 3 shows the proportions of iron in each of three size groups for kale extract and tea infusion. The proportions were calculated as in the iron-inhibitor binding study (Table 2).

From Table 3, the proportions of iron in the small size fraction (<1 kDa) were similar for all sample types. The highest proportion of iron was observed at pH 2.0. At an acidic pH of 2.0, iron was in the free form (or was associated in molecules of <1 kDa), except in the case of iron-spiked tea infusion, when precipitation was observed.

For the unspiked kale extract, the iron was concentrated in the FlFFF-observable range (>1 kDa, <500 kDa) at pH 5.0 and 7.0. The distribution profiles shown in Fig. 5a show that iron was associated with macromolecules of approximately the same molecular weight as in Fig. 2 (>1 kDa). Phytic acid, which binds to the iron, may be present in kale extract. Iron-spiked kale also gave iron distribution profiles

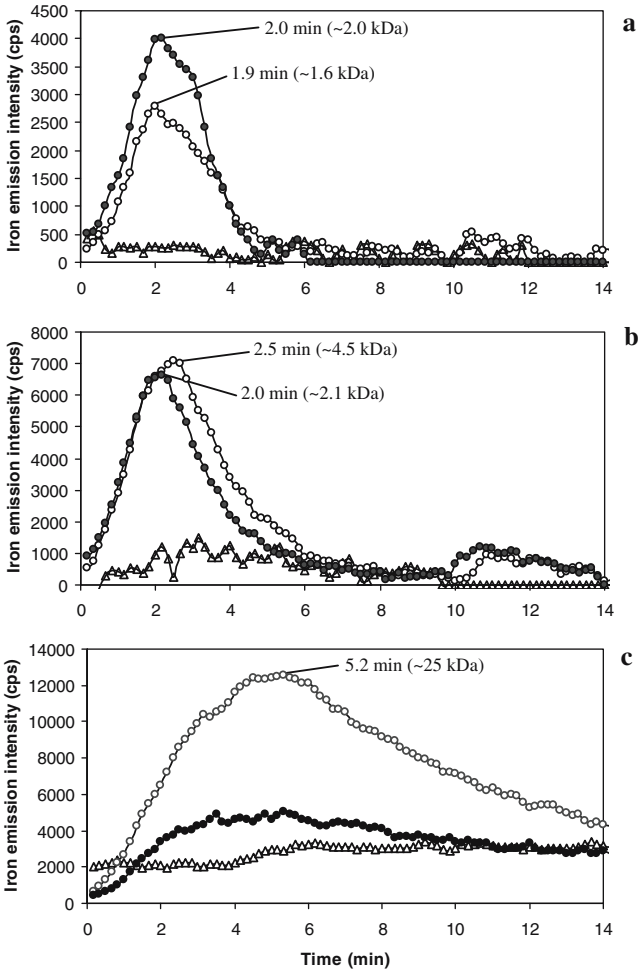

Fig. 5a–c Iron fractograms for iron in kale extract (**a**), iron-spiked kale extract (**b**) and iron-spiked tea infusion (**c**) at pH 2.0 (*triangles*), 5.0 (*unfilled circles*) and 7.0 (*filled circles*)

Table 3 Size-based distributions of iron for kale extract, iron-spiked kale extract and iron-spiked tea infusion at pH 2.0, 5.0, and 7.0

Sample	pH	Proportions of iron (%)		
		<1 kDa[a]	>1 kDa, <500 kDa[b]	>500 kDa[c]
Kale extract	2.0	100.0	0.0	0.0
	5.0	36.5	63.5	0.0
	7.0	4.2	95.8	0.0
Iron-spiked kale extract	2.0	100.0	n.d.	n.d.
	5.0	3.3	3.9	92.8
	7.0	3.0	3.5	93.5
Iron-spiked tea infusion	2.0	91.9	n.d.	8.1
	5.0	21.0	18.5	60.5
	7.0	18.5	7.2	74.3

[a] Obtained from the area of the iron profile yielded by FlFFF–ICP–OES without cross-flow field minus the value for (b)
[b] Obtained from the area of the iron profile yielded by FlFFF–ICP–OES with cross-flow field
[c] Obtained from the total iron minus (a) and (b)
n.d., not determined, as the concentration in this fraction was lower than the detection limit of 0.2 mg L^{-1}

Table 4 Size-based distributions of iron in iron-spiked tea infusion and kale extract at each stage of gastrointestinal digestion

Sample	Stage	Proportions of iron (%)		
		<1 kDa[a]	>1 kDa, <500 kDa[b]	>500 kDa[c]
Tea infusion (iron-spiked)	1 (pH 2.0)	94.8	nd	5.2
	2 (pH 5.0)	29.7	nd	70.3
	3 (pH 7.0)	15.5	nd	84.5
Kale extract	1 (pH 2.0)	82.8	nd	17.2
	2 (pH 5.0)	27.5	nd	72.5
	3 (pH 7.0)	21.2	nd	78.8

[a] Obtained from the area of the iron profile yielded by FlFFF–ICP–OES without cross-flow field minus the value for (b)
[b] Obtained from the area of the iron profile yielded by FlFFF–ICP–OES with cross-flow field
[c] Obtained from the total iron minus the values of (a) and (b)
n.d., not determined, as the concentration in this fraction was lower than the detection limit of 0.2 mg L^{-1}

that peaked in the FlFFF-observable range (>1 kDa, <500 kDa) at pH 5.0 and 7.0, as shown in Fig. 5b.

From Table 3, it is clear that most of the iron was distributed in the small molecular size fraction at pH 2.0. The iron was found in the large molecular size fraction when the pH was raised to 5.0 and 7.0. At pH 5.0, iron associated with macromolecules was observed, as the peak maximum occurred at 5 min or ~25 kDa (Fig. 5c), in agreement with the iron–tannic acid binding experiment (Fig. 4).

The fractograms for the kale extract (Fig. 5a) and the iron-spiked kale extract (Fig. 5b) show a similar degree of association in the range of >1 kDa but <500 kDa. Insufficient numbers of phytic acid binding sites in kale and the high iron concentration may have caused precipitation at slightly acidic (pH 5.0) and neutral (pH 7.0) conditions. Most of the unbound iron in iron-spiked kale precipitated and was distributed in the large molecular fraction (>500 kDa) at pH 5.0 and 7.0, as shown in Table 3.

IV. Size-based distributions of iron in kale and tea infusion after gastrointestinal digestion

To observe the change in the size-based distribution of iron as a result of gastrointestinal digestion, simulated enzymatic digestion was carried out by peptic and then pancreatic digestion. The iron distribution after each stage of gastrointestinal digestion of the kale extract and iron-spiked tea infusion is shown in Table 4. Both samples showed different iron distributions compared to those obtained after non-enzymatic incubation. No iron was observed in the FlFFF-observable size range (>1 kDa, <500 kDa). This shows that, upon gastrointestinal digestion, the iron-bound molecules were digested and converted to free irons and iron associated with molecules smaller than 1 kDa. The inhibitor in the sample was believed to bind with iron, forming an insoluble iron compound, especially at stages 2 and 3 of the simulated gastrointestinal digestion, as can be seen in Table 4.

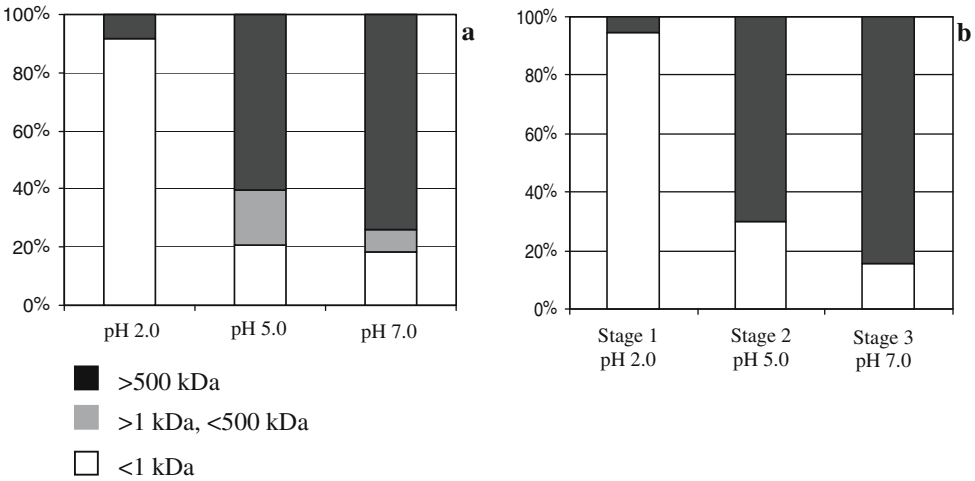

Fig. 6a–b Size-based distribution of iron in iron-spiked tea infusion after (**a**) non-enzymatic mixing at different pH values and (**b**) enzymatic gastrointestinal digestion

In the gastrointestinal digestion of iron-spiked tea infusion, iron did not completely precipitate after full gastrointestinal digestion at pH 7.0. This suggests that the tea infusion may contain less tannic acid than was added in the iron–tannic acid binding experiment.

In Fig. 6, size-based distributions of iron in the spiked tea infusion at different pH values both with and without enzymatic gastrointestinal digestion are compared. The distributions were found to be similar at pH 2.0. The results from the non-enzymatic study at pH 5.0 and 7.0 show that the soluble iron is partially associated with the inhibitor, as shown by the proportions in the range >1 kDa, <500 kDa. In contrast, the enzymatic digestion results in a negligible iron macromolecule binding fraction, as seen from the FlFFF fractogram. It seems probable that the iron in the molecular range of >1 kDa, <500 kDa is digested during enzymatic digestion; it is partially released as free forms and as some iron chelate precipitates.

All soluble iron was present as free iron or iron associated with molecules smaller than 1 kDa, which is absorbable. The iron bound to macromolecules may be digested to small molecules and released as free iron or precipitated after enzymatic digestion, depending on the nature and composition of the food sample.

Conclusion

A hybrid technique where flow field–flow fractionation (FlFFF) is coupled to inductively coupled plasma optical emission spectrometry (ICP–OES) has shown the potential to be an alternative investigation tool for monitoring the size-based distributions of elements in food suspensions during simulated gastrointestinal digestions. Using the technique, iron binding with food components—exemplified by phytic acid and tannic acid in this study—can be investigated. The FlFFF exhibited several advantages over chromatographic techniques due to its ability to investigate wider pH and molecular size ranges. However, the FlFFF has limitated applicability in other studies that require higher resolution.

With or without enzymatic digestion, iron strongly associates with phytic acid at every pH, whereas strong association with tannic acid was observed only when the pH was raised to 5.0 and 7.0. The investigation provides a better understanding of the elemental fractionation of iron–phytic acid and iron–tannic acid complexes during gastrointestinal digestion processes. Tea and kale, which contain tannic and phytic acids, respectively, exhibited the potential to bind with iron and yield similar distributions to those obtained for iron–phytic acid and iron–tannic acid. The ingestion of non-heme iron-containing foods with tea and kale may cause iron absorption to be inhibited during gastrointestinal digestion. The fractionation power of Fl-FFF coupled with the highly sensitivity of ICP–OES is potentially a useful technique for estimating the in vitro iron bioavailability, circumventing the need for a tedious and lengthy procedure. The study of bioavailability will lead to further management strategies for counteracting inhibition and promoting better mineral bioavailability.

Acknowledgement The authors are grateful for financial support from the Thailand Research Fund and the Center for Innovation in Chemistry: Postgraduate Education and Research Program in Chemistry, Higher Education Development Project, Ministry of Education.

References

1. Martinez-Navarrete N, Camacho MM, Martinez-Lahuerta J, Martinez-Monzo J, Fito P (2002) Food Res Int 35:225–231
2. Lopez HW, Leenhardt F, Coudray C, Remesy C (2002) Int J Food Sci Technol 37:727–739
3. Glahn RP, Wortley GM, South PK, Miller DD (2002) J Agric Food Chem 50:390–395
4. Brigide P, Canniatti-Brazaca SG (2006) Food Chem 98:85–89
5. Graf E, Mahoney JR, Bryant RG, Eaton JW (1984) J Biol Chem 259:3620–3624
6. Graf E, Empson K, Eaton J (1987) J Biol Chem 262:11647–11650
7. Graf E, Eaton JW (1990) Free Rad Biol Med 8:61–69
8. Vasca E, Materazzi S, Caruso T, Milano O, Fontanella C, Manfredi C (2002) Anal Bioanal Chem 374:173–178
9. Sandberg AS, Svanberg U (1991) J Food Sci 56:1330–1333
10. Engle-Stone R, Yeung A, Welch R, Glahn R (2005) J Agric Food Chem 53:10276–10284
11. South PK, Miller DD (1998) Food Chem 63:167–172
12. King A, Young G (1999) J Am Diet Assoc 99:213–218
13. Chung K-T, Wong TY, Wei C-I, Huang Y-W, Lin Y (1998) Crit Rev Food Sci Nutr 38:421–464
14. Brune M, Hallberg L, Skaanberg AB (1991) J Food Sci 56:128–167
15. Chou CL, Uthe JF, Guy RD (1993) J AOAC Int 76:794–798
16. Sadi BBM, Vonderheide AP, Becker JS, Caruso JA (2005) ACS Symp Ser 893:168–183
17. Wuilloud RG, Kannamkumarath SS, Caruso JA (2004) J Agri Food Chem 52:1315–1322
18. Siripinyanond A, Barnes RM (1999) J Anal Atom Spectrom 14:1527–1531
19. Stolpe B, Hassellov M, Andersson K, Turner DR (2005) Anal Chim Acta 535:109–121
20. Gimbert LJ, Andrew KN, Haygarth PM, Worsfold PJ (2003) Trends Anal Chem 22:615–633
21. Contado C, Blo G, Fagioli F, Dondi F, Beckett R (1997) Colloids Surf A 120:47–59
22. Bolea E, Gorriz MP, Bouby M, Laborda F, Castillo JR, Geckeis H (2006) J Chromatogr A 1129:236–246
23. Jackson BP, Ranville JF, Neal AL (2005) Anal Chem 77:1393–1397
24. Hurrell Richard F (2003) J Nutr 133:2973S–2977S
25. Evans WJ, Martin CJ (1991) J Inorg Biochem 41:245–252

Towards better understanding of *in vitro* bioavailability of iron through the use of dialysis profiles from a continuous-flow dialysis with inductively coupled plasma spectrometric detection†

Kunchit Judprasong,[ab] Atitaya Siripinyanond[a] and Juwadee Shiowatana*[a]

Received 11th January 2007, Accepted 19th March 2007
First published as an Advance Article on the web 11th April 2007
DOI: 10.1039/b700470b

A continuous-flow dialysis (CFD) method with an on-line inductively coupled plasma optical emission spectrometric (ICP-OES) simultaneous multielement measurement for the study of *in vitro* mineral bioavailability was previously reported. The method was based on a simulated gastric digestion in a batch system followed by a continuous-flow intestinal digestion—dialysis with on-line measurement of dialysed mineral concentration by ICP-OES. This study demonstrates how the dialysis profiles obtained could be exploited to understand differences of mineral dialysability and the effect of enhancers and inhibitors. The graphical plot of time-dependent cumulative dialysed mineral concentrations and percent dialysis was efficiently used for these purposes. Iron fortificants in various chemical forms were used to demonstrate the effect of their anionic parts on dialysability together with enhancement and inhibition effects from food acids.

Introduction

Mineral bioavailability has usually been determined by *in vivo* measurements. As an alternative to human and animal *in vivo* studies, the availability of minerals or trace elements has also been estimated by simple, rapid and inexpensive *in vitro* methods.[1] *In vitro* methods based on simulated gastrointestinal digestion with continuous-flow dialysis (CFD) were developed.[2–5] These methods measure the fraction of mineral accessible pool in diets which is of potential absorption. Although a true absorption is not determined, *in vitro* methods have frequently been used to predict and compare the bioavailability of minerals from different foods.[6,7]

In our previous reports, the CFD system was operated with flame AAS,[4] electrothermal AAS[5] and inductively coupled plasma optical emission spectrometric (ICP-OES)[8] detections for studies of minerals of nutritional importance (Ca, Mg, P, Fe and Zn). The objective of this study was to demonstrate the use of dialysis profiles to understand the differences of dialysability of minerals, taking the advantage of the time-dependent dialysis data obtained from the developed CFD method. Effects of the different chemical forms of mineral fortificant and the inhibition and enhancement effects from common components in food were elaborated.

Being carried out by an *in vitro* equilibrium batch dialysis method, previous studies provided no insight information to explain the dialysability results obtained. This work shows how to exploit the time-dependent dialysis information from the continuous-flow dialysis approach to clearly demonstrate the factors affecting *in vitro* bioavailability. Such investigation has been exemplified for Ca, Fe and Zn. In order to illustrate the concept, however, only Fe is described in this manuscript.

Experimental

Instrument and equipment

The detail of continuous-flow dialysis (CFD) system connected to a pH measurement module and ICP-OES detection unit has been described elsewhere.[8] A shaking water bath (Memmert®, Memmert GmbH, Germany), controlled at 37 ± 1 °C was used both for simulated gastric and intestinal digestions. The Orion SensorLink pH measurement system (ThermoOrion, USA), model PCM500, equipped with a PCMCIA slot and a personal computer, was used to monitor pH during digestion and dialysis.

Determination of iron by ICP-OES was performed using a SPECTRO CIROS CCD, axial configuration, equipped with a glass spray chamber (double pass, Scott-type) and a cross-flow nebuliser (all from SPECTRO, Kleve, Germany). The ICP-OES operating conditions were as follows: power 1350 W; nebuliser gas flow 1 L min^{-1}; and auxiliary gas flow 12 L min^{-1}. Selected emission lines were: Fe, 238.204 (II), 239.562 (II) and 259.940 (II). Emission lines for internal standards were: Y, 320.332 (II), 371.030 (II) and 442.259 (II) and Sc: 256.023 (II), 361.384 (II) and 440.037 (II) nm.

Reagents and solutions

The enzymes: pepsin (P-7000, from porcine stomach mucosa); pancreatin (P-1750, from porcine pancreas) and bile extract (B-6831, porcine) were from Sigma (St. Louis, Missouri, USA). The preparation procedures of the digestive enzyme

[a] *Department of Chemistry, Faculty of Science, Mahidol, 66 2 2015122, Thailand. E-mail: scysw@mahidol.ac.th*
[b] *Institute of Nutrition, Mahidol University, Salaya, Putthamonthon, Nakorn Pathom, 73170, Thailand. E-mail: nukjp@mahidol.ac.th*
† Presented at the Second Asia–Pacific Winter Conference on Plasma Spectrochemistry, Bangkok, Thailand, November 27–December 2, 2006.

pepsin, pancreatin bile extract (PBE) have been described elsewhere.[4]

Three sets of stock solution containing multi-element standards (QCS 01-5 at 100 μg mL^{-1}), Y (ICP-69N-1 at 1000 (μg mL^{-1}) and Sc (ICP-53N-1 at 1000 (μg mL^{-1}); as internal standards, were from Accutrace™ (AccuStandard®, Connecticut, USA). Standard solutions were prepared immediately before use by dilution of stock standard with 2% HNO_3.

Sample preparation

Five iron fortificants including iron(II) sulfate (Ajax Co. Ltd., Aubern, Australia), iron(II) fumarate (Vicky Consolidate Co. Ltd., Bangkok, Thailand), sodium iron(III) ethylenediaminetetraacetic acid (Akzo Nobel Functional Chemicals Co. Ltd., Arnhem, The Netherlands), iron(II) lactate, iron(III) ammonium citrate (Dr Paul Lohmann® Co. Ltd., Emmerthal, Germany) were investigated. The iron concentration for simulated gastrointestinal digestion experiment was approx. 1 mg metal mL^{-1}.

Ascorbic acid and citric acid (Fisher Scientific, Leicestershire, England) were selected to study enhancement of mineral absorption at molar ratio of enhancer to mineral of 3 : 1. For inhibition experiments, phytic acid (Sigma, USA), tannic acid (Fluka, Steinheim, Germany) and oxalic acid (BDH, Poole, England) were used at the same molar ratio of 3 : 1.

Simulated gastrointestinal digestion procedure and determination of dialysability

To study *in vitro* bioavailability of minerals, an *in vitro* gastric digestion was performed in a batch system (mimicking digestion in the stomach where no mineral absorption takes place), followed by an intestinal digestion in a CFD system. The CFD in the intestinal digestion step enables dialyzable components to be continuously removed for element detection. Gastric digestion was performed according to the procedure of Miller.[1] Dried samples were accurately weighed (0.5–1.0 g), mixed with 10 g of Milli-Q water, adjusted to pH 2.0 with 6 M HCl and adjusted to 12.5 g using pure water. To carry out pepsin–HCl digestion, 375 μL of pepsin solution (16% w/v) was added. The mixture was then incubated for 2 h at 37 ± 1 °C in a shaking water-bath. This mixture was further used in the following intestine digestion.

For intestinal digestion and dialysis, a CFD-ICP-OES system was used.[8] A portion of the mixture after gastric digestion (2.0 g) was injected into the flattened dialysis bag (MWCO 12–14 kDa) 10 mm flat wide, 17.6 cm in length (cellu-Sep®H1, Membrane Filtration Products, Texas, USA) in the dialysis chamber *via* a syringe. The dialysing solution of optimum concentration (3–9 × 10^{-4} M $NaHCO_3$) flowed through the chamber around the bag at 1 mL min^{-1} and the temperature was controlled at 37 ± 1 °C. A 625-μL freshly prepared pancreatin-bile extract (PBE) mixture containing 0.4% w/v pancreatin and 2.5% w/v bile extract was slowly injected after 30 min and dialysis was continued for an additional 2 h. The dialysable components were transported in the dialysing solution into the pH measurement cell and finally to the ICP-OES. To obtain good nebulisation performance and to ensure that iron remained soluble, the stream of dialysing solution was acidified by mixing with a stream of 4% nitric acid, which also contained 1 mg L^{-1} of Y and Sc, used as internal standards at 1.0 mL min^{-1}. A blank of gastrointestinal digestion-dialysis was also performed in each experiment.

The iron concentration of the dialysate (μg mL^{-1}) was obtained by on-line ICP-OES measurement with external calibration using standard solutions in $NaHCO_3$ of similar concentration to the dialysing solution. Total dialysed amount was determined by integration of the signal through the whole dialysis time using a computer program (Microcal Origin, Version 6.0). Dialysability in percent was calculated as follows: Dialysability (%) = 100 × D/C, where D = dialysed iron content (μg g^{-1} sample) and C = total iron content (μg g^{-1} sample).

Results and discussion

CFD-ICP-OES: Analytical recoveries and dialysability assessment

To validate the analytical procedure, the recoveries of iron were determined. The iron concentrations in the dialysate and the non-dialysed counterparts in the retentate were measured. Non-dialysed iron concentration in the retentate was determined after acid decomposition of the remains of sample suspension in the dialysis tube with subsequent ICP-OES detection. The total iron content of the sample was also determined after microwave decomposition of the sample. The summations of dialysed and non-dialysed amounts were compared with the total iron content. For all iron fortificants studied herein, the sum values of the dialysed and non-dialysed iron contents were close to the total values with recoveries ranging from 94.5 to 102.8%. Repeatability of percent dialysability of iron in all fortificants determined was better than 3% RSD.

Various chemical forms of iron fortificants provided significantly different iron dialysability. Iron(II) sulfate, iron(II) lactate, and iron(II) fumurate provided similar percent dialysability of 41–45%. Iron(III) ammonium citrate shows lowest percent dialysability (24–26%). The protected iron compound, NaFe(III)EDTA, gave the highest percent dialysability (79–83%). This phenomena can be explained by high stability constants of iron–EDTA complexes having the value log K of 25.7 for Fe(III) and 14.3 for Fe(II).[8,9] Formation of complexes prevents iron(III) in food from precipitating when pH rises resulting in high dialysability.

Dialysis profiles

While a batch dialysis system provides only a single value of dialysed amount at equilibrium, the continuous-flow dialysis system (CFD) offers both dialysed amount and time-based dialysis profile information. Dialysis profiles and pH change (Fig. 1 and 2, upper frame) and time-dependent cumulative plot of dialysed iron amount (Figs. 1 and 2, lower frame) can be obtained from the continuous measurement of dialysed iron concentrations and pH. The pH change (right axis of upper frame) from approx. 2.0 of the gastric digest to *ca.* 5.0 within 30 min of intestinal digestion and to *ca.* 7.0–7.5 after 1 h was close to what occurs in the human gastrointestinal tract. The

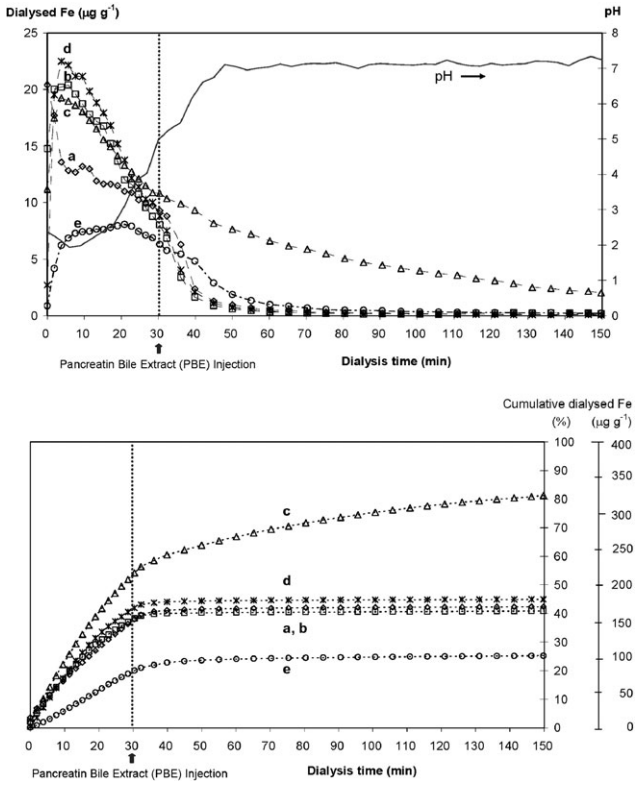

Fig. 1 Dialysis profiles of iron with pH change (upper frame) and corresponding cumulative plots (lower frame) for different chemical forms of iron fortificants: (a) iron(II) sulfate, (b) iron(II) fumarate, (c) NaFe(III)EDTA, (d) iron(II) lactate and (e) iron(III) ammonium citrate.

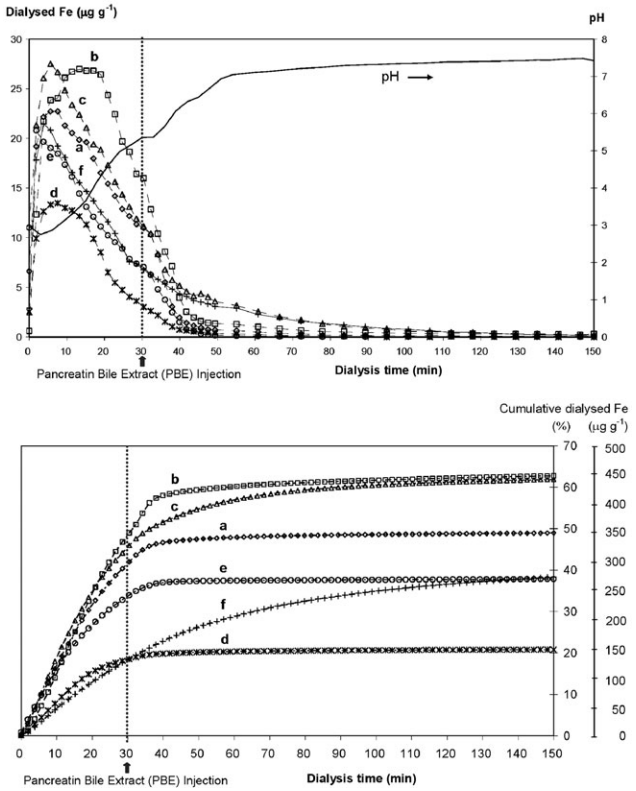

Fig. 2 Dialysis profiles of iron(II) sulfate with enhancers and inhibitors (upper frame) and their cumulative plots and percentage dialysis (lower frame): (a) $FeSO_4$ only; (b), (c), (d), (e), (f) for $FeSO_4$ with ascorbic, citric, phytic, tannic and oxalic acids, respectively.

graphical plot of dialysed iron concentration with respect to the dialysis time offers kinetic information of dialysis. The cumulative dialysed iron (Fig. 1 and 2, lower frame) increased before PBE injection, gradually increased after PBE injection and finally became constant. The slope of this graphical plot could demonstrate the rate of dialysis process. From this plot (Fig. 1, lower frame), iron fortificants can be divided into three groups according to their dialysability (low at 25% for iron(III) ammonium citrate; medium at 41–45% for iron(II) sulfate, iron(II) fumarate, iron(II) lactate; and high at 81% for NaFe(III)EDTA). The slopes are distinguished in two parts, before and after PBE injection at 30 min (Fig. 1, lower frame). The low dialysability (trace (e)) resulted from small slope before 30 min and almost zero thereafter. The medium dialysability (traces (a), (b) and (d)) can be seen to originate from higher slope before 30 min and almost zero thereafter. The high dialysability (trace (c)) was obtained from high slope before 30 min and small slope thereafter. The conversion of Fe(II) to $Fe(OH)_3$ is preferred at pH above 4.[10] Therefore, the dialysability of all studied iron fortificants ceased after 30 min (pH $\sim$ 5) except that of the protected compound NaFe(III)EDTA.

Effect of enhancers and inhibitors on iron dialysability

Many organic acids have been reported to show enhancement (ascorbic,[11–15] citric acids[16,17]) and inhibition (phytic, tannic and oxalic acids) effects. These compounds were used for the study of effect of enhancer and inhibitor on iron dialysability.

Fig. 2 (upper frame) shows profiles of iron dialysability of iron(II) sulfate with some enhancers (ascorbic and citric acids) and inhibitors (phytic, tannic and oxalic acids) at molar ratio of enhancer/inhibitor and iron between 3 : 1 to 4 : 1 (as used by Lynch and Stoltzfus[18]). Dialysis profiles of iron(II) sulfate were obviously affected by the presence of additives. The dialysis profile of iron(II) sulfate with ascorbic acid added at molar ratio of ascorbic acid to iron of 3 : 1 remarkably shows higher degree of dialysis in the first 30 min of dialysis. This is probably because ascorbic acid can decrease the transformation rate of iron(II) to iron(III) when pH increases. Iron(III) can be reduced by ascorbic acid only when the pH is below a limit, somewhere between pH 6.0 and 6.8. Above that pH limit, ascorbic acid is no longer an effective reducing agent for Fe(III).[19] In addition, ascorbic acid can form soluble complexes with iron at low pH that makes it remain soluble and absorbable at a more alkaline duodenal pH. Higher pH favors the conversion of Fe(II) to $Fe(OH)_3$. The reduction rate of iron(III) by ascorbic acid decreases markedly as the pH increases. Dialysability of iron(II) sulfate with ascorbic acid ceased at pH >6 (Fig. 2, upper frame). The dialysis rates (at 0–40 min, pH <6) of iron(II) sulfate with ascorbic and citric acids added were higher than that of iron(II) sulfate alone (Fig. 2, lower frame). The cumulative plots of iron(II) sulfate with and without enhancers and inhibitors are clearly distinguished.

The dominant increasing effect was observed before PBE injection in the case of ascorbic acid while citric acid showed significant effect after PBE injection. This is due to the chelating property of citric acid that presumably occurs through its carboxylic and hydroxyl groups, preventing iron from formation of insoluble iron hydroxides.[10] The stability constant (log *K*) of citric acid with Fe(II) and Fe(III) are 3.2 and 11.8, respectively.[9] So, the dialysability of the citrate complex of Fe(III) at pH >5 gradually increased.

On the other hand, dialyses of iron(II) sulfate with phytic or tannic acids, well-known strong iron inhibitors, were dramatically lower than that of iron(II) sulfate, especially in the first 30 min of dialysis (Fig. 2(d) and (e)). Since phytate and tannate are negatively charged, they can react with positively charged Fe ions, leading to the inhibition effect. After PBE injection (pH >5), the dialysis profile of iron(II) sulfate with oxalic acid showed a gradual increase of dialysed iron (Fig. 2(f), lower frame). The stability constant (log *K*) of oxalate with Fe(III) is 9.4, with the effective stability constants at pH 5, 6 and 7 being 2.9, 4.7 and 6.1, respectively.[9] As a result, dialysis of the oxalate complex of Fe(III) continues even at pH >5. In conclusion, the descending order of the iron dialysability is $FeSO_4$ with ascorbic acid (63%) $\sim$ with citric acid (62%) $>$ $FeSO_4$ only (49%) $>$ with oxalic acid (41%) $>$ with tannic acid (38%) $>$ with phytic acid (21%).

Conclusions

The CFD-ICP-OES-pH system was used for monitoring time-dependent dialysed minerals concentration and pH during dialysis. The system was applied to study the dialysability and effect of food components for iron fortificants. The mechanisms of enhancement and inhibition were investigated for the first time by a dynamic dialysis system. Dialysis profiles and their cumulative plots showed the changes of dialysis in the simulated intestinal digestion as affected by other food components. Such study is not possible using a batch dialysis system. The proposed approach is anticipated to be a useful tool to evaluate bioavailability of food or even non-food components consumed by humans.

Acknowledgements

The authors are grateful for financial support from the Thailand Research Fund and Center for Innovation in Chemistry: Postgraduate Education and Research Program in Chemistry, Higher Education Development Project, Ministry of Education.

References

1 D. D. Miller, B. R. Schricker, B. S. Rasmussen and D. Van Campen, *Am. J. Clin. Nutr.*, 1981, **34**, 2248–2556.
2 M. G. E. Wolters, H. A. W. Schreuder, G. Van Den Heuvel, H. J. Van Lonkhuijsen, R. J. J. Hermus and A. G. J. Voragen, *Br. J. Nutr.*, 1993, **69**, 849–861.
3 L. H. Shen, J. Luten, H. Robberecht, J. Bindels and H. Deelstra, *Z Lebensm.-Unters. -Forsch.*, 1994, **199**, 442–445.
4 J. Shiowatana, W. Kitthikhun, U. Sottimai, J. Promchan and K. Kunajiraporn, *Talanta*, 2006, **68**, 549–557.
5 J. Promchan and J. Shiowatana, *Anal. Bioanal. Chem.*, 2005, **382**, 1360–1367.
6 M. J. Roig, A. Alegria, R. Barbera and M. J. Lagarda, *Food Chem.*, 1999, **65**, 353–357.
7 K. J. H. Wienk, J. J. M. Marx and A. C. Beynen, *Eur. J. Nutr.*, 1999, **38**, 51–75.
8 K. Judprasong, M. Ornthai, A. Siripinyanond and J. Shiowatana, *J. Anal. At. Spectrom.*, 2005, **20**, 1191–1196.
9 T. E. Furia, in *CRC Handbook of Food Additives*, CRC Press, Boca Raton, FL, USA, 2nd edn, 1980.
10 S. Salovaara, A.-S. Sandberg and T. Andlid, *J. Agric. Food Chem.*, 2003, **51**, 7820–7824.
11 L. Hallberg, M. Brune and L. Rossander, *Hum. Nutr. Appl. Nutr.*, 1986, **40**, 97–113.
12 B. Nayak and K. M. Nair, *Food Chem.*, 2003, **80**, 545–550.
13 S. Salovaara, A.-S. Sandberg and T. Andlid, *J. Agric. Food Chem.*, 2003, **51**, 7820–7824.
14 L. Davidsson, P. Galan, P. Kastenmayer, F. Cherouvrier, M. A. Juillerat, S. Hercberg and R. F. Hurrell, *Pediatr. Res.*, 1994, **36**, 816–822.
15 D. Siegenberg, R. D. Baynes, T. H. Bothwell, B. J. Macfarlane, R. D. Lamparelli, N. G. Car, P. Macphail, U. Schmidt, A. Tal and F. Mayet, *Am. J. Clin. Nutr.*, 1991, **53**, 537–541.
16 M. Gillooly, T. H. Bothwell, J. D. Torrance, A. P. MacPhail, D. P. Derman, W. R. Bezwoda, W. Mills, R. W. Charlton and F. Mayet F, *Br. J. Nutr.*, 1983, **49**, 331–342.
17 D. P. Derman, D. Ballot, T. H. Bothwell, B. J. MacFarlane, R. D. Baynes, A. P. MacPhail, M. Gillooly, J. E. Bothwell, W. R. Bezwoda and F. Mayet F, *Br. J. Nutr.*, 1987, **57**, 345–353.
18 S. R. Lynch and R. J. Stoltzfus, *J. Nutr.*, 2003, **133**, 2978S–2984S.
19 Y.-H. P. Hsieh and Y. P. Hsieh, *J. Agric. Food Chem.*, 1997, **45**, 1126–1129.

Available online at www.sciencedirect.com
SCIENCE DIRECT
Talanta 68 (2006) 549–557
Talanta
www.elsevier.com/locate/talanta

Dynamic continuous-flow dialysis method to simulate intestinal digestion for in vitro estimation of mineral bioavailability of food

Juwadee Shiowatana*, Wutthika Kitthikhun, Upsorn Sottimai, Jeerawan Promchan, Kanokwan Kunajiraporn

Department of Chemistry, Faculty of Science, Mahidol University, Rama VI Rd., Bangkok 10400, Thailand

Available online 13 June 2005

Abstract

A system for dynamic continuous-flow dialysis during intestinal digestion for an in vitro simulation of gastrointestinal digestion is presented as an alternative to human and animal in vivo methods for estimation of the bioavailability of minerals. The method is based on the in vitro batch dialysis method described by Miller, which was developed into a continuous-flow system of a simple design to perform dynamic dialysis in the intestinal digestion stage. A flow dialysis system has the advantages of simulation being close to in vivo physiological conditions because pH change during dialysis is gradual and dialyzed components are continuously removed. The proposed new design performed dialysis during a continuous flow of dialyzing solution ($NaHCO_3$) around a dialysis bag containing peptic digest, which is placed inside a glass dialysis chamber. Gradual change of dialysis pH, similar to that occurring in the gastrointestinal tract, was obtained by optimization of flow rate and concentration of $NaHCO_3$. The dialysate collected in fractions was analyzed to determine dialyzed minerals and pH change in the course of dialysis. The method was tested by determination of calcium bioavailability of powder milk and calcium carbonate tablets.

Keywords: In vitro method; Bioavailability; Continuous-flow

1. Introduction

The total concentration of a mineral micronutrient in food does not provide information about its bioavailability. Speciation of a micronutrient or the determination of its chemical forms in food and in the gastrointestinal tract is essential to the understanding and the prediction of its availability for absorption [1]. This is often difficult to perform. Nutrient bioavailability has usually been estimated by in vivo human study. In vivo experiments, however, are time consuming and very expensive and often give variable results caused by uncontrollable physiological factors. Laboratory in vivo experiments in animals are sometime used as a model for human. Experiments with animals are less expensive but are limited by uncertainties with regard to differences in metabolism between animals and human. As an alternative to in vivo human and animal studies, nutrient bioavailability has also been estimated through in vitro methods [2–9]. These methods have gained popularity because of their simplicity, precision, speed of analysis and relatively low cost.

Interest in development of in vitro methods for estimating bioavailability of essential mineral elements dates back to at least the early 1930s [2]. These methods provide insights on minerals and trace element nutrition that are not achievable by human or animal experiments. The earliest trial [2] assumed ionizable minerals as potentially available and determined ionizable iron in food by extracting with complexing agents such as α,α′-dipyridyl and bathophenanthroline. Another approach attempted to simulate gastrointestinal digestion conditions and determined soluble or dialyzable minerals [3–9]. Particularly, the in vitro method developed in 1981 by Miller et al. [5] has been reported to provide availability measurements that correlate well with in vivo studies for iron. This method has been the basis for several in vitro methods for estimation of the bioavailability of iron and other minerals such as calcium and zinc [10,11]. The in vitro method

* Corresponding author. Tel.: +66 2 201 5124; fax: +66 2 354 7151.
E-mail address: scysw@mahidol.ac.th (J. Shiowatana).

0039-9140/$ – see front matter © 2005 Elsevier B.V. All rights reserved.
doi:10.1016/j.talanta.2005.04.068

involves a simulated gastrointestinal digestion with pepsin at pH 2 for 2 h during the gastric stage and with a mixture of pancreatin and bile salts along with a gradual pH change from 2 to 7 during the intestinal stage. The proportion of the compounds diffusing across a semipermeable membrane during the intestinal stage is used as a prediction of the elemental bioavailability.

In Miller's method, equilibrium dialysis is performed to obtain dialyzable compounds during intestinal digestion. The drawback is that dialyzed components are not removed during dialysis, as occurred in the real situation of the digestive tract. This may cause lower dialyzability. Therefore, a modified continuous dialysis in vitro method was developed by Minihane et al. [12] in which dialyzed components were removed continuously. The model developed by Minihane et al. used an Amicon stirred cell for continuous dialysis. The pH was adjusted gradually over a 30 min period from 2.0 to 7.0 before dialysis was started. Minihane's method was further modified by Shen et al. [13] to obtain a gradual pH change during the dialysis instead of adjusting the pH before dialysis. Shen et al. performed continuous dialysis by introducing a gradual pH adjustment using a small dialysis bag filled with an amount of $NaHCO_3$ equivalent to the predetermined titratable acidity of the peptic digest. The dialysis was carried out in a vessel under a pressure of 50 psi.

Wolters et al. [9] developed an in vitro method for continuous dialysis of minerals and trace elements based on a hollow-fiber system. The hollow-fiber system for continuous dialysis consists of a reaction vessel placing in a water bath at 41 °C. The food suspension in this vessel is pumped via a peristaltic pump through a suction tube into the hollow-fiber membrane. A fine filter cloth stretched across the inlet of the hollow-fiber and a magnetic stirrer was used to prevent clogging of the hollow-fiber by large particles. Components in the suspension that could pass through the hollow-fiber membrane were dialyzed and collected in a plastic bottle for subsequent analysis. That part of the suspension that could not pass through the hollow-fiber membrane was pumped back into the reaction vessel where these components could be digested further and recirculated into the hollow-fiber for complete dialysis.

A multicompartmental computer controlled simulated gastrointestinal digestion system has been developed [14] and applied [15,16] for evaluation of bioavailability. The system consists of several successive compartments to simulate the digestion in the stomach, duodenum, jejunum and ileum. Compartments are connected by peristaltic valve pumps to regulate the transfer of digestive enzymes. The system was also equipped with rotary pumps, syringe pumps for water pressure and secretion controls. Because the model aimed to mimic the whole GI-tract from stomach to ileum, it was rather complicated and not easy to perform. A simple method to access maximum bioaccessibility based on flow injection leaching of food sample by artificial saliva, gastric juice and intestinal juice was recently developed [17]. The method has the advantages of rapidity and simplicity. However, because leaching was accomplished in only a few minutes, the food sample may only be partially digested and leached.

In the present study, a simple setup for continuous-flow dialysis to perform an in vitro simulated intestinal digestion was developed. Considering that mineral absorption takes place mainly at the intestinal digestion stage [5], this setup was designed for dialysis in the intestinal digestion stage to occur by a continuous flow of dialyzing solution (dilute $NaHCO_3$ solution) around the dialysis tubing containing the gastric digestate. The gastric digestion was performed in a batch manner to effect high sample throughput because a large number of samples could be digested at the same time. In the simulated intestinal digestion stage, gradual change of pH, similar to that occurring in the intestinal tract, was obtained by optimization of flow rate and concentration of $NaHCO_3$. The dialysate collected in fractions was analyzed to determine the amount of dialyzed minerals. The graphical plot of dialyzed minerals with time of dialysis provides kinetic information of the dialysis process. The feasibility of the developed system was tested by applying it to evaluate dialyzability of calcium in calcium carbonate tablets and powder milk.

2. Experimental

2.1. Design and setup of continuous-flow dialysis system

A continuous-flow dialysis system was designed to serve three objectives: a gradual pH change at the early stage of dialysis, a convenient means of addition of enzymes at will and continuous removal of dialyzable components during dialysis.

The proposed dialysis system is presented schematically in Fig. 1. A dialysis chamber was designed to allow containment of a dialysis tubing, around which dialyzing solution could flow during dialysis. The chamber (ca. 20 cm in length and 0.8 cm inner diameter) and its cover were constructed in-house from borosilicate glass. Dialysis tubing MMCO 12,000–14,000 Da (Spectra/Por, Thomas Scientific, USA) was used. To prepare the dialysis chamber, a dialysis tubing

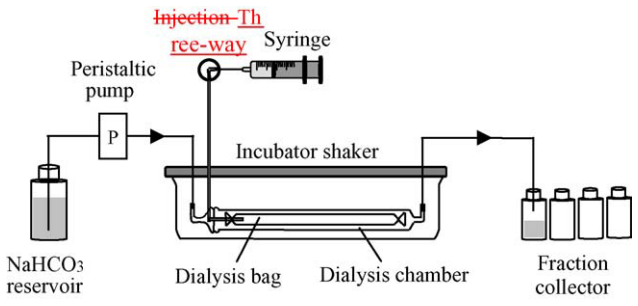

Fig. 1. Schematic diagram of the proposed continuous flow in vitro dialysis setup.

of 10 mm flat width and ca. 17.5 cm in length was tied at both ends, one end with a silicone tube (2 mm inner diameter and 5 cm long) inserted for the injection of a peptic digest sample and required enzymes. The other end of this silicone tube is pierced through an aperture in the chamber cover to allow convenient addition of a peptic digest aliquot and PBE mixture via a three-way valve by a 3 ml disposable syringe (both were purchased from a local medical equipment supplier). The cover was tightly sealed onto the chamber with a silicone gasket and a rubber band. The dialysis chamber was placed in a shaking water bath at $37 \pm 1\,^{\circ}C$. The dialyzing solution ($NaHCO_3$) from the reservoir was pumped through the chamber using a peristaltic pump (Eyela, Model MP-3N, Japan). The dialysis flow can be adjusted between 0.5 and 10 ml min^{-1} but 1.0 ml min^{-1} was found to be optimal. Dialyzable components in the peptic digest suspension could pass through the dialysis membrane and collected in plastic collectors.

To perform dialysis, the prewashed [18] dialysis tubing is prepared as above. Before adding the peptic digest, the dialysis tubing is flattened to remove any air bubbles or liquid inside using a syringe connecting to the silicone tube insert. Peptic digest aliquot of 2.5 ml is then injected through the same silicone tube. The dialyzing solution of optimum concentration is flowed through at 1.0 ml min^{-1} or at the required flow rate.

2.2. Instrument and equipment

Determination of calcium by flame atomic absorption spectrometer (FAAS) was performed using a Perkin-Elmer Model 3100 equipped with deuterium background correction (CT, USA), providing a background corrected signal. The operating parameters for measurement of calcium were 422.7, 0.7 nm band width and air–acetylene flame. The calcium contents of the dialysate and digested samples were determined using standard addition method.

A pH meter of Denver Instrument Model 215 (USA) with a glass combination electrode was used for all pH measurements. Commercial standard buffers (Damstadt, Germany) of pH 4.00 ± 0.01 and 7.00 ± 0.01 were employed for the pH meter calibration.

An incubator shaker from Grant Instrument, Model SS40-D2 (Cambridge, England), was used to shake and incubate samples at $37 \pm 1\,^{\circ}C$.

2.3. Chemicals and test materials

Enzymes pepsin (P-7000, from porcine stomach mucosa), pancreatin (P-1750, from porcine pancreas) and bile extract (B-6831, porcine) were from Sigma (St. Louis, MO, USA). Ca standard solution (1000 mg l^{-1}) was a certified NIST standard.

A pepsin solution was prepared by dissolving 0.16 g pepsin (P-7000, from porcine stomach mucosa) in 1 ml of 0.1 M of hydrochloric acid.

A pancreatin–bile extract (PBE) mixture was prepared by weighing 0.004 g pancreatin and 0.025 g bile extract into a beaker and dissolving in 5 ml of 0.001 M sodium bicarbonate. The concentration of sodium bicarbonate in PBE solution was prepared at 0.001 M so that addition of PBE (after 30 min of intestinal digestion) will not disturb the pH change already optimized.

Calcium carbonate tablets (dietary supplement) were from Vitamin World (New York, USA). Milk samples were obtained from a local supermarket.

2.4. Determination the total calcium content in test materials and in residues after dialysis

To determine the total calcium content of each calcium source, the sample (250 mg for tablet and 10.0 g for milk powder) was dissolved by wet digestion with nitric acid to clear solution and diluted to 100.0 ml with pure water. For residues after dialysis, the food suspension after dialysis was transferred from the dialysis tube into a beaker (100 ml) and rinsed with two aliquots (3 ml each) of 0.01 M EDTA washing and two aliquots (10 ml each) of 2% HNO_3 washing before subsequent digestion to clear solution. The calcium contents were determined by flame atomic absorption spectrometry using standard addition method.

2.5. Peptic digestion and determination of titratable acidity

Peptic digestion was performed according to the procedure of Miller [5]. For calcium carbonate tablet, 90 ml of pure water was added to one tablet (250 mg) and the pH was adjusted to 2.0 with diluted HCl. For milk samples, powder milk of 10.0 g and pure water were added into a 100 ml flask and the mixture was shaken to obtain a suspension of 90 ml. The pH was adjusted to 2.0 by addition of a dilute HCl solution. To each sample suspension, 1.5 ml of pepsin solution was added and pH was adjusted again to 2.00 before the total volume was adjusted to 100.0 ml with pure water and the sample was incubated in a shaking water bath at 37 °C for 2 h. The pH was adjusted to 2.00 every 30 min.

Titratable acidity of peptic digest was determined by titrating a 2.5 ml aliquot to which 625 μl of PBE mixture was added, using standard 0.01 M NaOH as a titrant to a pH of 7.5.

2.6. In vitro equilibrium dialysis method

A 2.5 ml portion of the peptic digest was added into the dialysis bag in the dialysis chamber. Then, 3.0 ml of dialyzing solution containing an amount of $NaHCO_3$ equivalent to the titratable acidity of the peptic digest was injected into the dialysis chamber to fill the space in the chamber outside of the dialysis bag. The sample was incubated in a shaking water bath at 37 °C for 30 min before 625 μl of PBE mixture was added and incubation continued for an additional 2 h.

The dialysate was collected for subsequent determination of calcium content.

2.7. Optimization of flow rate and concentration of sodium bicarbonate for continuous-flow dialysis

Firstly, standard calcium solution in 0.01 M HCl was subjected to continuous-flow dialysis with varying flow rate of sodium bicarbonate. The sample (2.5 ml) was introduced into the flattened dialysis tubing. The dialysis was performed using 0.001 M sodium bicarbonate and the dialysate fractions were collected continuously for calcium determination. The flow rate that gave a complete dialysis in a short time without too much dilution effect of dialysate was considered as optimal.

Then, the optimal sodium bicarbonate flow rate was used to study the effect of its concentration on pH change. Peptic digest samples of varying titratable acidities, including peptic digest containing 0.01 M HCl, peptic digest containing 0.01 M HCl with 0.04 M ascorbic acid, and peptic digest containing 0.01 M HCl with 0.09 M ascorbic acid, were used. These peptic digests had pH values and titratable acidities of 2.0, 0.01 M; 2.0, 0.05 M and 2.0, 0.10 M, respectively. Each sample (2.5 ml) was subjected to the simulated intestinal digestion.

2.8. In vitro dialysis method with continuous flow

To start the simulated pancreatic intestinal digestion, a segment of dialysis tubing was prepared and placed in the dialysis chamber as described earlier. A silicone gasket was placed on the outlet, and the chamber cover was securely clamped. The chamber was connected to the sodium bicarbonate reservoir and the collector containers using tygon tubings and placed in a water bath. A 2.5 ml pepsin digest sample was injected into the dialysis tubing via the silicone tube insert using a syringe. The bath temperature was maintained at $37 \pm 1\,^{\circ}C$. The peristaltic pump was switched on to start the dialysis. The dialysis flow rate was 1 ml min^{-1}. The dialysate was collected at 10 ml intervals in plastic containers for 30 min before a 625 μl freshly prepared PBE mixture was added and dialysis was continued for an additional 2 h. The dialysate fractions were subjected to FAAS measurement after all fractions were collected. Then, the dialyzed amount of an element was calculated by summation of the amounts in all dialysate fractions.

2.9. Calculation of dialyzability

The amount of dialyzed calcium is expressed as a percentage of the total amount present in the sample as follows:

$$\text{Dialyzability}\,(\%) = \frac{(D - B) \times 100}{W \times A}$$

where D and B are the total and blank amounts (μg), respectively, of mineral dialyzed, W the dry weight (g) of sample used for dialysis and A is the concentration of calcium in the dry sample (μg g^{-1}). For equilibrium dialysis, the dialyzed calcium is calculated as twice of the amount dialyzed when the volumes of the peptic digest and the dialyzing solution were equal because the dialyzed amount accounted for only one half of the dialyzable amount in equilibrium dialysis. When the volumes were not equal, correction was made accordingly.

3. Results and discussion

3.1. Design of continuous-flow system for in vitro determination of mineral bioavailability

As the absorption of minerals and trace elements is taking place in the earlier part of the small intestine, simulation of the conditions prevailing in the small intestine is the most critical step for in vitro methods aiming at prediction of the bioavailability of minerals and trace elements. Variation in the pH conditions in the course of intestinal digestion is a major cause of variability of results of dialyzability [13,19–21]. Therefore, this study has given particular attention to the process resulting in pH change and considered it important to provide a pH profile during dialysis corresponding to the dialysis profile. The dynamic in vitro methods developed by Miller [5], Minihane [12] and Shen et al. [13], Wolters et al. [9] and this study have slight differences in the pH change during dialysis and duration of dialysis as summarized in Table 1.

Optimization of the flow rate and concentration of dialyzing solution has been performed to achieve the following requirements for a close simulation of intestinal digestion in human:

1. Change of pH from 2.0 to about 5.0–6.0 in 30 min and to approximately 7.0–7.5 in 60 min and being constant thereafter.
2. Addition of digestive enzymes at required time via a three-way valve.
3. Continuous removal of dialyzed minerals from the dialysis system for determination.

Aiming at the above requirements, firstly a flow rate was selected. Then, the concentration of sodium bicarbonate was optimized.

Although the proposed dialysis system can be connected to the FAAS instrument for online detection, this study chose to collect the dialysate fractionwise (every 5 or 10 min) for subsequent calcium determination. By this way, dialysate samples are not totally consumed and can be kept for pH measurements and for repeated confirmation.

3.2. Selection of dialyzing solution flow rate

The peptic digestion was performed in pepsin solution at pH 2 in a batch system. For intestinal digestion, in contrast to

Table 1
A diagram comparing in vitro gastrointestinal digestion procedures

Item		Time (min) 0 30 60 90 120 150
1. pH adjustment and dialysis process		
(Miller) [5]	Place dialysis bag containing equivalent amount of $NaHCO_3$ in the digestion vessel; dialysis occurs through this dialysis bag	
(Minihane & Shen) [13]	Place a small dialysis bag containing equivalent amount of $NaHCO_3$ in an Amicon stirred cell; dialysis occurs through dialysis membrane at the bottom of the Amicon cell	
(This work)	Flow suitable concentration of $NaHCO_3$ to adjust pH and to continuously remove dialyzable minerals from peptic digest inside a dialysis tube	
2. Addition of PBE (same for all methods)		↓ PBE addition
3. pH change		
(Miller)		2.0 5.0 7.0
(Minihane & Shen)		2.0 7.0 7.0
(This work)		2.0 7.0 7.0
4. Dialysis process and duration of dialysis		
(Miller)	passive diffusion + equilibrium	
(Minihane)	diffusion under pressure of 50 psi + continuous removal of dialyzed minerals	
(Shen)	diffusion under pressure of 50 psi + continuous removal of dialyzed minerals	
(This work)	dialyzing solution flow accelerated diffusion + continuous removal of dialyzed minerals	
5. Dialysis membrane		
(Miller)	MMCO 6,000-8,000 Da	
(Minihane)	MMCO 1,000 Da	
(Shen)	MMCO 1,000 Da	
(This work)	MMCO 12,000-14,000 Da	

the equilibrium dialysis method where samples are incubated in sodium bicarbonate solution of sufficient concentration, optimal concentration of sodium carbonate solution was continuously flowed around the dialysis tubing containing peptic digest and the dialysate was collected fractionwise. Thus, the optimal flow rate was selected and the effect of concentration of sodium bicarbonate on pH change during the course of dialysis was studied. In theory, a faster flow rate can facilitate removal of the dialyzed minerals from the system and can speed up the dialysis. However, a fast flow can result in dilution of the dialyzed minerals in the dialyzing solution. The optimal flow rate should assist fast transfer of dialyzable mineral through the membrane and should not cause too much dilution of the dialyzed minerals. The dialysis profiles were obtained at different flow rates as shown in Fig. 2. Dialysis profiles show the kinetics of dialyzable calcium penetrating through the semipermeable membrane for 0.5, 1.0 and 2.5 ml min^{-1} flow rates.

It can be seen that faster flow rate at 2.5 ml min^{-1} could remove dialyzable calcium faster and quantitative dialysis was obtained in about 50 min while slow flow rate at 0.5 ml min^{-1} took a longer time (ca. 100 min) to complete the removal. However, the concentration of calcium in dialysate was lower for the faster flow as a result of dilution effect. Therefore, 1.0 ml min^{-1} flow rate was considered as a compromised flow rate for this application because the dialysis could be completed within 1 h and the dilution effect was acceptable.

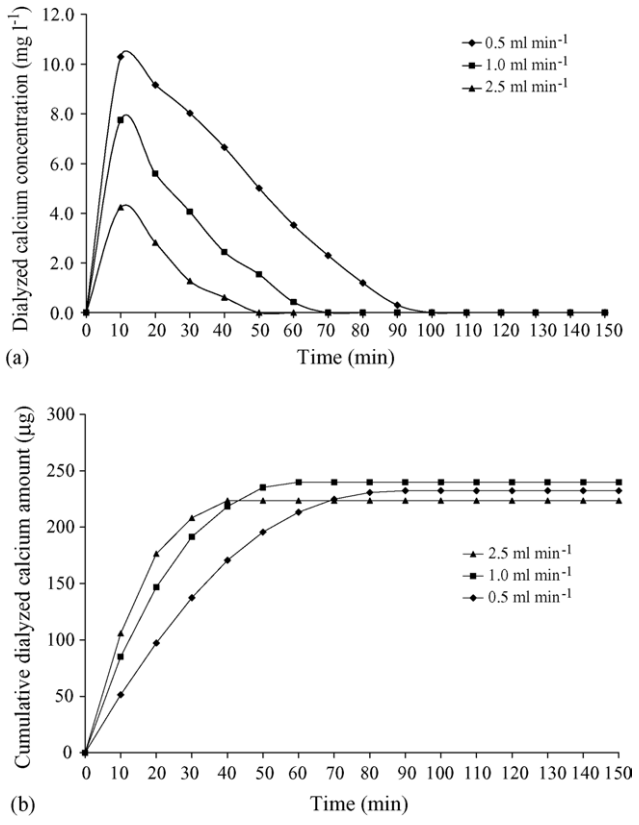

Fig. 2. Profiles of dialyzed amount (a) and cumulative dialyzed amount (b) of calcium at varying flow rate of dialyzing solution. Standard calcium (100 mg l^{-1}) 2.5 ml was used.

3.3. Optimization of concentration of sodium bicarbonate dialyzing solution

The concentration of dialyzing solution has to be optimized to obtain the required pH increase during the course of dialysis. It was found that $NaHCO_3$ concentration of 0.002 M was optimal for peptic digest of calcium carbonate tablets having titratable acidity of 0.05 M (Fig. 3b). The dialysis pH profiles for peptic digest of 0.01 and 0.1 M titratable acidities at various concentrations of dialyzing solution are also

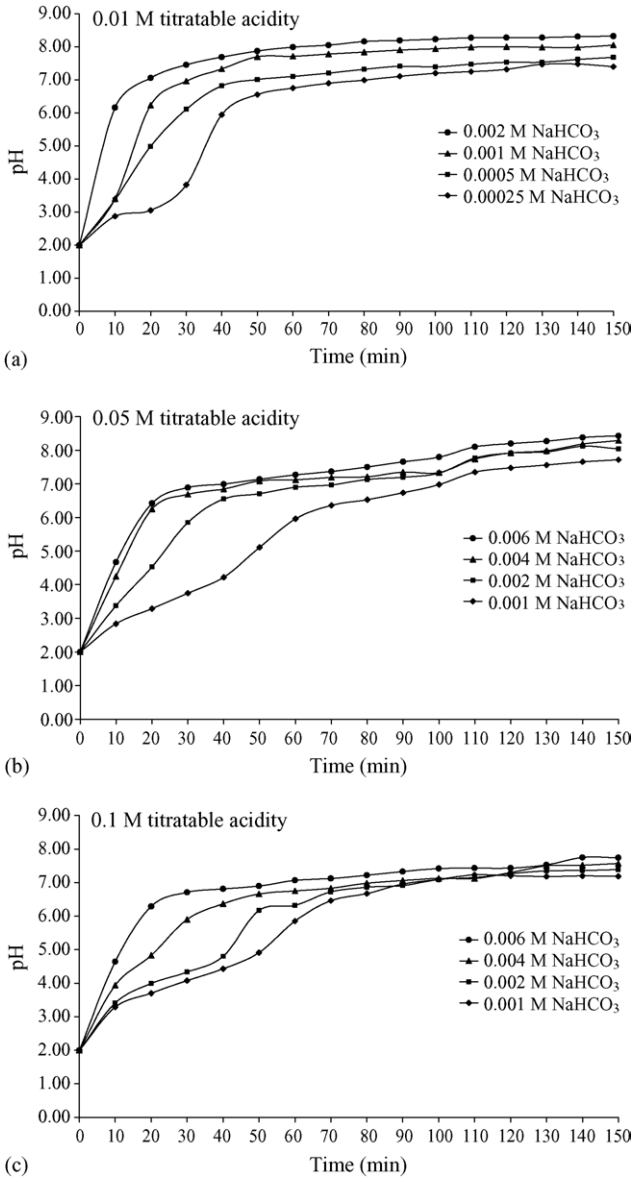

Fig. 3. Effect of concentration of dialyzing solution ($NaHCO_3$) on pH change during dialysis for peptic digests of different titratable acidities. Flow rate 1.0 ml min^{-1}.

Table 2
Analytical recovery of calcium for powder milk sample (three individual replicates are shown)

Sample	Dialyzed		Non-dialyzed		%Recovery
	Amount (mg kg^{-1})	%Dialyzability	Amount (mg kg^{-1})	%Remaining	
Powder milk-based formula	4680	68.1	1800	26.2	94.3
	4500	65.4	2270	33.1	98.4
	4780	69.5	2080	30.3	99.8
Average	4650 ± 140	67.6 ± 2.1	2060 ± 240	29.9 ± 3.4	97.5 ± 2.9

Total calcium 6890 ± 120 mg kg^{-1}.

shown in Fig. 3a and c. From the results of Fig. 3, optimum concentration of dialyzing solution was found to show an approximate linear relationship with the titratable acidity and the following equation can be drawn:

$$\text{Optimum } NaHCO_3 \text{ concentration} = \frac{\text{titratable acidity in M}}{25}$$

The optimal $NaHCO_3$ concentration for more than 10 peptic digests of calcium carbonate tablet samples with different titratable acidities were calculated using the above equation and the pH profiles were found to demonstrate satisfactory pH change during dialysis. So this equation will be used to obtain appropriate concentration of dialyzing solution for calcium carbonate peptic digests. It should be noted that the above equation can be applied for calcium carbonate and other tablets, and may not be applied to other types of food digest. For peptic digests of powder cow milk, the optimum dialyzing solution was found to be one fiftieth of the titratable acidity in M. This difference is probably due to the higher concentration of suspended matter in peptic digest of powder cow milk which resulted in slow rate of mass transfer in the dialysis tube and across the dialysis membrane. Therefore, this should be determined when different new types of sample are to be studied.

3.4. Method validation by analytical recovery study

Since there is no reference materials providing bioavailability data available, validation of the proposed method can only be done by studying of analytical recoveries of the mineral of interest. A milk sample was subjected to the proposed analytical procedure to determine the dialyzable calcium in the dialysate and the non-dialyzable calcium in the retentate. The results are given in Table 2. It can be seen that percent dialyzability of calcium is reproducible and the percent recoveries are acceptable.

3.5. Application of the proposed method to estimate calcium dialyzability of calcium carbonate tablets and milk samples

As examples to show the applicability of the dialysis system developed, calcium dialyzability for calcium carbonate tablets and milk samples was studied. Table 3 shows the results of dialyzable calcium determined by the developed continuous-flow method and the equilibrium method together with some previously reported values.

Since there has not been an accepted standard procedure for in vitro method for estimation of bioavailability, different authors used different procedures or conditions in their work. Furthermore, components in the samples (especially for formulated milk, which may contain different additives)

Table 3
Comparison of percent bioavailability (or dialyzability) of calcium for milk samples and calcium carbonate by different authors and procedures

Sample	In vitro		In vivo	Ref.
	Continuous flow	Equilibrium		
Powder cow milk	42.7 ± 2.5[a]	16.3 ± 1.1[a] (32.6 ± 2.2)	–	This work
Powder milk-based formula	67.7 ± 2.1	–	–	This work
Cow milk	–	20.2 ± 1.4	–	[22]
Cow milk	–	17.0 ± 0.8	–	[18]
Milk-based formula	13.9 ± 2.6[b]	10.2 ± 0.7	–	[13]
Milk-based formula	4.3 ± 0.6[c]	–	–	[13]
Cow milk	–	–	46.3 ± 9.5	[23]
Whole milk	–	–	31 ± 3	[24]
Powder cow milk	–	–	37.4 ± 8.7	[25]
Calcium carbonate	72.8 ± 2.2[a]	32.4 ± 1.5[a] (64.8 ± 3.0)	–	This work
Calcium carbonate	–	–	43.0 ± 5.9	[25]
Calcium carbonate	–	–	39 ± 3	[24]

[a] $n = 3$, in brackets are corrected values as indicated in Section 2.9.
[b] By Shen's method.
[c] By Minihane's method.

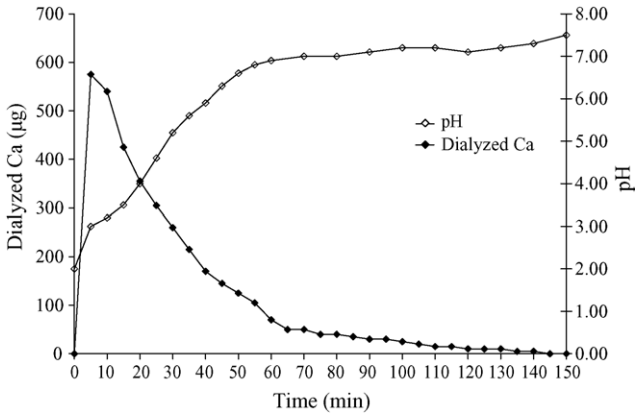

Fig. 4. Profile of dialyzed calcium and the pH change for peptic digest of calcium carbonate tablet by a continuous flow in vitro method.

may inhibit or promote dialyzability. This makes it rather impossible to compare results of different authors.

For milk samples, it was found in this work that dialyzability of calcium in powder cow milk was 32.6 and 42.7% for equilibrium and continuous-flow methods, respectively. The powder milk-based formula has a high dialyzability at 67.7%. Many authors have reported different values of bioavailability of calcium in milk ranging from 4.3 [13] to 46.3% [23]. This probably was attributed to the different sample compositions, procedures and conditions being used. For calcium carbonate tablet, our results of %dialyzability were very high at 64.8 and 72.8 for equilibrium and continuous-flow methods, respectively. Some authors indicated that incomplete disintegration and/or dissolution of the tablet could limit the degree of dialysis [26]. In this study, the peptic digest was seen to be clear after 2 h of peptic digestion at pH 2.0 indicating of solubilization very close to completion. This could possibly be the reason for high dialyzability. The dialyzability for equilibrium method gave slightly lower value probably due to loss during transfer of the dialysate from the dialysis chamber for AAS measurement, the step not required in the continuous-flow method. The in vivo result from a balance study [24,25] reported lower bioavailability values (43.0 and 39%).

Because in vitro dialysis method is a relative rather than an absolute estimation, the use of this method to estimate bioavailability has to be done with careful consideration of dialysis conditions [20,21] and report should serve as a relative evaluation under the same dialysis procedure and conditions. To confirm the similar conditions of dialysis being performed, this work considers monitoring of pH during dialysis a crucial necessity. Fig. 4 shows the dialysis profiles and the pH change during dialysis for calcium carbonate after peptic digestion. The pH profiles demonstrate pH change following the physiological conditions. The dialyzed calcium profiles show maximum value at the first dialysate fraction and gradually lower values similar to the profile of Fig. 2. The dialysis took about 60 min to complete. Similar observation was also evident for milk samples (not shown).

The continuous-flow dialysis profile and pH change are expected to be useful for comparative study of dialyzability of different foods and the study of the effects of food components on dialyzability. Such detailed investigation is not possible using the equilibrium dialysis system.

4. Conclusions

Simulated intestinal digestion has been developed for estimation of nutrient bioavailability. The continuous flow in vitro method is believed to be more representative of in vivo physiological conditions than that based on equilibrium dialysis because dialyzable components are continuously removed from the simulated intestinal digestion system during dialysis. In this study, a simple in vitro continuous-flow dialysis method was developed and used for estimation of calcium availability in comparison with the conventional in vitro equilibrium dialysis method. The most important part for successful simulation of the intestinal absorption was the pH adjustment during intestinal digestion. This was obtained by flowing dialyzing solution of appropriate concentration through a glass dialysis chamber containing the dialysis tubing with peptic digest inside. The optimum conditions for continuous flow in vitro method were a flow rate of 1.0 ml min^{-1} and varying concentration of dialyzing solution ($NaHCO_3$) depending on titratable acidity of the sample. In order that the PBE mixture would not drastically affect the pH change on its addition, PBE was prepared in 0.001 M sodium bicarbonate instead of 0.1 M as in the equilibrium dialysis. As a result, this proposed method achieved a gradual change of pH. The results from continuous-flow dialysis system not only can be used for estimating dialyzability of minerals but also provide dialysis profiles for detailed investigation. Since pH change during dialysis can greatly affect dialyzability due to precipitation for some elements, simultaneous monitoring of the pH change was also performed. The dialysis profiles of dialyzed mineral together with corresponding pH change can help understand the dialysis changes with time and the effect of food components on mineral dialyzability.

Although other elements, elemental detection systems and online measurement can be performed to demonstrate additional advantages of this proposed system, only calcium with a FAAS and off-line detection was attempted to prove the feasibility of the concept in this report. Future studies with online and other elemental detection systems such as inductively-coupled plasma spectrometry will be performed to cover more elements and to show the usefulness of the dialysis profiles obtained.

Acknowledgements

The authors are grateful for the financial support from the Thailand Research Fund and the Postgraduate Education and Research Program in Chemistry, Higher Education Development Project, Ministry of Education.

References

[1] L.H. Allen, Am. J. Clin. Nutr. 35 (1982) 783.
[2] L. Shackleton, R.A. McCance, Biochem. J. 30 (1936) 583.
[3] B.S. Narasinga Rao, T. Prabhavathi, Am. J. Clin. Nutr. 31 (1978) 169.
[4] S. Lock, A.E. Bender, Br. J. Nutr. 43 (1980) 413.
[5] D.D. Miller, B.R. Schricker, R.R. Rasmussen, D. Van Campen, Am. J. Clin. Nutr. 34 (1981) 2248.
[6] B.R. Schricker, D.D. Miller, R.R. Rasmussen, D. Van Campen, Am. J. Clin. Nutr. 34 (1981) 2257.
[7] T. Hazell, I.T. Johnson, Br. J. Nutr. 57 (1987) 223.
[8] R.F. Hurrell, S.R. Lynch, T.P. Trinidad, S.A. Dassenko, J.D. Cook, Am. J. Clin. Nutr. 47 (1988) 102.
[9] M.G.E. Wolters, H.A.W. Schreuder, G. Van Den Heuvel, H.J. Van Lonkhuijsen, R.J.J. Hermus, A.G.J. Voragen, Br. J. Nutr. 69 (1993) 849.
[10] P. Hocquellet, M.D. L'Hotellier, J. AOAC Int. 80 (1997) 920.
[11] J. Veenstra, M. Minekus, P. Marteau, R. Havenaar, Int. Food Ingredients 3 (1993) 1.
[12] A.M. Minihane, T.E. Fox, S.J. Fairweather-Tait, Proceedings of Bioavailability'93 Nutritional, Chemical and Food Processing Implications of Nutrient Availability, Part II, FRG, 1993, p. 175.
[13] L.H. Shen, I. Luten, H. Robberecht, J. Bindels, H. Deelstra, Lebensm Unters Forsch 199 (1994) 442.
[14] M. Minekus, P. Marteau, R. Havenaar, J.H.J. Huis in't Veld, Altern. Lab. Anim. (ATLA) 23 (1995) 197.
[15] M. Larsson, M. Minekus, R. Havenaar, J. Sci. Food Agric. 74 (1997) 99.
[16] C. Krul, A. Luiten-Schuite, R. Baan, H. Verhagan, G. Hohn, V. Feron, R. Havenaar, Food Chem. Toxicol. 38 (2000) 783.
[17] M. Chu, D. Beauchemin, J. Anal. At. Spectrom. 19 (2004) 1213.
[18] P. Chaiwanon, P. Puwastien, A. Nitithamyong, P.P. Sirichakwal, J. Food Comp. Anal. 13 (2000) 319–327.
[19] D.R. Van Campen, R.P. Glahn, Field Crop. Res. 60 (1999) 93.
[20] C. Ekmekcioglu, Food Chem. 76 (2002) 225.
[21] D. Bosscher, Z.L. Lu, R. Van Cauwenbergh, M. Van Callie-Bertrand, H. Robberecht, H. Deelstra, Int. J. Food Sci. Nutr. 52 (2001) 173.
[22] M.J. Roig, A. Alegria, R. Barbera, R. Farre, M.J. Lagarda, Food Chem. 65 (1999) 353.
[23] R.P. Heaney, C.M. Weaver, S.M. Hinders, B. Martin, P.T. Packard, J. Food Sci. 58 (1993) 1378.
[24] M.S. Sheikh, C.A. Santa Ana, M.J. Niocar, L.R. Schiller, J.S. Fordtran, N. Engl. J. Med. 317 (1987) 532.
[25] M.C. Kruger, B.W. Gallaher, L.M. Schollum, Nutr. Res. 23 (2003) 1229.
[26] M.J. Brennan, W.E. Duncan, L. Wartofsky, V.M. Butler, H.L. Wray, Calcif. Tissue Int. 49 (1991) 308.

JOURNAL OF AGRICULTURAL AND FOOD CHEMISTRY

Enhancement Effect Study of Some Organic Acids on the Calcium Availability of Vegetables: Application of the Dynamic in Vitro Simulated Gastrointestinal Digestion Method with Continuous-Flow Dialysis

JUWADEE SHIOWATANA,* SOPON PURAWATT, UPSORN SOTTIMAI, SUTTHINUN TAEBUNPAKUL, AND ATITAYA SIRIPINYANOND

Department of Chemistry, Faculty of Science, Mahidol University, Rama VI Road, Bangkok 10400, Thailand

The effect of added organic acids on the calcium availability of vegetables was investigated using the dialysis profiles obtained from an in vitro simulated gastrointestinal digestion with continuous-flow dialysis method. Citric acid was the most effective enhancer followed by tartaric, malic, and ascorbic acids. For amaranth, which has a low calcium availability (5.4%), a significant increase of availability was observed with increasing concentrations of all acids studied. With the continuous-flow dialysis approach, organic acids could be observed to promote the dialyzability even at an elevated intestinal pH. An enhancement effect from added organic acids was not clearly observed for Chinese kale, which itself contains a high amount of available calcium (52.9%).

KEYWORDS: Calcium availability; vegetables; organic acid; in vitro method; continuous flow

INTRODUCTION

Vegetables, especially green leafy vegetables, are known as a rich source of dietary calcium. Unfortunately, some vegetables with high contents of calcium show very low availability. The low calcium availability in vegetables was derived from the presence of some substances (phytate, oxalate, and dietary fiber components) which bind calcium to form unabsorbable compounds (*1*, *2*).

The effect of some organic acids on calcium availability has been documented. An enhancement effect by ascorbic acid (*3*) and citric acid (*4*, *5*) was reported. Many literature data on the effect of an enhancer or an inhibitor on the mineral availability are available. These studies were often carried out by adding the enhancer or inhibitor directly to foods followed by an in vitro or an in vivo availability evaluation. The in vitro method was widely performed by the method or modified methods of Miller (*6*) using a simulated gastrointestinal digestion with an equilibrium dialysis procedure. The methods involve enzymatic digestion with pepsin at pH 2 followed by digestion−dialysis in the presence of pancreatin−bile extract (PBE) at a gradual pH change from 2 to 7.5. The earlier conventional dialysis procedure provides a single value of the dialyzable amount of the element of interest at the equilibrium condition. It is simple and has been well accepted. However, in the equilibrium method, the dialyzed components are not continuously removed, as occurred in the intraluminal digestive tract, and therefore, this approach does not mimic the dynamic absorption process in the body and does not give information of time-dependent changes of dialysis during the course of gastrointestinal digestion.

Therefore, in vitro gastrointestinal digestion with continuous-flow dialysis procedures have been proposed as a closer simulation of the in vivo physiological conditions as opposed to that based on equilibrium dialysis, because dialyzable components are continuously removed from the digestion mixture during dialysis (*7*−*10*). The continuous-flow procedures also are readily adaptable to automatic computer control (*9*) and on-line detection (*11*, *12*). The computer-controlled in vitro dynamic system was applied for many case studies of the bioavailability of both minerals (*13*, *14*) and food mutagens (*15*).

Continuous monitoring of dialyzed minerals and pH change during dialysis provides profiles which are believed to be useful for the interpretation of enhancing or inhibiting effects. The aim of this work was to apply the dynamic in vitro simulated gastrointestinal digestion with continuous-flow dialysis method for the first time to demonstrate the use of dialysis profiles to investigate the effect of some organic acids on the calcium dialyzability of vegetables by looking into the time-dependent profiles obtained. Amaranth and Chinese kale were selected in this study to represent vegetables of low and high calcium availability, respectively (*16*). Four common organic acids, i.e., ascorbic, citric, tartaric, and malic acids, were studied.

EXPERIMENTAL DETAILS

Equipment and Materials. For measurement of calcium in dialysates, a Perkin-Elmer model 3100 flame atomic absorption/emission spectrometer (FAAS/FAES) was used. Calibration standards were

* To whom correspondence should be addressed. Phone: +66-2-201-5122. Fax: +66-2-354-7151. E-mail: scysw@mahidol.ac.th.

10.1021/jf062073t CCC: $33.50
Published on Web 11/08/2006

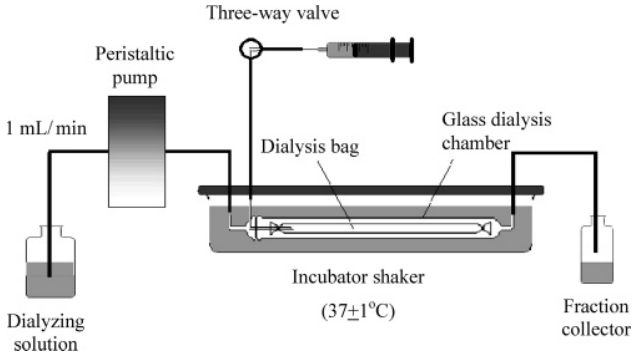

Figure 1. Diagram of the proposed continuous-flow in vitro dialysis system.

prepared in sodium bicarbonate of the same concentration as the dialyzing solution. The measurement was carried out with an air−acetylene flame. The calcium emission intensity was monitored at 422.7 nm with a 0.7 nm slit width.

A pH meter (Denver Instrument model 215, Colorado) with a glass combination electrode was used for all pH measurements. Commercial standard buffers (Merck, Darmstadt, Germany) of pH 4.00 ± 0.01 and 7.00 ± 0.01 were employed for the pH calibration. An incubator shaker from Grant Instrument, model SS40-D2 (Cambridge, England), was used to incubate the samples at 37 ± 1 °C.

Chemicals and Samples. The enzymes pepsin (P-7000, from porcine stomach mucosa), pancreatin (P-1750, from porcine pancreas), and bile extract (B-6831, porcine) were from Sigma (St. Louis, MO). A pepsin solution was prepared by dissolving 0.16 g of pepsin in 1 mL of 0.1 M hydrochloric acid and a PBE mixture by dissolving 0.004 g of pancreatin and 0.025 g of bile extract in 5 mL of 0.001 M sodium bicarbonate (*6*). Calcium standard solution (1000 mg/L) was prepared by dissolving an appropriate amount of calcium carbonate (Carlo Erba, Italy) in 1% (v/v) hydrochloric acid. The dialyzing solution was prepared by dissolving an appropriate amount of sodium bicarbonate in 1 L of purified water. The optimum concentration of sodium bicarbonate was determined from the titratable acidity, which was determined by titrating a 2.5 mL aliquot of peptic-digested sample to which 625 μL of PBE mixture was added, using standard 0.01 M NaOH as a titrant, to a pH of 7.5 (*10*). Ascorbic, malic, citric, and tartaric acids were obtained from Fluka Chemicals (Switzerland) and were confirmed to contain an undetectable amount of calcium at the concentrations being used.

Fresh amaranth, Chinese kale, and other vegetables were purchased from local markets and were cleaned and rinsed with purified water. Only the edible parts were then dried at 65 °C to constant mass and ground to store in a desiccator for use throughout the study to ascertain that similar vegetable lots were used.

Determination of the Total Calcium Content of Food Samples. A 0.5 g amount of sample was accurately weighed in a TFM vessel, and 10 mL of a HNO_3/H_2O_2 (3:2 v/v) mixture was added. Then acid dissolution was performed in a microwave digestion system (Milestone, model MLS-1200 Mega, Connecticut) according to the manufacturer's instructions. The clear solution was diluted with purified water to obtain a volume of 50.0 mL. The solution was then transferred to a polyethylene bottle. The calcium content was determined by flame atomic emission spectrometry using standard addition calibration.

Design and Setup of the Continuous-Flow Dialysis System (*10*). A continuous-flow dialysis (CFD) system was designed to serve three objectives as follows: to facilitate a gradual pH change at the early stage of dialysis (30 min), with the pH being maintained at 7.5 at the later stage (after 60 min), to provide a convenient means of addition of enzymes at the time and amount required, and to enable continuous removal of dialyzable components during dialysis.

The proposed dialysis system is presented schematically in **Figure 1**. A dialysis chamber was designed to allow containment of the dialysis tubing, around which the dialyzing solution could flow during dialysis. The chamber (ca. 20 cm in length and 0.8 cm inner diameter) and its covers were constructed in-house from borosilicate glass. Dialysis tubing of MWCO 12000−14000 (Spectro/Por, Thomas Scientific) was used. To prepare the dialysis chamber, dialysis tubing of 10 mm flat width and ca. 17.5 cm length was tied at both ends, one end with a silicone tube (2 mm inner diameter and 5 cm long) inserted for the injection of a peptic digest sample and required enzymes. The other end of this silicone tube was pierced through an aperture in the chamber cover to allow convenient addition of a peptic digest aliquot and PBE mixture via a three-way valve by a syringe. The cover was tightly sealed onto the chamber with a silicone gasket and a rubber band. The dialysis chamber was placed in a shaking water bath at 37 ± 1 °C. The dialyzing solution ($NaHCO_3$) from the reservoir was pumped through the chamber using a peristaltic pump (Eyela, model MP-3N, Japan) with a flow rate of 1.0 mL/min. Dialyzable components in the peptic digest suspension could pass through the dialysis membrane and be collected in plastic collectors.

Although the proposed dialysis system can be connected to the pH meter and elemental detection instrument for on-line detection, in this study we chose to collect the dialysate fractionwise for subsequent calcium determination. In this way, dialysate samples are not totally consumed and can be kept for further analyses or later confirmation.

Simulated Gastrointestinal Digestion Procedure with Continuous-Flow Dialysis. Simulated gastrointestinal digestion of food samples was carried out starting with peptic digestion with pepsin in a batch system, followed by pancreatic digestion with PBE in the CFD system (see the flow chart in **Figure 2**).

In the simulated peptic digestion step, a dried homogeneous vegetable sample (0.5 g) or cooked vegetable (equivalent to a 0.5 g dry mass) was suspended in 10 mL of purified water and adjusted to pH 2 with 6 M hydrochloric acid. The sample suspension volume was finally adjusted to 12.5 mL with purified water and spiked with 375 μL of pepsin solution. This digestion process was performed in an incubator shaker at 37 ± 1 °C for 2 h. The titratable acidity of the peptic digest was determined by titrating a 2.5 mL aliquot to which 625 μL of PBE mixture was added, using standard 0.01 M NaOH as a titrant, to a pH of 7.5. This titratable acidity was used for calculation of the optimal concentration of the dialyzing solution (*10*).

After the simulated peptic digestion, intestinal digestion with continuous-flow dialysis was carried out. The dialysis chamber was prepared as described earlier. Before use, the dialysis tubing was flattened to remove any air bubbles or liquid inside. Then, the 2.5 g peptic-digested sample was added via the three-way valve using a syringe connected to the silicone tube insert. The dialysis temperature was maintained at 37 ± 1 °C. The peristaltic pump was switched on to start the pancreatic digestion with a flow rate of 1 mL/min. The dialysate from the chamber was collected at 10 mL intervals in plastic vials for 60 min and then at 10 or 30 mL intervals for an additional 90 min. The freshly prepared PBE mixture (625 μL) was added into the dialysis bag by means of syringe injection via the three-way valve at 30 min. All dialysate fractions were subjected to pH measurement and calcium determination after completion of the pancreatic digestion.

Simulated Gastrointestinal Digestion Procedure with Equilibrium Dialysis. The peptic digestion was carried out similarly as mentioned above. Then a 2.5 mL portion of the peptic digest was added into the dialysis bag in the chamber of the dialysis system setup. However, instead of flowing the dialyzing solution, 3.0 mL of dialyzing solution containing an amount of $NaHCO_3$ equivalent to the titratable acidity of the peptic digest was injected into the dialysis chamber to fill the space in the chamber outside the dialysis bag. The sample was incubated in a shaking water bath at 37 ± 1 °C for 30 min before 625 μL of pancreatin−bile extract mixture was added and incubation continued for an additional 2 h. The dialysate was collected for subsequent determination of the calcium content.

Estimation of Calcium Availability. The amount of dialyzed calcium in a sample after the simulated gastrointestinal digestion was calculated from the summation of dialyzed calcium in all dialysate fractions and was expressed as a percentage of the total amount of calcium present in the sample:

$$\text{availability (\%)} = (D \times 100)/(WA)$$

where D = total amount of dialyzed calcium (μg), W = amount of sample used (g) as the dry mass of the original sample, and A = concentration of calcium in the original dry sample (μg/g).

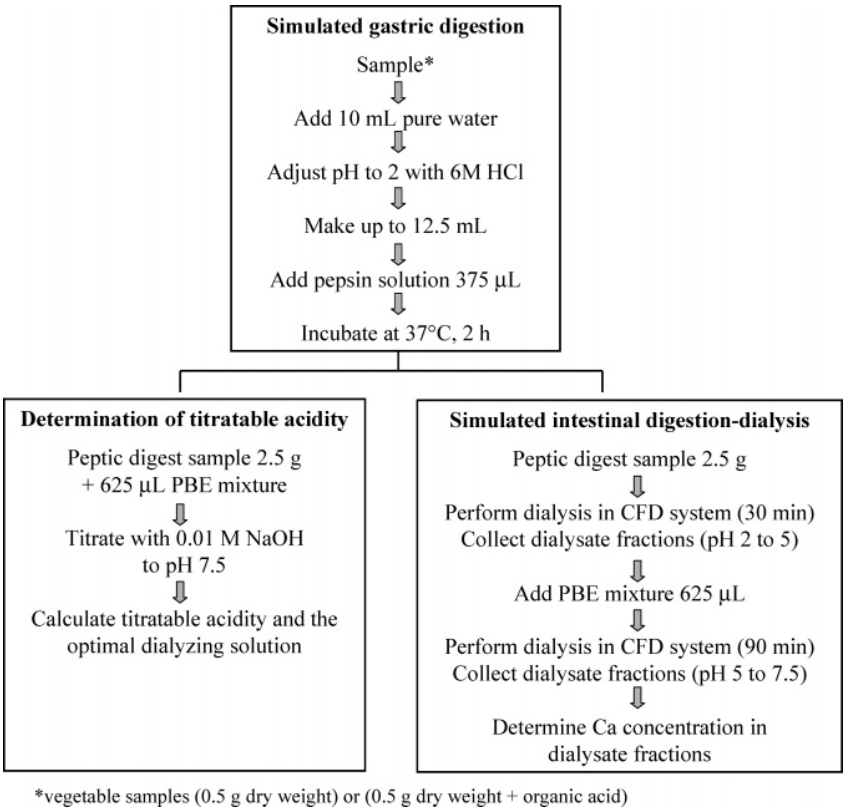

Figure 2. Flow chart of the simulated gastrointestinal digestion with continuous-flow intestinal digestion–dialysis.

RESULTS AND DISCUSSION

In Vitro Simulated Gastrointestinal Digestion: Equilibrium vs Dynamic Dialysis Approaches. The differences between the in vitro gastrointestinal dialysis with traditional equilibrium and the continuous-flow dialysis approaches are important to consider. Only a single value of the dialyzable amount of minerals at the equilibrium condition is obtained from the equilibrium dialysis procedure, whereas a time-dependent change of the dialyzed amount of mineral during the course of gastrointestinal digestion is obtained from the continuous-flow approach. A dynamic in vitro method with continuous removal of dialyzed components should be a better estimation of availability than the equilibrium in vitro method. Naturally, the results obtained from the two approaches are different, owing to the fact that the equilibrium method is based on the dialysis equilibrium of minerals between both sides of the dialysis membrane. Dialysis ceases when the concentrations of dialyzable components on both sides are equal. On the other hand, in the dynamic continuous-flow in vitro method, all the dialyzable components could possibly permeate through the membrane because fresh dialyzing solution was fed to the system continuously. To demonstrate this fact, standard 100 μg/mL calcium carbonate in 1% (v/v) HCl was subjected to the two dialysis procedures using the procedure described. The calcium availability as determined by the continuous-flow in vitro method was higher than that obtained from the equilibrium dialysis method (**Table 1**). The dialyzed amounts obtained from the equilibrium approach were found to be dependent on the volume ratio of the peptic digest and the dialyzing solution as summarized in **Table 1**. For a given case in which the volumes of the peptic digest and the dialyzing solution are equal (10 mL each), the dialyzed amount from the continuous-flow in vitro method was approximately 2 times that of the equilibrium in vitro method. In other words, the dialyzed amount accounted for only half of the dialyzable amount in the equilibrium dialysis. Since the continuous-flow approach provides the total dialyzable amount through continuous removal of dialyzable minerals, the results from the equilibrium dialysis should be corrected to match the value obtained from the continuous-flow dialysis procedure using the following equation:

$$D_{\text{corrected}} = D_{\text{uncorrected}}(V_s + V_d)/V_d$$

where $D_{\text{corrected}}$ (%) = the corrected D (%), $D_{\text{uncorrected}}$ (%) = the D (%) obtained from the amount dialyzed in the equilibrium dialysis, V_s = sample volume (mL), and V_d = dialyzing solution volume (mL).

This rationale was confirmed by examining the effects of the sample volume and dialyzing solution volume on the dialyz-

Table 1. Effect of the Sample Volume to Dialyzing Solution Volume Ratio (S:D) on Dialyzability in the Equilibrium Dialysis Method[a]

dialysis method	sample vol (mL)	dialyzing solution vol (mL)	S:D	D[b] (%) $D_{\text{uncorrected}}$ (%)	D[b] (%) $D_{\text{corrected}}$ (%)
equilibrium	10.0	20.0	0.5	28.1 ± 1.0	42.2 ± 1.5
	10.0	10.0	1.0	22.0 ± 1.1	44.0 ± 2.2
	10.0	5.0	2.0	12.6 ± 0.8	37.8 ± 2.4
continuous flow	2.5	flowing		41.2 ± 1.4	

[a] The sample was a 100 μg/mL (2.5 mL) standard calcium carbonate solution ($n = 3$). [b] D for the equilibrium method is provided as uncorrected values ($D_{\text{uncorrected}}$) and corrected values ($D_{\text{corrected}}$), while that of the continuous-flow method needs no correction. Each $D_{\text{corrected}}$ value shows no significant difference with the D obtained from the continuous-flow method as evaluated by the t test at $P = 0.05$.

Table 2. Total Calcium Content and Availability of Calcium from Various Vegetables As Determined by in Vitro Simulated Gastrointestinal Digestion with Continuous-Flow and Equilibrium Dialysis

		availability (%) ($n = 3$)			
			equilibrium in vitro method		
vegetable	total calcium concn (mg/g dried sample) ($n = 3$)	continuous-flow in vitro method[a]	uncorrected	corrected[b]	availability (%) (other researchers)
amaranth, leaves	26.7 ± 0.4	5.4 ± 0.4	3.0 ± 0.5	6.0 ± 1.0	4.1[c] (Kamchan et al. (*16*))
awltree, leaves	38.7 ± 0.6	10.1 ± 1.2	5.1 ± 1.0	10.2 ± 2.0	
cabbage, edible parts	4.5 ± 0.4	48.2 ± 1.3	21.6 ± 0.5	43.2 ± 1.0	64.9[d] (Weaver et al. (*20*))
Chinese kale, edible parts	16.1 ± 0.3	52.9 ± 1.1	22.2 ± 1.7	44.4 ± 3.4	58.8[d] (Weaver et al. (*20*))
cumin, leaves	23.6 ± 0.6	13.2 ± 0.6	5.5 ± 0.2	11.0 ± 0.4	
hairy basil, leaves	20.4 ± 0.5	31.2 ± 0.3	13.3 ± 0.9	26.6 ± 1.8	
Indian penny wort, leaves	15.3 ± 0.5	39.6 ± 0.7	17.1 ± 0.3	34.2 ± 0.6	
ivy gourd, leaves and tips	9.3 ± 0.6	38.4 ± 0.8	16.1 ± 0.6	32.2 ± 1.2	
kitchen mint, leaves	18.5 ± 0.4	33.9 ± 1.7	16.5 ± 1.6	33.0 ± 3.8	
betel, leaves	22.8 ± 0.5	2.25 ± 0.1	1.3 ± 0.2	2.6 ± 0.4	2.5[c] (Kamchan et al. (*16*))
sesbania, tender tips	10.1 ± 0.4	24.8 ± 0.2	10.1 ± 0.7	20.2 ± 1.4	
spinach, edible parts	10.3 ± 0.5	4.6 ± 0.5	1.9 ± 0.2	3.8 ± 0.4	4.6[d] (Peterson et al. (*19*))

[a,b] The correlation plot of data from the continuous-flow (*a*) and equilibrium (*b*) methods shows that $b = 0.853a + 0.638$, $r^2 = 0.991$. [c] Values from the in vitro method. [d] Values from the in vivo method.

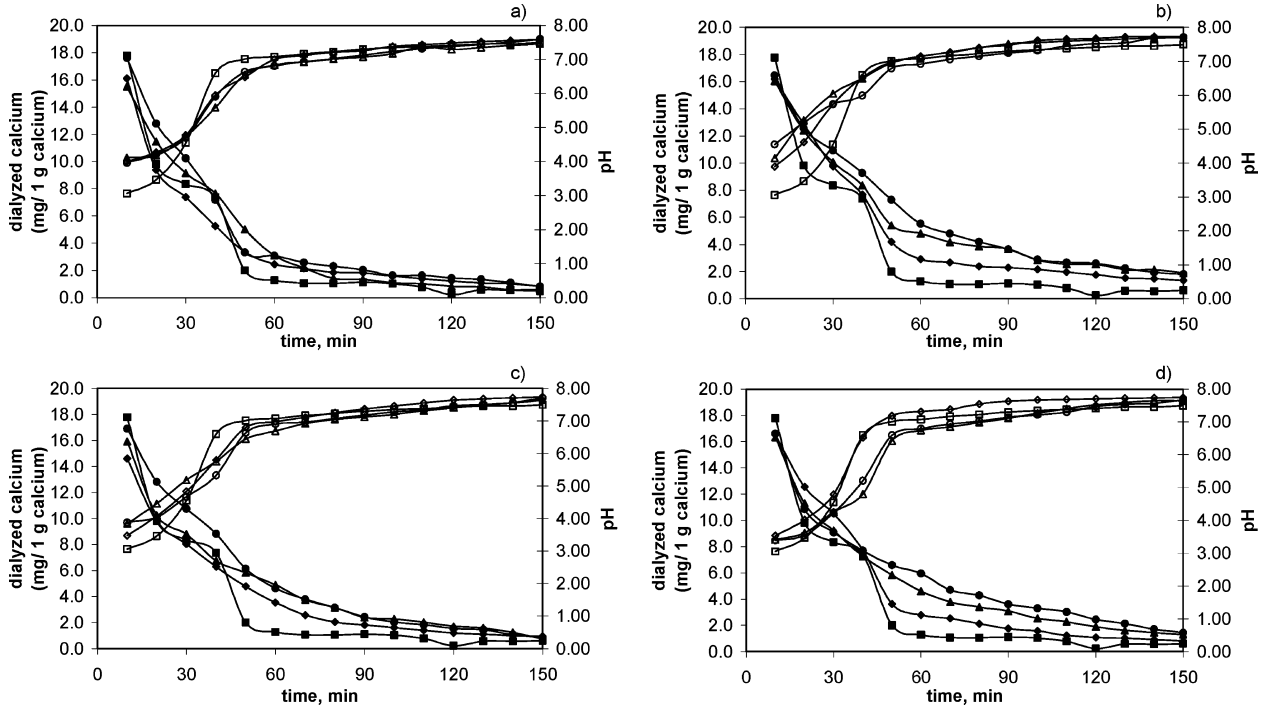

Figure 3. Dialyzed calcium and pH change during simulated intestinal digestion for amaranth with addition of varying concentrations of ascorbic acid (**a**), citric acid (**b**), malic acid (**c**), and tartaric acid (**d**), where ■, ◆, ▲, and ● represent amaranth with 0%, 1.0%, 2.5%, and 5% (w/w) acid, respectively. The corresponding pH profiles are presented with open symbols of the same type.

ability of a calcium standard as presented in **Table 1**, which shows a lower $D_{\text{uncorrected}}$ when the dialyzing solution volume is increased. $D_{\text{corrected}}$ gave results comparable with those of continuous-flow dialysis. This correction method should always be applied to get $D_{\text{corrected}}$, which is an accurate value expressing the dialyzable fraction for the equilibrium method.

In Vitro Availability of Calcium for Various Local Vegetables. The calcium availability of some vegetables as determined by the in vivo method has been reported (*16*−*20*). Total calcium and its availability of various local vegetables by an in vitro method based on continuous-flow dialysis and equilibrium approaches were determined, and the results are shown in **Table 2**. Some reported availability data are given in the last column for comparison. The results show that the corrected availability values of the equilibrium method were approximately 85% of the values obtained from the continuous-flow dialysis as calculated from the correlation plot ($b = 0.853a + 0.638$, $r^2 = 0.991$). The slightly lower availability values (%) from the equilibrium method could be due to systematic error from the correction factors obtained from the sample and dialyzing solution volumes used for correction. The accurate volumes were difficult to measure since the dialysis membrane may swell during use. This observation can also suggest that the results from the continuous-flow method should be more reliable than those obtained from the equilibrium method.

The in vitro availability of calcium for cabbage, Chinese kale, and spinach by the continuous-flow method was found to be 48.2%, 52.9%, and 4.6%, respectively. These results are close

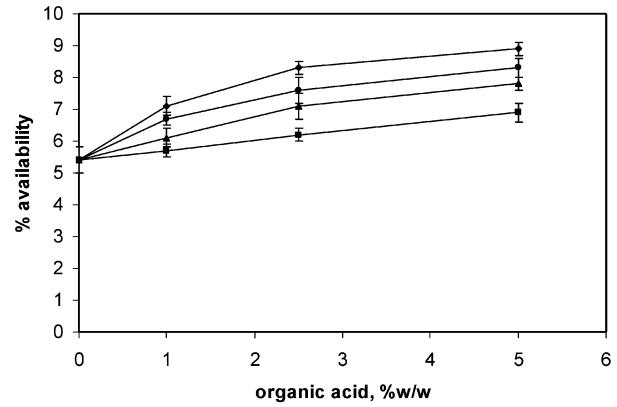

Figure 4. Relationship between the concentration (%) of organic acids added and the calcium availability (%) for amaranth: ascorbic acid (■), citric acid (◆), malic acid (▲), and tartaric acid (●).

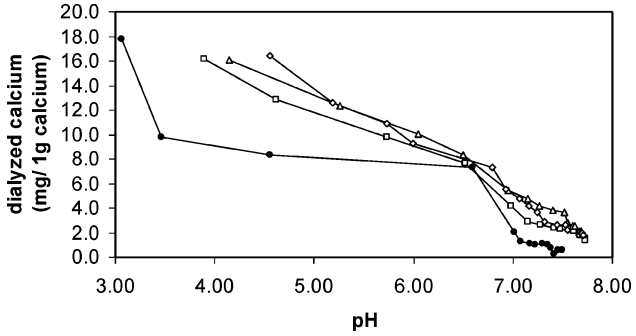

Figure 5. Dialysis profile as a graphical plot of dialyzed calcium against the pH value of the dialysate for amaranth with addition of varying concentrations of citric acid: 0% (●), 1% (□), 2.5% (△), and 5% (◇). Data were obtained from **Figure 3b**.

to the values of in vivo study reports of 64.9%, 58.8% (*20*), and 4.6% (*19*), respectively.

Some vegetables such as amaranth, awltree, cumin, betel leaves, and spinach were found to contain high amounts of calcium but a very low in vitro availability (%). The reasons for the low availability were reported to be related to the inhibitors (phytate, oxalate, and dietary fiber components) which bind calcium to form unabsorbable compounds (*1*, *2*).

Amaranth and Chinese kale were selected as representative vegetables for low and high calcium availability, respectively, for the study of the effect of organic acids on availability.

Effect of Organic Acids on the Calcium Availability of Amaranth. Chemical bindings of calcium with food components are major factors affecting availability. Some food components favorably promote mineral absorption. The influence of various organic acids on calcium availability has been investigated. Some authors reported an enhancing effect by organic acids (*4*, *5*). Therefore, the effect of organic acids, commonly found in foods, on the calcium availability of vegetables was systematically studied. Ascorbic, citric, tartaric, and malic acids were directly added into the chosen vegetables at concentrations of 1% (w/w), 2.5% (w/w), and 5% (w/w) of the vegetable (dry mass), and the calcium availability was determined in the same manner. The results are depicted in **Figure 3**.

The dialysis profiles obtained from the dynamic continuous-flow system, showing the effect of the concentration of added organic acids, are illustrated in **Figure 3**. The changes in the dialyzed amount could be observed from the dialysis profiles. The profiles show an enhancing effect on calcium dialyzability at increased concentrations of organic acids. For example, the dialysis profiles of amaranth without citric acid dropped to the baseline when the pH of dialysis approached 7. On the contrary, dialysis went on even at pH higher than 7 when 1−5% citric acid was added. Other organic acids gave similar results. From

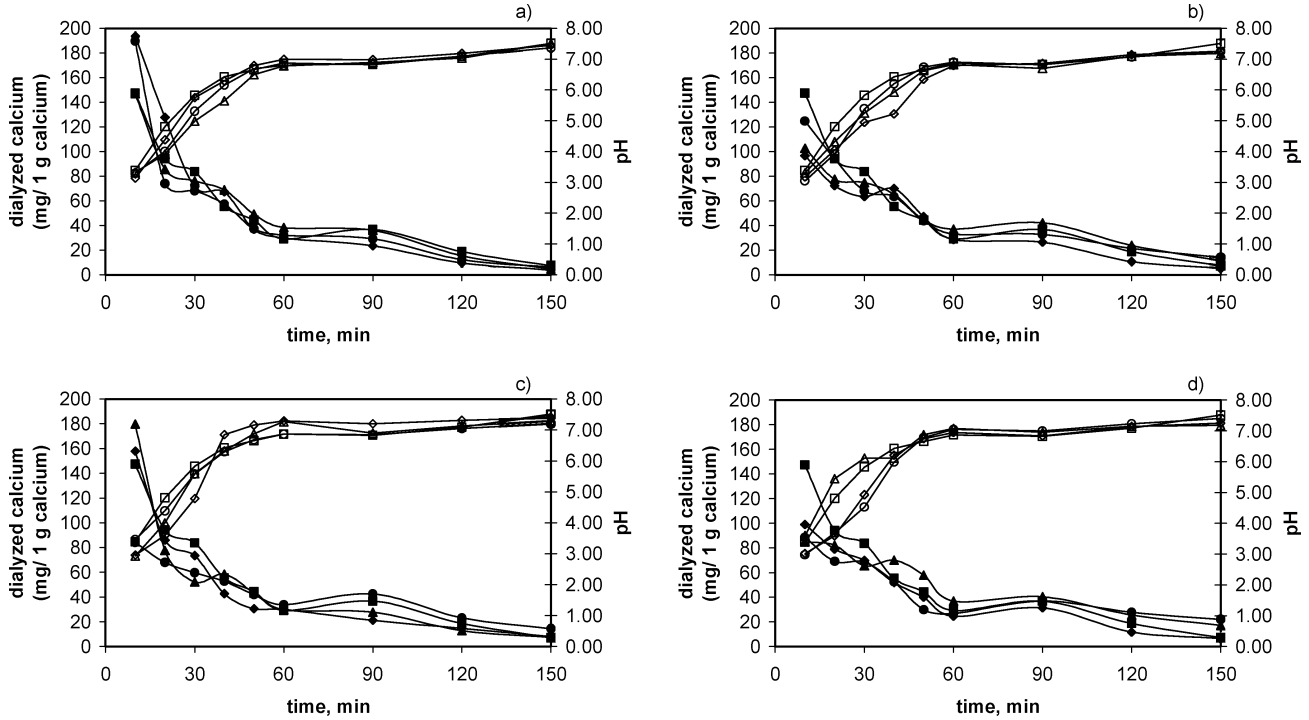

Figure 6. Dialyzed calcium and pH change during simulated intestinal digestion for Chinese kale at varying concentrations of ascorbic acid (**a**), citric acid (**b**), malic acid (**c**), and tartaric acid (**d**), where ■, ◆, ▲, and ● represent Chinese kale with 0%, 1.0%, 2.5%, and 5% (w/w) acid, respectively. The corresponding pH profiles are presented with open symbols of the same type.

the dialysis profiles (**Figure 3**), the enhancement effect was most pronounced when citric and tartaric acids of 5% were added.

Figure 4 illustrates the effect of the percentage of organic acid added on calcium availability, as calculated from the summation of dialyzed calcium in all dialysate fractions, for the amaranth sample. The effect on calcium dialyzability in a decreasing order is as follows: citric acid > tartaric acid > malic acid > ascorbic acid. This appears to be the same order as that of the first stability constants (log K_1) of calcium complexation with these organic ligands: citric acid (3.50), tartaric acid (1.80), malic acid (1.80), and ascorbic acid (0.19) (*21*).

From the observation of dialysis profiles, the following can be speculated. Most of the calcium in vegetables is bound with other dietary constituents. During the simulated gastrointestinal digestion, these constituents are broken down, and calcium is released as dialyzable forms. At low pH, the dialyzability is naturally higher than at high pH, owing to the favorable binding of anions with protons, leaving calcium as an ionic soluble form. When the pH increases, binding with various ligands occurs. Oxalate and phytate can bind with calcium to form precipitates which are not dialyzed. However, with the presence of organic acids, the organic acids favorably bind with calcium even at an elevated pH, resulting in the enhancement of calcium dialyzability. To demonstrate the dialysis of calcium at high pH in the presence of the organic acids studied, **Figure 3b** was replotted to obtain **Figure 5** showing the effect of citric acid on the dialyzed calcium at various pH values. This graph illustrates that the change in dialyzability was not solely contributed by the pH change, but also due to the organic acid added. This information cannot be obtained from the equilibrium dialysis approach.

Effect of Organic Acids on the Calcium In Vitro Availability of Chinese Kale. The dialysis profiles showing the effect of added organic acids in Chinese kale are presented in **Figure 6**. No enhancement of calcium dialyzability was observed when various organic acids were added at various concentrations. Because of the naturally existing promoters (citric and malic acids) in Chinese kale, most calcium was already present in readily dialyzable forms. The dialysis profiles (**Figure 6**) show continuing dialysis even after pH has reached 7.0. In relation to the high calcium availability of Chinese kale, some authors reported a low concentration of inhibitors (precipitators) such as phytate and oxalate in Chinese kale (*16*). Moreover, high concentrations of enhancers such as citric and malic acids were found as the major organic acids in Chinese kale at 22.13 and 1.51 mg/g, respectively (*22*). Lucarini et al. (*23*) presented *brassica* vegetables (e.g., broccoli, green cabbage, and kale) as a good source of dietary calcium and showed that dialyzable calcium in these vegetables was in both ionic and bound forms with a large fraction in the bound forms. Hence, the added organic acid did not show an observable effect on the calcium dialyzability in Chinese kale.

Conclusion. The calcium availability of various vegetables was determined by the in vitro simulated gastrointestinal digestion with continuous-flow dialysis method. The calcium in vitro availability in the vegetables studied was found to vary between 4.6% and 52.9%. The in vitro availability obtained as compared to the reported availability data from the in vivo measurement was very similar. This indicates the possibility of using the in vitro method as a rapid evaluation method for the availability study.

The study of the effect of organic acids on calcium dialysis showed a significant increase of availability at increasing concentrations of acid for amaranth. Citric acid was the most effective enhancer followed by tartaric, malic, and ascorbic acids as could be predicted from their stability constants of complexation with calcium. An enhancement effect was not clearly observed for Chinese kale, which was a representative vegetable of high calcium availability.

The dialysis profiles from continuous-flow dialysis, showing a time-dependent dialyzed amount and pH change, provide information which is not obtained from the equilibrium method. Thus, the enhancement effect of some organic acids on calcium availability was proved to be caused by calcium remaining dialyzable even at elevated pH conditions in the intestinal digestion stage. The dialysis profiles were proved to be useful for understanding the effect of food components on mineral dialyzability in the simulated gastrointestinal digestion model.

LITERATURE CITED

(1) Kennefick, S.; Cashman, K. D. Investigation of an *in vitro* model for predicting the effect of food components on calcium availability from meals. *Int. J. Food Sci. Nutr.* **2000**, *51*, 45−54.

(2) Aletor, V. A.; Adeogun, O. A. Nutrient and anti-nutrient components of some tropical leafy vegetables. *Food Chem.* **1995**, *53*, 375−379.

(3) Mehansho, H.; Kanerva, R. L.; Hudepohl, G. R.; Smith, K. T. Calcium bioavailability and iron-calcium interaction in orange juice. *J. Am. Coll. Nutr.* **1989**, *8*, 61−68.

(4) Wolters, M. G.; Diepenmaat, H. B.; Hermus, R. J. J.; Voragen, A. G. J. Relation between *in vitro* availability of minerals and food composition: a mathematical model. *J. Food Sci.* **1993**, *58*, 1349−1355.

(5) Pak, C. Y. C.; Harvey, J. A.; Hsu, M. C. Enhanced calcium bioavailability from a solubilized form of calcium citrate. *J. Clin. Endocr. Metab.* **1987**, *65*, 801−805.

(6) Miller, D. D.; Schricker, B. R.; Rasmussen, R. R.; Campen, D. V. An *in vitro* method for estimation of iron availability from meals. *Am. J. Clin. Nutr.* **1981**, *34*, 2248−2256

(7) Shen, L. H.; Luten, I.; Robberecht, H.; Daeel, P. V.; Deelstra, H. Modification of an in-vitro method for estimating the bioavailability of zinc and calcium from foods. *Lebensm. Unters. Forsch.* **1994**, *199*, 442−445.

(8) Wolters, M. G. E.; Schreuder, H. A. W.; Heuvel, G. V. D.; Lonkhuijsen, H. J. V.; Hermus, R. J. J.; Voragen, A. G. J. A continuous *in vitro* method for estimation of the bioavailability of minerals and trace elements in foods: Application to breads varying in phytic acid content. *Br. J. Nutr.* **1993**, *69*, 849−861.

(9) Larsson, M.; Minekus, M.; Havenaar, R. Estimation of the bioavailability of iron and phosphorus in cereals using a dynamic *in vitro* gastrointestinal model. *J. Sci. Food Agric.* **1997**, *74*, 99−106.

(10) Shiowatana, J.; Kitthikhun, W.; Sottimai, U.; Promchan, J.; Kunajiraporn, K. Dynamic continuous-flow dialysis method to simulate intestinal digestion for *in vitro* estimation of mineral bioavailability of food. *Talanta* **2006**, *68*, 549−557.

(11) Promchan, J.; Shiowatana, A dynamic continuous-flow dialysis system with on-line electrothermal atomic-absorption spectrometric and pH measurements for *in-vitro* determination of iron bioavailability by simulated gastrointestinal digestion. *Anal. Bioanal. Chem.* **2005**, *382*, 1360−1367.

(12) Judprasong, K.; Ornthai, M.; Siripinyanond, A.; Shiowatana, J. A continuous-flow dialysis system with inductively coupled plasma optical emission spectrometry for *in vitro* estimation of bioavailability. *J. Anal. At. Spectrom.* **2005**, *20*, 1191−1196.

(13) Larsson, M.; Minekus, M.; Havenaar, R. Estimation of the bioavailability of iron and phosphorus in cereals using a dynamic *in vitro gastrointestinal model. J. Sci. Food Agric.* **1997**, *74*, 99−106.

(14) Dominy, N. J.; Davoust, E.; Minekus, M. Adaptive function of soil consumption: an *in vitro* study modeling the human stomach and small intestine. *J. Exp. Biol.* **2004**, *207*, 319−324.
(15) Krul, C.; Luiten-Schuite, A.; Baan, R.; Verhagen, H.; Mohn, G.; Feron, V.; Havenaar, R. Application of a dynamic *in vitro* gastrointestinal tract model to study the availability of food mutagens, using heterocyclic aromatic amines as model compounds. *Food Chem. Toxicol.* **2000**, *38*, 783−792.
(16) Kamchan, A.; Puwastien, P.; Sirichakwal, P. P.; Kongkachauichai, R. *In vitro* calcium bioavailability of vegetables, legumes and seed. *J. Food Compos. Anal.* **2004**, *17*, 311−320.
(17) Toba, Y.; Takada, Y.; Tanaka, M.; Aoe, S. Comparison of the effects of milk components and calcium source on calcium bioavailability in growing male rats. *Nutr. Res.* **1999**, *19*, 449−459.
(18) Heaney, R. P.; Recker, R. R.; Weaver, C. M. Absorbability of calcium sources: the limited role of solubility. *Calcif. Tissue Int.* **1990**, *46*, 300−304.
(19) Peterson, C. A.; Eurell, J. A. C.; Erdman, J. W. Bone composition and histology of young growing rats fed diets of varied calcium bioavailability: spinach, nonfat dry milk, or calcium carbonate added to casein. *J. Nutr.* **1992,** *122*, 137−144.
(20) Weaver, C. M.; Plawecki, K. L. Dietary calcium: Adequacy of a vegetarian diet. *Am. J. Clin. Nutr.* **1994**, *59* (Suppl.), 1238s−1241s.
(21) Thomas, E. F. *CRC Handbook of Food Additives*; Taylor and Francis, CRC Press: Boca Raton, FL, 1972.
(22) Ayaz, F. A.; Glew, R. H.; Millson, M.; Huang, H. S.; Chuang, L. T.; Sanz, C.; Ayaz, S. H. Nutrient contents of kale (*Brassica oleraceae* L. *var. acephala* DC.). *Food Chem.* **2006**, *96*, 572−579.
(23) Lucarini, M.; Canali, R.; Cappelloni, M.; Di, Lullo, G.; Lombardi-Boccia, G. *In vitro* calcium availability from *brassica* vegetables (*Brassica oleracea* L.) and as consumed in composite dishes. *Food Chem.* **1999**, *64*, 519−523.

Received for review July 22, 2006. Revised manuscript received September 22, 2006. Accepted September 29, 2006. We are grateful for financial support from the Thailand Research Fund and the Postgraduate Education and Research Program in Chemistry, Higher Education Development Project, Ministry of Education.

JF062073T

ARTICLE

JAAS
www.rsc.org/jaas

A continuous-flow dialysis system with inductively coupled plasma optical emission spectrometry for *in vitro* estimation of bioavailability†

Kunchit Judprasong,[ab] Mathuros Ornthai,[a] Atitaya Siripinyanond[a] and Juwadee Shiowatana*[a]

[a] *Department of Chemistry, Faculty of Science, Mahidol University, Rama VI Rd., Bangkok 10400, Thailand. E-mail: scysw@mahidol.ac.th; Fax: 66 2 3547151; Tel: 66 2 2015122*

[b] *On study leave from Institute of Nutrition, Mahidol University, Salaya, Putthamonthon, Nakorn Pathom 73170 Thailand. E-mail: nukjp@mahidol.ac.th; Fax: 66 2 4419344; Tel: 66 2 8002380*

Received 17th June 2005, Accepted 8th September 2005
First published as an Advance Article on the web 22nd September 2005

A continuous-flow dialysis (CFD) method with on-line inductively coupled plasma optical emission spectrometric (ICP-OES) simultaneous multielement measurement for the study of *in vitro* mineral bioavailability was developed. The method was based on a simulated gastric digestion in a batch system followed by a continuous-flow intestinal digestion. The simulated intestinal digestion was performed in a dialysis bag placed inside a channel in a flowing stream of dialyzing solution ($NaHCO_3$). The mineral concentrations in the dialysate were determined by ICP-OES using Y and Sc as internal standards. The pH of the dialysate was also monitored on-line to ensure pH changes similar to the situation in the gastrointestinal tract.The developed system was applied to determining the dialysability of five essential elements (Ca, Mg, P, Fe, Zn) for various kinds of foods, *i.e.*, milk-based infant formula reference material (NIST SRM 1846), milk powder, kale, mungbean, chicken meat, jasmine rice, and *Acacia pennata*. The dialysis profiles of elements and pH change profiles can be useful in understanding the dialysis change and factors affecting dialysability. All studied elements were rapidly dialysed in the first 30 min of simulated intestinal digestion. It is expected that this system will be useful for estimation of dialysability and for studying the mutual effects of components in food.

Introduction

Mineral deficiency is usually caused by a low mineral content in the diet when rapid body growth is occurring and/or when minerals from the diet are poorly absorbed. Mineral bioavailability has usually been determined by *in vivo* measurement.[1] Ideally, mineral bioavailability studies should be performed *in vivo* and in humans; however, they are difficult, expensive, and provide limited data with each experiment.[2] While animal assays are less expensive, they are somewhat limited by uncertainties with regard to differences in metabolism between animals and humans. As an alternative to human and animal *in vivo* studies, the availability of minerals or trace elements has also been estimated by simple, rapid and inexpensive *in vitro* methods.[3] The earlier *in vitro* methods estimated bioavailability by measuring the dialysability of minerals through a semipermeable membrane in equilibrium after simulated enzymatic digestion of foods, which was known as ''Miller's method''. However, in this equilibrium method, the dialysed components are not continuously removed, as occurrs in the intraluminal digestive tract. Many modifications have been made to Miller's method in an attempt to improve the analytical methodology. Continuous-flow dialysis (CFD) *in vitro* methods were developed[4–6] in which dialysed components were continuously removed. These methods measure the fraction of the available mineral pool in diets which is potentially capable of absorption. Although a true absorption is not determined, *in vitro* methods have frequently been used to predict and compare the availability of different foods because they are simple, rapid, inexpensive and easy-to-control. In addition, certain parameters can be monitored during *in vitro* dialysis. Some studies reported poor correlation between *in vitro* and *in vivo* bioavailability,[7,8] whereas some studies reported good correlation between results obtained from the two methods.[9,10] An example of disagreement between the two methods was reported for bioavailability estimation of Ca.[8] The *in vivo* studies of Ca showed higher values than *in vitro* studies because some of the Ca bound species was released into the large intestine and might be absorbable.[8] Therefore, to obtain a reliable and meaningful *in vitro* bioavailability study, a clear need exists for the development of a dialysis method that can mimic *in vivo* functions.

A CFD system, by which dialysed components were continuously removed during simulated intestinal digestion, has been developed to obtain a closer simulation of the mineral absorption in the body.[6] It involves an *in vitro* gastric digestion in a batch system (mimicking digestion in the stomach where no mineral absorption takes place), then intestinal digestion in a CFD system. The CFD in the intestinal digestion step enables dialysable components to be continuously removed for element detection. Moreover, the proposed CFD system offers information on dialysis kinetics, which could be extrapolated to be of some use for absorption studies. In our previous reports, the CFD system was operated with off-line flame AAS,[6] and on-line electrothermal AAS detection[11] for the study of Ca and Fe dialysability, respectively. However, many essential minerals are of nutritional interest, for example Ca and P are two essential elements for optimal bone mineralization.[12] The roles

† Presented at the First Winter Conference on Plasma Spectrochemistry, Chiang Mai, Thailand, April 25–30, 2005.

DOI: 10.1039/b508639f

of other major and trace elements (Mg, Fe, Zn, Cu, Se, *etc.*) are also of particular interest. Magnesium, Zn, and Fe serve metabolic and enzymatic functions. Zinc is essential for normal growth and development of the immune response.[13] So, the CFD system with multielement detection capability for the determination of major and trace elements was aimed in this direction. An inductively coupled plasma optical emission spectrometric (ICP-OES) detection was chosen for this study. An ICP-OES spectrometer was connected on-line sequentially after an on-line pH measurement module to the CFD system to continuously monitor the dialysed multielement content and pH change during dialysis. The developed method was validated and applied for determination of mineral (Ca, Mg, P, Zn and Fe) dialysability for various kinds of food.

Experimental

Reagents and solutions

All reagents were of analytical grade, and ultrapure water of 18 MΩ cm specific resistivity obtained from a Milli-Q purification system (Millipore Corp., MA, USA) was used throughout. Glass and polyethylene containers were soaked in 10% nitric acid for at least 24 h and then rinsed three times with ultrapure water before use.

A pepsin solution was prepared by dissolving 0.16 g of pepsin (P-7000, porcine stomach mucosa, Sigma, St.Louis, MO, USA) in 1 mL of 0.1 mol L^{-1} HCl. A pancreatin–bile extract (PBE) mixture was prepared by dissolving 0.004 g of pancreatin (P-1750, porcine pancreas, Sigma) and 0.025 g of bile extract (B-6831, porcine, Sigma) in 5 mL of 0.001 mol L^{-1} $NaHCO_3$. Flat dialysis membranes (MWCO 12–14 kDa) 10 mm wide and 17.6 cm in length (cellu-Sep®H1, Membrane Filtration Products, Texas, USA) were used in the intestinal digestion procedure. The membranes were boiled for 30 min in 40% ethanol, soaked in 1 mM ethylenediamine tetraacetic acid (EDTA; BDH Ltd., Poole, UK) for 30 min, rinsed several times with Milli-Q water, stored in 0.01 M $NaHCO_3$ and rinsed with Milli-Q water before use. A multielemental stock solution (QCS 01–5 at 100 μg mL^{-1}), Y (ICP-69N-1 at 1000 g mL^{-1}) and Sc (ICP-53N-1 at 1000 g mL^{-1}), as internal standards, were from AccutraceTM (AccuStandard®, USA). Standard solutions were prepared immediately before use by dilution of stock standard with 2% HNO_3.

Instrument and equipment

The CFD system used in this study was described elsewhere.[6] The outlet of the CFD system was connected to a pH measurement module and ICP-OES detection unit (Fig. 1). A shaking water bath (Memmert®, Memmert GmbH, Germany), controlled at 37 ± 1 °C, was used for both gastric and intestinal digestions. The Orion SensorLink pH measurement system (ThermoOrion, USA), Model PCM500, equipped with PCMCIA slot and personal computer, was used to determine pH during digestion and dialysis.

Determination of minerals by ICP-OES was performed using a SPECTRO CIROS CCD, axial configuration, equipped with a glass spray chamber (double pass, Scott-type) and a cross-flow nebulizer (all from SPECTRO Analytical Instruments, Germany). The ICP-OES operating conditions were as follows: power 1350 W; nebulizer gas flow 1 L min^{-1}; and auxiliary gas flow 12 L min^{-1}. Selected emission lines were: Ca, 396.847 (II), 317.933 (II), and 422.673 (I); Mg, 279.553 (II), 279.079 (II) and 280.270 (II); P, 177.495 (I) and 214.914 (I); Fe, 238.204 (II), 239.562 (II), 259.940 (II); and Zn, 202.548 (II), 206.191 (II), 213.856 (II) nm. Emission lines for internal standards were: Y, 320.332 (II), 371.030 (II) and 442.259 (II); and Sc: 256.023 (II), 361.384 (II), and 440.037 (II) nm. A closed microwave digestion unit (Milestone MLS 1200 mega, Italy) equipped with 6 Teflon vessels was used to mineralize 0.5–1 g of food samples with 10.0 mL of concentrated nitric acid prior to determination of the total mineral contents by ICP-OES.

Sample collection and preparation

Milk-based infant formula (NIST SRM 1846) was used for method validation. Representative samples of cow milk, kale (*Brassica oleracea* var. alboglabra, Bail.), *Acacia pennata* (L., Willd. Subsp.), mungbean (*Phaseolus aureus* Roxb.), chicken meat, and jasmine rice (*Orya sativa*) were examined. Three samples for each food item, 1–3 kg, were purchased randomly in three local markets in metropolitan areas of Bangkok, Thailand. After purchase, the samples were transported as soon as possible to the laboratory. Milk powder, jasmine rice, and mungbean were used as purchased. Kale, *Acacia pennata* and chicken meat were cleaned once with tap water, and twice with Milli-Q water. The inedible portions of each sample were recorded and discarded. The edible parts in all samples except milk powder and infant formula were cooked by boiling,

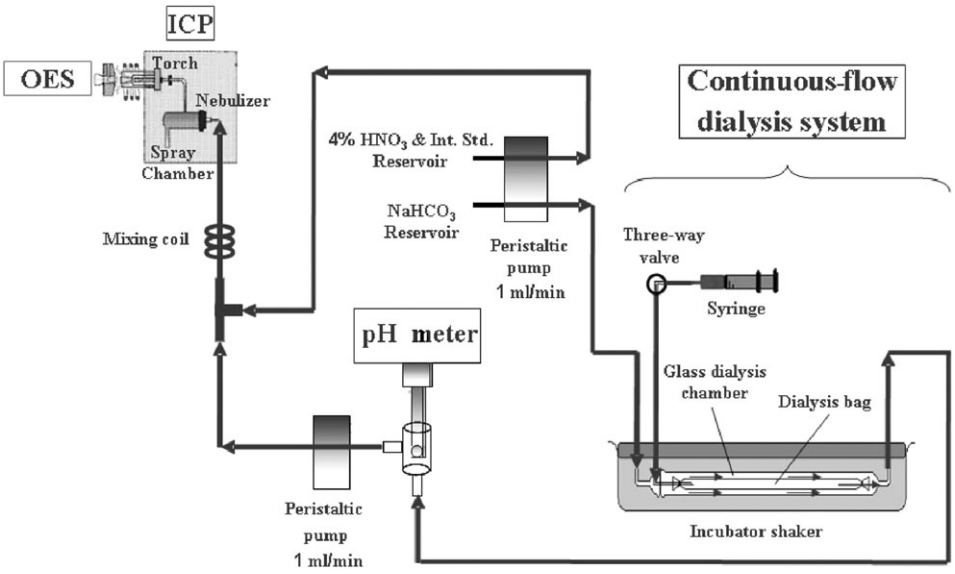

Fig. 1 Schematic diagram of continuous-flow dialysis system with on-line ICP-OES and pH measurements. A 2.5 mL pepsin digest sample was injected into the dialysis bag using a syringe. A 625 μL aliquot of pancreatin–bile extract was introduced into the dialysis bag after the first 30 min of the dialysis process. Dialysis was continued for 150 min. The dialysate flow was sequentially subjected to pH and ICP-OES measurements.

Table 1 Optimum concentrations of $NaHCO_3$ for each food sample

Sample	Optimum $NaHCO_3$/mol L^{-1}
Jasmine rice	7.77×10^{-4}
Chicken meat	1.89×10^{-3}
Mungbean	1.32×10^{-4}
Acacia pennata	1.59×10^{-3}
Milk powder	1.14×10^{-3}
Kale	1.44×10^{-3}

homogenized by a food processor (Tefal® Kaleo Blender, France), kept in an acid-washed screw-capped plastic bottle, and stored at −20 °C. A representative portion of the homogenized samples was dried at 60 °C and ground to fine particles, and then stored in a sealed plastic bag in a desiccator at room temperature until analysis.

Analytical procedure

***In vitro* gastrointestinal digestion method.** Gastric digestion was performed according to the procedure of Miller.[3] Dried samples were weighed (0.5–1 g), mixed with 10 g of Milli-Q water, adjusted to pH 2.0 with 6 M HCl and adjusted to 12.5 g using pure water. To carry out pepsin–HCl digestion, 375 µl of pepsin solution was added. The mixture was then incubated for 2 h at 37 °C in a shaking water bath.

For intestinal digestion and dialysis, a dynamic CFD system was used (Fig. 1). A portion of the mixture after gastric digestion (2.0–2.5 g) was injected into the flattened dialysis bag in the dialysis chamber *via* a syringe. The dialysing solution, $NaHCO_3$ of optimum concentration, determined by titratable acidity[6] for each food sample as summarized in Table 1, flowed through the outer surface of the bag at 1 mL min^{-1} and the temperature was controlled at 37 °C. The dialysable components in the dialysing solution were transported into the pH measurement cell and finally to the ICP-OES. To obtain good nebulization performance and to ensure that the analyte elements remained soluble, the stream of dialysing solution was acidified by mixing with a stream of 4% nitric acid, which also contained 1 mg L^{-1} of Y and Sc, used as internal standards at 1.0 mL min^{-1} (see Fig. 1). Blanks for gastric and intestinal digestions were also performed in each experiment to control possible contamination problems.

Mineral content determination. A known amount of sample (approximately 1.0 g) was digested by microwave digestion using 10.0 mL of concentrated HNO_3. The microwave digestion program comprised five steps: 1, 250 W for 1 min; 2, no power for 1 min; 3, 250 W for 5 min; 4, 400 W for 5 min; and 5, 650 W for 5 min. Digestion was performed to obtain a clear solution. In each digestion round, five vessels were used for food samples and one vessel was left for blank HNO_3 to check for the presence of contamination during each run. Acid digestion of an SRM 1846 milk-based infant formula standard reference material was also performed using a microwave digestion system to check for analytical recovery. The mineral total contents were measured by ICP-OES.

In the CFD method, the concentration of each mineral in the dialysate (µg mL^{-1}) was obtained by on-line ICP-OES measurement by external calibration using freshly prepared standard solution in $NaHCO_3$ of similar concentration to the dialysing solution, which was acidified to contain 2% HNO_3 before use. The total amount of dialysed minerals was determined by integration of the signal through the whole dialysis time using a computer program (Microcal Origin, Version 6.0).

Dialysability in percent was calculated as follows: dialysability (%) = $100 \times D/C$, where D represents dialysed mineral content (µg g^{-1} sample) and C represents the total mineral content (µg g^{-1} sample). After dialysis, mineral contents in the residue inside the dialysis bag were determined by ICP-OES after acid digestion, and the percentages of mineral remaining were calculated.

Results and discussion

I. Setup of continuous-flow dialysis system with on-line detections

The design of the continuous-flow dialysis (CFD) system for *in vitro* determination of mineral bioavailability, the selection of dialysing solution flow rate and optimization of dialysing solution ($NaHCO_3$) have been reported elsewhere.[6] The optimum flow rate of dialysing solution in the CFD and the uptake rate of ICP-OES were similar at 1 mL min^{-1}, therefore they can be readily coupled. Nonetheless, to obtain good nebulization performance, sample solution was acidified before reaching the nebulizer by merging the stream of sample solution with a stream of 4% nitric acid. The signal intensities of Ca and Fe in acidified samples were increased remarkably, in comparison with those which were not acidified.

II. Validation of analytical method

Because a reference material, which would provide bioavailability data, is not available, validation of the proposed method was performed by studying the analytical recoveries of all elements of interest. Milk-based infant formula reference material (SRM 1846) was subjected to the proposed analytical procedure to determine the dialysable minerals in the dialysate and the non-dialysable ones in the retentate. The non-dialysable mineral in the retentate was determined by ICP-OES after acid digestion of the remaining of food suspension in the dialysis tube. The total mineral content of the sample was determined after total digestion of the sample. The results are given in Table 2. The results of total concentration obtained by ICP-OES after acid digestion agreed well with the certified values for all elements studied, suggesting good performance of ICP-OES detection. In addition, a summation of the dialysed

Table 2 Validation of method using milk-based infant formula (SRM 1846) ($n = 3$)

	Mineral contents				
	Ca	Mg	P	Fe	Zn
Certified value/µg g^{-1}	3670 ± 200	538 ± 29	2610 ± 150	63.1 ± 4.0	60.0 ± 3.2
Total minerals/µg g^{-1}[a]	3760 ± 160	541 ± 17	2490 ± 96	66.6 ± 1.5	62.8 ± 1.8
dialysed minerals/µg g^{-1}[a]	2800 ± 140	428 ± 10	1730 ± 200	17.7 ± 2.2	51.5 ± 3.7
Non-dialysed minerals/µg g^{-1}[a]	792 ± 46	86 ± 12	1040 ± 94	42.4 ± 5.5	7.8 ± 1.0
dialysed + non-dialysed mineral/µg g^{-1}	3600 ± 140	514 ± 6	2690 ± 145	60.1 ± 5.0	59.0 ± 4.9
Dialysis (%)	76 ± 4	80 ± 2	70 ± 5	27 ± 3	82 ± 6
Element retained (%)	22 ± 1	16 ± 2	42 ± 4	64 ± 5	18 ± 2
Sum (%)	98 ± 4	96 ± 1	104 ± 6	90 ± 5	94 ± 9

[a] Blank subtracted.

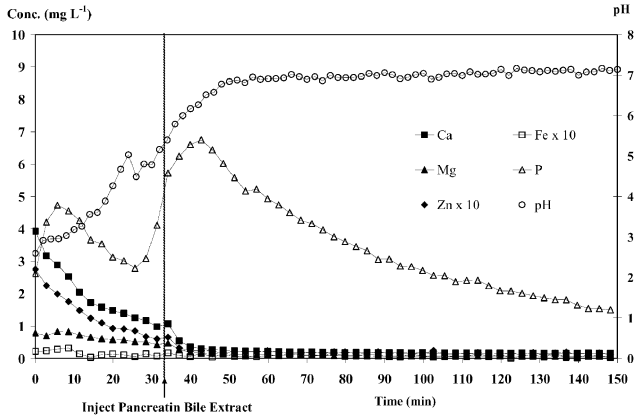

Fig. 2 Dialysis profiles and pH changes obtained from the CFD-pH-ICP-OES system for blank analysis.

minerals (by CFD-ICP-OES) and non-dialysed minerals contents was similar to the certified values with recoveries ranging from 90 ± 5% for Fe to 104 ± 6% for P, suggesting good performance of the CFD system and the absence of matrix interferences from the dialysable components and therefore the reliability of an on-line ICP-OES determination of dialysable minerals without prior acid digestion. With the proposed CFD-ICP-OES system, a quantitative recovery was obtained.

III. Dialysis profile

Not only was the percent dialysability obtained but also the dialysis profiles of elements and pH change profiles, which can be useful in understanding the dialysis change and factors affecting dialysability. The pH changes (right axis of Fig. 2) from approximately 2.0 for gastric digests to *ca*. 5.0 within 30 min of intestinal digestion and to *ca*. 7.0–7.5 after 1 h were

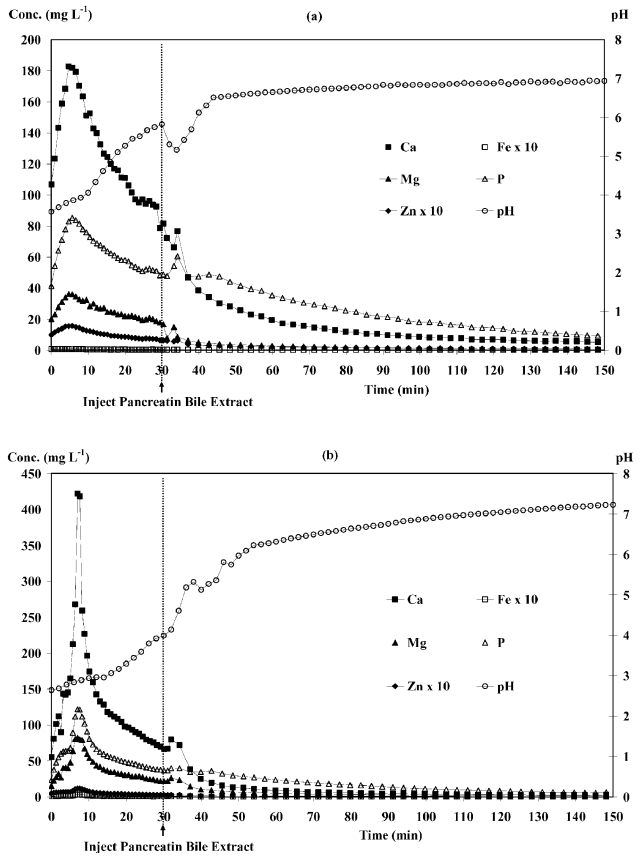

Fig. 3 Dialysis profiles and pH changes in milk powder (a) and kale (b).

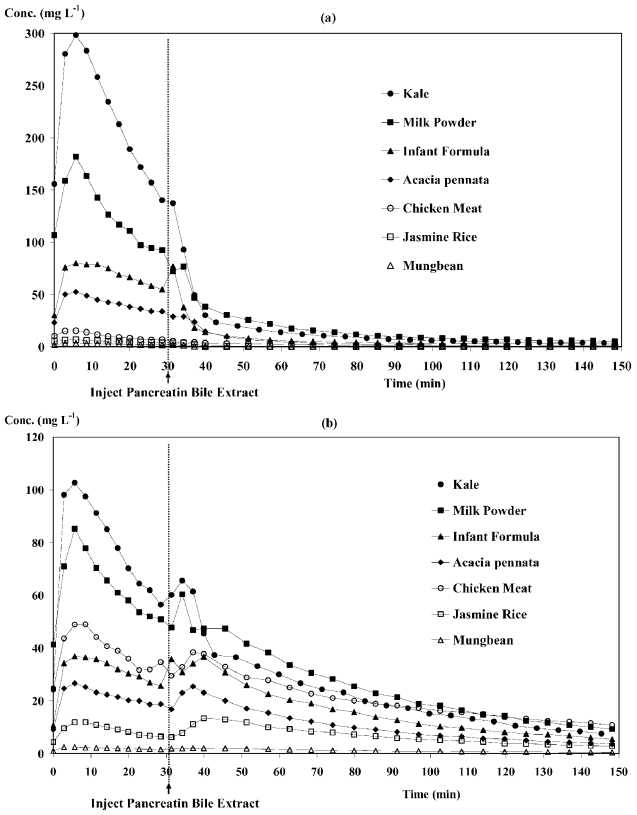

Fig. 4 Dialysis profiles of calcium (a) and phosphorus (b) in various foods.

close to what occurs in the human gastrointestinal tract.[4] The blank dialysis (Fig. 2) was found to give low values (<4 mg L^{-1} for all elements, highest for P at 3–7 mg L^{-1}, which was considerably low and could be estimated to be less than 10% of the dialysable components). Nevertheless, blank correction was performed and subtracted in all analyses. Figs. 3(a) and 3(b) show dialysis profiles of Ca, Mg, P, Fe and Zn for milk powder and kale digests, respectively. All elements show similar profiles, giving peak maxima at about 10 min of dialysis and a gradual decrease to baseline; in this system, such profiles equate to "absorption", seen here as loss of mineral from the model intestine. The irregular pH change and dialysis profiles at 30–40 min were probably affected by PBE injection at 30 min.

Fig. 4 shows dialysis profiles of Ca (a) and P (b) in different food digests. Calcium and phosphorus in kale and milk powder were rapidly dialysed in the first 30 min. It was found that P dialysis profiles showed a second peak after PBE injection, as illustrated in Fig. 4(b), as a result of digestion of food components by PBE enzymes. The descending order of the total calcium content (Table 3) is as kale > milk powder > infant formula > *Acacia pennata* > chicken meat > jasmine rice > mungbean (ranged from 13 867 to 56 μg g^{-1}) considering their dialysed calcium.

IV. Profile of molar ratio plot

From a nutritional point of view, the ratio of Ca and P intake is believed to be important: the optimum molar ratio of Ca/P is 1, although a Ca/P ratio of 1/1.5 is acceptable. Injurious effects can appear when this relationship is not met.[14] It is important to maintain a good ratio of Ca and P intake for optimal bone mineralization.[15] Anderson,[16] in a review of the relationship of Ca and P and human bone development, stated that a potential mechanism for the development of low bone mass in the United States was related to a low ratio of Ca/P intake. Consumed diets with low Ca in dairy foods can also potentially

Table 3 Total and dialysed minerals (as per dry weight) in various kinds of foods ($n = 3$)

	Jasmine rice	Chicken meat	Mungbean	*Acacia pennata*	Milk powder	Kale
Calcium						
Total minerals/μg g^{-1}	56 ± 3	299 ± 13	819 ± 43	1650 ± 30	6890 ± 120	13 870 ± 540
Dialysed minerals/μg g^{-1}	44 ± 2	279 ± 9	714 ± 35	1220 ± 55	5560 ± 280	8520 ± 430
Non-dialysed minerals/μg g^{-1}	8 ± 2	12 ± 5	119 ± 27	482 ± 25	1030 ± 30	5520 ± 240
Dialysed + non-dialysed minerals/μg g^{-1}	52 ± 4	290 ± 13	842 ± 26	1760 ± 91	6580 ± 280	14 030 ± 520
Dialysis (%)	78 ± 3	93 ± 3	87 ± 4	74 ± 3	81 ± 4	61 ± 3
Element retained (%)	14 ± 3	4 ± 2	15 ± 3	31 ± 2	15 ± 0.5	40 ± 2
Sum (%)	94 ± 6	100 ± 4	103 ± 3	105 ± 6	96 ± 4	101 ± 4
Magnesium						
Total minerals/μg g^{-1}	157 ± 3	878 ± 30	1410 ± 3	1980 ± 12	763 ± 29	4690 ± 310
Dialysed minerals/μg g^{-1}	95 ± 4	814 ± 13	1050 ± 40	1640 ± 44	628 ± 46	3130 ± 100
Non-dialysed minerals/μg g^{-1}	34 ± 6	47 ± 2	459 ± 3	417 ± 7	69 ± 3	1470 ± 40
Dialysed + non-dialysed minerals/μg g^{-1}	129 ± 3	861 ± 14	1507 ± 43	2080 ± 50	697 ± 45	4600 ± 90
Dialysis (%)	60 ± 2	93 ± 2	74 ± 3	84 ± 2	82 ± 6	67 ± 2
Element retained (%)	22 ± 4	5 ± 0.2	33 ± 0.2	21 ± 1	9 ± 0.4	31 ± 1
Sum (%)	82 ± 2	98 ± 2	107 ± 3	105 ± 2	91 ± 6	98 ± 2
Phosphorus						
Total minerals/μg g^{-1}	839 ± 41	6060 ± 209	4000 ± 60	8540 ± 220	6610 ± 310	5990 ± 60
Dialysed minerals/μg g^{-1}	77 ± 8	2720 ± 90	525 ± 13	3250 ± 120	3680 ± 180	3240 ± 210
Non-dialysed minerals/μg g^{-1}	699 ± 26	2490 ± 340	3750 ± 40	5390 ± 260	1610 ± 30	1840 ± 40
dialysed + non-dialysed minerals/μg g^{-1}	776 ± 25	5210 ± 370	4280 ± 60	8630 ± 340	5160 ± 140	5280 ± 60
Dialysis (%)	9 ± 1	45 ± 1	13 ± 0.3	38 ± 1	56 ± 3	54 ± 3
Element retained (%)	83 ± 3	45 ± 1	94 ± 1	63 ± 3	23 ± 2	31 ± 1
Sum (%)	92 ± 3	90 ± 2	107 ± 1	101 ± 4	79 ± 2	88 ± 1
Iron						
Total minerals/μg g^{-1}	3.8 ± 0.1	15.2 ± 0.8	46.8 ± 2.1	113.4 ± 10.2	69.0 ± 1.4	90.9 ± 8.6
dialysed minerals/μg g^{-1}	0.2 ± 0.1	0.7 ± 0.2	2.2 ± 0.3	11.8 ± 0.9	3.7 ± 0.7	4.8 ± 0.4
Non-dialysed minerals/μg g^{-1}	3.2 ± 0.1	14.0 ± 0.3	41.4 ± 1.4	104.9 ± 1.9	55.5 ± 3.1	85.5 ± 2.8
dialysed + non-dialysed minerals/μg g^{-1}	3.5 ± 0.1	14.7 ± 0.4	43.6 ± 1.4	116.7 ± 2.7	59.2 ± 3.4	90.4 ± 2.6
Dialysis (%)	6 ± 1	5 ± 1	5 ± 1	10 ± 1	5 ± 1	5 ± 1
Element retained (%)	84 ± 3	92 ± 2	89 ± 3	92 ± 2	80 ± 4	94 ± 3
Sum (%)	91 ± 3	96 ± 2	93 ± 3	103 ± 2	86 ± 5	100 ± 3
Zinc						
Total minerals/μg g^{-1}	19.4 ± 0.6	27.5 ± 1.8	29.6 ± 0.4	44.0 ± 3.2	50.7 ± 2.3	32.0 ± 4.0
Dialysed minerals/μg g^{-1}	10.8 ± 1.3	22.9 ± 0.7	21.3 ± 0.2	15.9 ± 0.6	38.3 ± 1.7	18.2 ± 0.9
Non-dialysed minerals/μg g^{-1}	6.5 ± 0.7	6.9 ± 0.2	10.4 ± 0.8	22.9 ± 0.8	7.2 ± 0.1	15.1 ± 0.8
Dialysed + non-dialysed minerals/μg g^{-1}	17.3 ± 1.4	29.8 ± 0.7	31.5 ± 0.6	38.8 ± 0.6	44.3 ± 1.1	32.6 ± 0.8
Dialysis (%)	55 ± 7	83 ± 2	72 ± 1	36 ± 1	76 ± 3	57 ± 3
Element retained (%)	33 ± 4	25 ± 1	35 ± 3	52 ± 2	14 ± 0.2	47 ± 2
Sum (%)	89 ± 7	108 ± 3	106 ± 2	88 ± 2	87 ± 2	102 ± 3

contribute to a low Ca/P ratio.[17] Wyatt and co-workers[18] found that beans and corn tortillas were the main contributors of Ca and P in the diet, contributing higher levels of P than Ca, which resulted in Ca/P of 1 : 1.8.

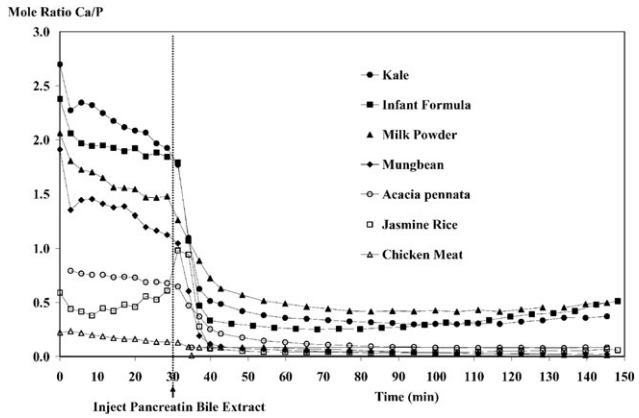

Fig. 5 Dialysis profiles of molar ratio Ca/P for various foods.

From the Ca and P levels found in the dialysed samples, the Ca/P ratio was calculated. The molar ratio plot of Ca/P in various kinds of food is markedly different (see Fig. 5). The ratio of Ca/P of dialysed amount is higher than that of the total mineral content in the same food (Table 4). The molar ratio of Ca/P from total mineral content in milk powder is 0.81 in this study, which is similar to an earlier report.[19] In contrast, the Ca/P ratio from total mineral content in kale is 1.80, which differs from the values in an earlier study[20] of 2.44–3.01, possibly owing to the fact that kales were from different geographical areas and might be of different species. However, this ratio for dialysed amount is, in all cases, higher because Ca gives higher % dialysis than P in all food samples (see Table 3). Although the Ca/P is important in determining their biological activity, this does not extend to absorption. Nonetheless, the study of the molar ratio profile might be of potential use in the future.

V. Application of the proposed system to estimate mineral dialysability of various foods

Dialysability was calculated by the summation of dialysed amounts of mineral during intestinal digestion. The results

Table 4 Molar ratio of Ca/P in dialysed and total minerals (calculated from Table 3)

	Jasmine rice	Chicken meat	Mungbean	*Acacia pennata*	Milk powder	Kale
Molar ratio of Ca/P (dialysed)	0.44	0.08	1.05	0.29	1.17	2.03
Molar ratio of Ca/P (total)	0.05	0.04	0.16	0.15	0.81[a]	1.80[b]

[a] A value of 0.81 reported.[19] [b] 2.44–3.01 reported.[20]

from the determination of the dialysability of essential elements from different kinds of food by the proposed method are shown in Table 3. Total Ca content was low in jasmine rice (56 ± 3 μg g^{-1}) and high in kale ($13\,870 \pm 540$ μg g^{-1}). The percentage of dialysis in all samples ranged from 61 to 93%, the percentage of Ca remained ranged from 4 to 40% and the sum of these values ranged from 94 to 105%. Magnesium content in studied foods ranged from 157 ± 3 μg g^{-1} in jasmine rice to 4690 ± 310 μg g^{-1}in kale. The percentage of dialysis varied from 60% in jasmine rice and 93% in chicken meat. Percent Mg remaining ranged from 5 to 33% and the sum of these values ranged from 82 to 105%. Most studied foods contained high amounts of total P (more than 2490 μg g^{-1}) except that of jasmine rice (839 μg g^{-1}). The percent dialysis of P was lower than 56% and the sum of percent dialysis and percent remained minerals was 79–107%. The percent dialysis of Fe was lowest at 5–10%, and the recovery was 86–103%. For Zn, the summation of dialysed and remaining Zn was also acceptable (87–108%).

In summary, total element and percent dialysability of each element is markedly influenced by the nature of the food. Kale and milk powder contained high total amounts of Ca, Mg, P, and Zn. Chicken meat contained a high total Fe content, whereas mungbean was high in total Mg content. The dialysabilities of Ca, Mg, and Zn are relatively high (36–93%). All studied foods had varying P dialysability, 9 ± 1% in jasmine rice and 56 ± 3% in milk powder. In contrast, the Fe dialysability is lowest at 5–10%.

Conclusions

The developed CFD-pH-ICP-OES system is simple, rapid and capable of continuous multielement detection. The system can be used for simultaneous monitoring of dialysed minerals concentration and pH during dialysis. The developed system was successfully applied to estimate the essential minerals dialysability of various kinds of foods. Information about minerals dialysability can be useful for the nutritional evaluation of foods and for the study of the effect of food components on mineral bioavailability. The dialysis profiles of elements and pH change profiles can be useful to understand the dialysis change and factors affecting dialysability. All studied elements were rapidly dialysed in the first 30 min of simulated intestinal dialysis. Not only was the profile of dialysed minerals obtained but also the molar ratio profiles of elements, which can be useful for nutritional evaluation of foods. Knowledge of mineral bioavailability is useful for managing mineral intake and for reduction of the health risk from mineral deficiency.

Acknowledgements

The authors are grateful for financial support from the Thailand Research Fund and the Postgraduate Education and Research Program in Chemistry, Higher Education Development Project, Ministry of Education.

References

1 K. Van Dyck, S. Tas, H. Robberecht and H. Deelstra, *Int. J. Food Sci. Nutr.*, 1996, **47**, 499–506.
2 M. Hansen, B. Sandstrom and B. Lonnerdal, *Pediatr. Res.*, 1996, **40**(4), 547–552.
3 D. D. Miller, B. R. Schricker, B. S. Rasmussen and D. Van Campen, *Am. J. Clin. Nutr.*, 1981, **34**, 2248–2556.
4 M. G. E. Wolters, H. A. W. Schreuder, G. Van Den Heuvel, H. J. Van Lonkhuijsen, R. J. J. Hermus and A. G. J. Voragen, *Br. J. Nutr.*, 1993, **69**, 849–861.
5 L. H. Shen, J. Luten, H. Robberecht, J. Bindels and H. Deelstra, *Z. Lebensm. Unters. Forsch.*, 1994, **199**, 442–445.
6 J. Shiowatana, W. Kitthikhun, U. Sottimai, J. Promchan and K. Kunajiraporn, *Talanta*, 2005, in the press; DOI: 10.1016/j.talanta.2005.04.068.
7 M. J. Roig, A. Alegria, R. Barbera and M. J. Lagarda, *Food Chem.*, 1999, **65**, 353–357.
8 M. Santaella, I. Martinez, G. Ros and J. Periago, *Meat Sci.*, 1997, **45**, 473–483.
9 M. Lucarini, R. Canali, M. Cappelloni, G. Di Lullo and G. Lombardi-Boccia, *Food Chem.*, 1999, **64**, 519–523.
10 K. J. H. Wienk, J. J. M. Marx and A. C. Beynen, *Eur. J. Nutr.*, 1999, **38**, 51–75.
11 J. Promchan and J. Shiowatana, *Anal. Bioanal. Chem.*, 2005, **382**, 1360–1367.
12 J. M. Pettifor, 'Rickets', in *Dietary Calcium Deficiency*, ed. F. H. Glorieux, Raven Press, New York, 1991, pp. 123–143.
13 F. Cámara, M. A. Amaro, R. Barberá and G. Clemente, *Food Chem.*, 2004, **92**, 481–489.
14 P. Aranda and J. Llopis in *Nutrition Dietetic: Aspects Sanitarios*, Consejo General de Colegios Oficiales de Farmaceuticos, Madrid, 1993, pp. 183–233.
15 I. Martinez, M. Santaella, G. Ros and J. Periago, *Food Chem.*, 1998, **63**(3), 299–305.
16 J. J. B. Anderson, *J. Nutr.*, 1996, **126**, 1153s–1158s.
17 J. J. Barger-Lux, R. P. Heaney, P. T. Packard, J. M. Lappe and R. R. Reeker, *Clin. Appl. Nutr.*, 1992, **2**, 39–45.
18 C. J. Wyatt, M. E. Hemandez-Lozano, R. O. Mendez and M. E. Valencia, *Nutr. Res.*, 2000, **20**(3), 427–437.
19 A. Lante, G. Lomolino, M. Cagnin and P. Spettoli, *Food Control*, 2004, in the press (DOI:10.1016/j.foodcont.2004.10.010).
20 M. Umetaa, C. E. West and H. Fufaa, *J. Food Compos. Anal.*, 2005, **18**, 803–817.

Anal Bioanal Chem (2005) 382: 1360–1367
DOI 10.1007/s00216-005-3288-z

ORIGINAL PAPER

Jeerawan Promchan · Juwadee Shiowatana

A dynamic continuous-flow dialysis system with on-line electrothermal atomic-absorption spectrometric and pH measurements for in-vitro determination of iron bioavailability by simulated gastrointestinal digestion

Received: 10 February 2005 / Revised: 20 April 2005 / Accepted: 23 April 2005 / Published online: 10 June 2005

Abstract A dynamic continuous-flow dialysis (CFD) method with on-line electrothermal atomic absorption spectrometric (ETAAS) and pH measurements for study of simulated gastrointestinal digestion has been developed for prediction of iron bioavailability. The method used to estimate mineral bioavailability was based on gastric digestion in a batch system then dynamic continuous-flow intestinal digestion. The intestinal digestion was performed in a dialysis bag placed inside a chamber containing a flowing stream of dialyzing solution. Mineral concentration and dialysate pH were monitored by ETAAS and use of a pH meter, respectively. The amount of dialyzed minerals in the intestinal digestion stage was used to evaluate the dialyzability. The dialysis profile and pH change can be used to understand or examine differences between the dialyzability of different food samples. To test the proposed system it was used to estimate the iron dialyzability of different kinds of milk. Iron dialyzability for powdered cow milk, cereal milk, and two brands of soymilk was found to be 1.7, 20.4, 24.9, and 37.7%, respectively. The developed CFD–ETAAS–pH system is a simple, rapid, and inexpensive tool for bioavailability studies, especially for minerals at ultratrace levels.

Keywords Continuous-flow · Dialysis · Gastrointestinal digestion

Abbreviation ETAAS: Electrothermal atomic-absorption spectrometry · CFD: Continuous-flow dialysis

J. Promchan · J. Shiowatana (✉)
Department of Chemistry, Faculty of Science,
Mahidol University, Rama VI Road, Bangkok 10400,
Thailand
E-mail: scysw@mahidol.ac.th
Tel.: +66-2-2015122
Fax: +66-2-3547151

Introduction

Minerals are needed by the body in different amounts, depending on the element, to maintain good health. The terms trace minerals or trace elements can refer to essential, non-essential, or toxic elements which are found in very small amounts in human body [1]. Trace minerals are found in foods from both plant and animal sources. An adequate dietary intake of an essential trace element does not guarantee that the body can meet its needs; absorption efficiency must also be considered. Some food constituents for example phytates, oxalates, tannins, and polyphenols can inhibit absorption of trace elements whereas other food components can promote bioavailability [2–7].

Bioavailability of trace minerals has attracted increasing interest in studies of nutrition. Bioavailability is a term used to describe the proportion of a nutrient in food that can be utilized for normal body functions. Many techniques have been proposed for quantification of bioavailability. The most reliable methods for bioavailability studies are in-vivo measurement of absorption in humans with or without using a labeling technique [7–13]. Human in-vivo studies are, however, time-consuming, very expensive, and complicated, and produce variable results. Laboratory animal in-vivo studies are less expensive but are limited by uncertainties with regard to differences between the metabolism of animals and human. In-vitro methods have several advantages, for example simplicity, rapidity, precision, and low cost, but their results may not always agree with those from real human body mineral absorption studies. Many in-vitro methods were presented in the last half of the twentieth century [14–20]. The in-vitro method developed in 1981 by Miller et al. [16], in particular, has been shown to provide availability measurements that correlate well with human in vivo studies. The method involves simulated gastrointestinal digestion then measurement of dialyzable minerals in the intestinal stage.

This method has been the basis for several in-vitro methods for estimation of the bioavailability of iron and other minerals [18, 19]. In Miller's equilibrium dialysis method the dialyzed components are not continuously removed, as occurs in the intraluminal digestive tract. Continuous-flow dialysis (CFD) in-vitro methods were therefore developed by Wolters et al. [18] and Shen et al. [19] in which dialyzed components were continuously removed. A dynamic multicompartmental computer-controlled in-vitro gastrointestinal-tract model was designed by Minekus et al. [20] to simulate various parts of the digestive tract—stomach, duodenum, jejunum, and ileum. Because the objective of the method was to imitate the whole gastrointestinal tract, it was very complicated and not easy to follow.

In this work, a simple and inexpensive CFD method has been developed. It involves simulated gastric digestion in a batch system then simulated intestinal digestion in a CFD system. The batch system in the gastric digestion stage enables high sample-throughput, because many samples can be digested in parallel. The CFD in the intestinal digestion step enables dialyzable components to be continuously removed for element detection. For on-line detection the system is connected to an electrothermal atomic-absorption spectrometer (ETAAS) and a pH meter to continuously monitor dialyzed mineral content and pH change during dialysis. The objective of using ETAAS as a detector is to enable the determination of minerals at very low levels. Monitoring of pH is necessary to ensure the dialysis pH is close to physiological pH. To evaluate the usefulness of the proposed method the iron dialyzability of different kinds of milk was determined and results were compared those from the widely used equilibrium dialysis method.

Experimental

Chemicals and materials

Deionized water (Milli Q plus, 18.2 MΩ cm^{-1}) was used throughout the experiments. All glassware was washed with liquid detergent, rinsed with water, soaked overnight in 10% HNO_3, rinsed again, and dried. All chemicals were analytical grade.

Pepsin solution was prepared by dissolving 0.16 g pepsin (P-7000, from porcine stomach mucosa) in 1.0 mL 0.1 mol L^{-1} hydrochloric acid.

Pancreatin bile extract (PBE) mixture contained 0.02 g pancreatin (P-1750, from porcine pancreas) and 0.125 g bile extract (B-6831, porcine) dissolved in 5.0 mL 0.1 mol L^{-1} sodium bicarbonate.

Dialysis tubing was prewashed before use. The tubing was boiled for 10 min in 40% ethanol, and washed with distilled water, and rewashed with 0.01 mol L^{-1} EDTA in 2% $NaHCO_3$ solution to remove trace element impurities. The tubing was then rinsed several times with deionized water. The ready-to-use dialysis tubing was kept in 0.001 mol L^{-1} $NaHCO_3$ in the refrigerator (4°C). It was rinsed again a few times with deionized water before use [21].

All Fe(II) working standard solutions were prepared by diluting 1010 mg L^{-1} Fe(II) standard solution (AccuStandard, USA) with 0.001 mol L^{-1} $NaHCO_3$ solution.

Test samples, ultra-high-temperature (UHT) corn milk, UHT cereal milk, UHT soymilk, and powdered cow milk, were obtained from a local supermarket. All milk samples were used as obtained except powdered cow milk, which was prepared by dissolving 25 g in 200 mL deionized water.

Instrument and equipment

The iron content of the solution was determined by means of a Perkin–Elmer Analyst 100 atomic absorption spectrometer equipped with a deuterium arc background corrector and a Perkin–Elmer HGA-800 heated-graphite atomizer. The Perkin–Elmer Model AS-72 autosampler was used to introduce standard and necessary solutions into the graphite tube. Pyrolytically coated graphite tubes with integrated platforms from the same manufacturer were used throughout and measurements were based on peak area. An iron hollow-cathode lamp was operated at 25 mA and the wavelength 248.3 nm was used. The spectral bandwidth was 0.7 nm. The furnace operating conditions for iron measurement are given in Table 1. The atomic signals were monitored by means of a Compaq computer with a Hewlett–Packard 870 printer to print out the analytical data. Standard stock solution (1010 mg Fe L^{-1}) was used to prepare working standard solutions of iron. Peak area was used to construct calibration plots. A six-point calibration plot in the range 0–40 μg Fe L^{-1} was constructed. When peak area under these operating conditions (Table 1) was used, standard solutions in different matrices in this work were found to give the same calibration slope. Therefore, a single calibration plot can be used for samples with different matrices.

An Orion Model PCM500 SensorLink pH Measurement System equipped with a PCMCIA slot laptop was used. The PCMCIA card was connected to a small glass combination electrode (6-mm diameter) from Orion. Commercial standard buffer solutions of pH 4.00 ± 0.01, 7.00 ± 0.01, and 10.00 ± 0.01 from Merck, Germany, were used to calibrate the pH meter.

Table 1 Furnace operating conditions for iron

Step	Temperature (°C)	Ramp/hold time (s)	Argon flow (mL min^{-1})
Drying	150	10/30	250
Pyrolysis	1300	1/10	250
Pre-atomization	500	1/5	250
Atomization	2400	0/5	0
Clean up	2600	1/3	250

An incubator shaker from Grant Instrument, model SS40-D2 (Cambridge, UK), was used to shake and incubate samples at 37 ± 1°C.

Design of the CFD system

A dialysis system was designed to serve three objectives. First, a gradual pH change from 2.0 of gastric digestion to 7.0–7.5 of intestinal digestion within 60 min of the CFD must be achieved. Second, pancreatin-bile extract can be added to the digestion mixture at the time required. Finally, dialyzed components must be continuously removed throughout the duration of the simulated intestinal digestion.

The proposed dialysis system is presented schematically in Fig. 1. A dialysis chamber was designed to enable containment of a dialysis tubing, and through which dialyzing solution could flow during dialysis. The chamber and its cover were constructed from borosilicate glass (ca. 20 cm in length and 0.8 cm inner diameter). Dialysis tubing was Spectro/Por MMCO 12,000–14,000 Da (Thomas Scientific, USA) and dialysis was performed with a piece 17.6 cm long (10 mm flat width). Although larger tubing can be used, this size is preferred to give a large contact surface with the surrounding dialysis solution. The tubing was tied at both ends, one end having silicone rubber tubing of 2 mm inner diameter and 7 cm long inserted for introduction of the sample and the required enzymes. The other end of this silicone tubing was inserted through an aperture in the glass chamber cover to enable convenient addition of a peptic digest sample and pancreatin-bile extract mixture through a three-way valve by means of a syringe. The cover was tightly sealed on to the chamber with a silicone rubber gasket. The dialysis chamber was placed in a water bath at 37 ± 1°C for pancreatic digestion. The dialyzing solution ($NaHCO_3$) was pumped through the chamber using a peristaltic pump (Eyela model MP-3N, Japan). The dialysis flow was adjusted to 1 mL min^{-1}. Dialyzable components in the peptic digest suspension could pass through the dialysis membrane and were carried by the dialyzing solution to the ETAAS sampling cup, to the pH measurement cell, and finally to the fraction collector.

To perform dialysis, the prewashed dialysis tubing was prepared as above. Before adding the peptic digest, the dialysis tubing was flattened to remove any air bubbles or liquid inside using a syringe connected to the silicone tube insert. A peptic digest sample (2.5 g) was then injected through the same silicone rubber tube. The dialyzing solution of optimum concentration flowed through at 1 mL min^{-1}. Although it took approximately 4 min for dialyzing solution to reach the ETAAS sampling cup for first ETAAS detection, this first ETAAS measurement was taken as the amount dialyzed at $t = 0$ in the dialysis profile to indicate the first point of data collection.

ETAAS sampling cup and pH measurement cell

An ETAAS sampling cup (Fig. 1) was constructed from borosilicate glass to have a small inner cone volume to enable real-time measurement of the element in the flowing stream [22]. The i.d. of the inner and outer cones of the sampling cup were 3 and 8 mm, respectively, and the inner cone volume was 60 μL. The dialysate from the CFD system flowed through the inlet at the bottom of the sampling cup, overflowed to the top of the inner cone, and drained to the outlet of the sampling cup. Determination of the concentration of iron (ng mL^{-1}) in the dialysate was performed by an ETAAS with an autosampler which sampled 20 μL dialysate every 2 min (or less frequently when the dialyzed iron concentration was steady at the later stage of dialysis). A pH measurement cell was designed to have a slightly larger size than the microelectrode (6-mm diameter) to enable the microelectrode to fit into the cell using a rubber O-ring. The dialysate flowed into the cell for continuous pH measurement.

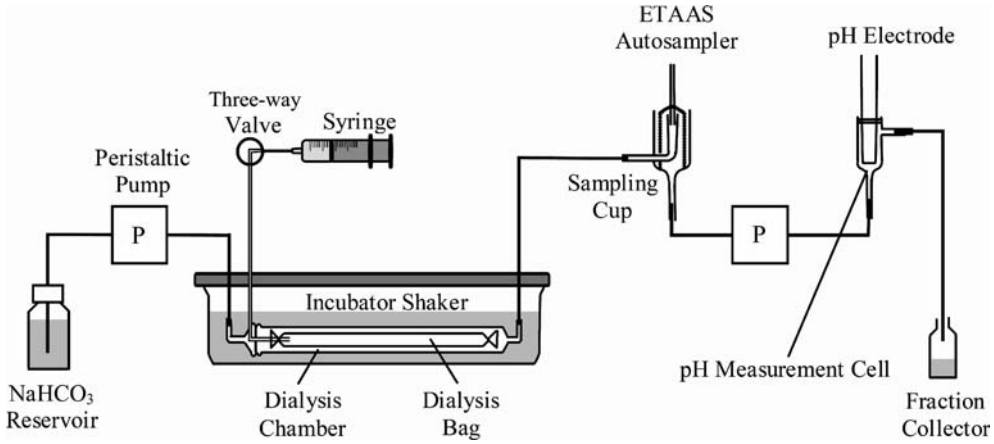

Fig. 1 Diagram of the CFD system with on-line ETAAS and pH measurement

Simulated gastrointestinal digestion procedures

Equilibrium dialysis method

Gastric digestion The in-vitro simulated gastric digestion with equilibrium dialysis was performed according to Miller et al. [16]. Deionized water (5 mL) was added to a test sample (5 mL) in a 125-mL conical flask and the pH was adjusted to 2.0 with 6 mol L^{-1} HCl. The sample was made up to 12.5 g with deionized water and 375 μL freshly prepared pepsin solution was added. The mixture was subsequently incubated in an incubator shaker at 37 ± 1°C for 2 h.

Intestinal digestion After the simulated gastric digestion, a triplicate 2.5 g peptic digest sample was weighed and introduced into the proposed dialysis bags that were placed in glass dialysis chambers. After transferring the peptic digest samples into the dialysis bag, 3.0 mL dialyzing solution was injected to the dialysis chamber. The temperature of the incubator was maintained at 37 ± 1°C. The freshly prepared PBE mixture (625 μL) was added into the dialysis bag via a three-way valve after 30 min intestinal digestion and incubation was continued for an additional 2 h. The dialysate was collected for subsequent determination of iron content.

Determination of the optimum concentration of $NaHCO_3$ The optimum $NaHCO_3$ concentration for equilibrium dialysis can be calculated from titratable acidity [16]. Titratable acidity was defined as the number of equivalents of NaOH required to titrate the amount of digest to a pH of 7.5. It was determined, using standard 0.01 mol L^{-1} NaOH as titrant, on a 2.5 g aliquot of the peptic digest to which 625 μL of PBE mixture had been added.

Continuous-flow dialysis method

Gastric digestion The simulated gastric digestion procedure was the same as the equilibrium method.

Intestinal digestion The system setup as shown in Fig. 1 was used. After simulated gastric digestion 2.5 g peptic digest was weighed and introduced into a dialysis bag. The chamber was connected to the sodium bicarbonate solution reservoir and the collector vials using Tygon tubing and placed in an incubator shaker. The other end of the chamber was connected to a sampling cup for ETAAS and to the pH measurement system. The temperature of the incubator was maintained at 37 ± 1°C. The peristaltic pump was switched on to start the intestinal digestion. The dialyzing solution flow rate was 1 mL min^{-1}. The dialysate from the CFD chamber was analyzed for iron content and pH change by means of ETAAS and a pH meter, respectively. The freshly prepared PBE mixture (625 μL) was added into the dialysis bag via a three-way valve after 30 min intestinal digestion. The dialyzed iron content and pH change were measured for an additional 2 h.

Determination of the optimum concentration of $NaHCO_3$ The optimum $NaHCO_3$ concentration for the CFD method depends on the titratable acidity of the sample and the dialysis flow rate. Titratable acidity was determined as already described. For the dialysis flow rate of 1 mL min^{-1} the optimum concentration of $NaHCO_3$ was calculated by dividing the titratable acidity by 50. This concentration of $NaHCO_3$ was found to change the pH of the dialysate to 5.0 after 30 min of dialysis and gradually increase it to 7.0–7.5 on addition of the PBE mixture.

A reagent blank was analyzed for iron content to correct for impurities in the reagents or enzymes being used (Fig. 2).

Determination of the total iron content of milk samples and in residues after dialysis

A known amount of sample (approx. 1.0 g) was digested using 10.0 mL HNO_3 and 30% H_2O_2 mixture (3:2) at 80°C. Digestion was performed until the mixture was clear. For residues after dialysis, the food suspension after dialysis was transferred from the dialysis tube into a beaker (100 mL) and the dialysis tubing was rinsed with 0.01 mol L^{-1} EDTA (2×3 mL) and 2% HNO_3 (2×10 mL), into the same beaker, before subsequent digestion to furnish a clear solution. The accurate weight of digested samples was reconstituted with deionized water and the iron content was determined by ETAAS.

Calculation of dialyzability

The amount of dialyzed mineral in dialysate from the simulated gastrointestinal digestion was used to calculate the percentage of the total amount of mineral present in the sample (or dialyzability). The dialyzability was calculated according to the equation:

$$\text{Dialyzability}(\%) = [(D - B) \times 100]/(W \times A)$$

where D is the total amount of dialyzed mineral in the dialysate (μg), B the total amount of dialyzed mineral in the blank (μg), W the weight of sample used for intestinal digestion (g), and A the total concentration of mineral in the sample (μg g^{-1}).

For the equilibrium method amounts of dialyzable minerals were calculated as twice the amount dialyzed when the volumes of peptic digest and dialyzing solution were equal, because the dialyzed amount accounted for only one half of the dialyzable iron in equilibrium dialysis [18]. When the volumes were not equal, correction was made accordingly.

In the CFD method the concentration of iron in the dialysate (ng mL^{-1}) was obtained by ETAAS

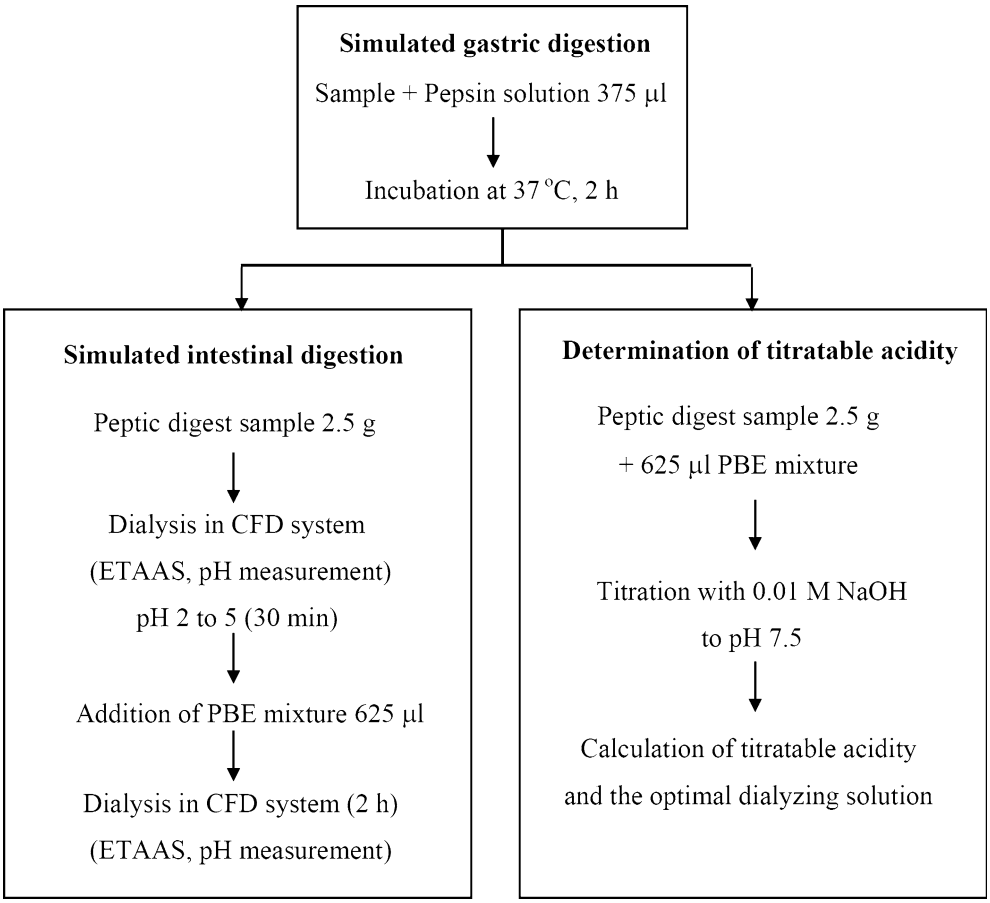

Fig. 2 Flow chart of simulated gastrointestinal digestion with the CFD–ETAAS–pH system

measurement. This concentration represented the concentration of iron in the dialysate at the time of sampling. Because a flow rate of 1 mL min^{-1} was used, the amount of iron in ng min^{-1} was obtained by multiplying the iron concentration in ng mL^{-1} by 1 mL min^{-1}. Total amount of dialyzed iron was determined by integration of the signal in ng min^{-1} through the whole dialysis time using a computer program, Microcal Origin Version 6.0.

Results and discussion

Dialysis profile

On-line ETAAS detection and pH measurement were coupled with the CFD system to enable simultaneous monitoring of low levels of dialyzed minerals and pH change during dialysis.

The dialysis profiles of iron and pH change during dialysis for different kinds of milk are shown in Fig. 3. Iron can gradually dialyze through the semipermeable membrane during intestinal digestion and dialysis decreases as pH increases. The pH of dialysate changed slowly to reach pH 5 in approximately 30 min, similar to physiological conditions in the human intestine [23]. The pH then increased rapidly to 7.0 as a result of PBE addition. After reaching a neutral pH, iron dialysis ceased except for UHT cereal milk and UHT soymilk 2, for which dialysis continued. This is probably because of the different components in these types of milk, which may help promote dialyzability. As a result, UHT soymilk 2 has higher iron dialyzability than UHT soymilk 1 although the total iron content is lower (Table 2).

In Fig. 3a, dialysis profiles for two types of calcium-fortified milk are compared. The results showed that iron dialyzability was very low (1.7%) for powdered cow milk 1 and too low to be determined for powdered cow milk 2. Many researchers have reported that calcium can inhibit iron absorption [11–13, 24]. However, the effect of calcium is complex and the mechanisms by which it reduces iron absorption are unknown. Further study of the effect of added calcium on the dialysis profiles of both elements is in progress to understand the mechanism more clearly.

Dialysis of UHT soymilk (Fig. 3b) also resulted in different profiles for iron. These UHT soymilk samples contained soy protein, different vitamins, and different amounts of calcium. Vitamin C or ascorbic acid has been reported as a most potent enhancer of iron absorption [4, 5]. At high enough concentrations ascorbic acid was found to overcome the inhibitory effect of phytic acid in cereal and in soy formula. Addition of vitamins A and C to a meal was also found to improve iron absorption [6]. Some proteins found in

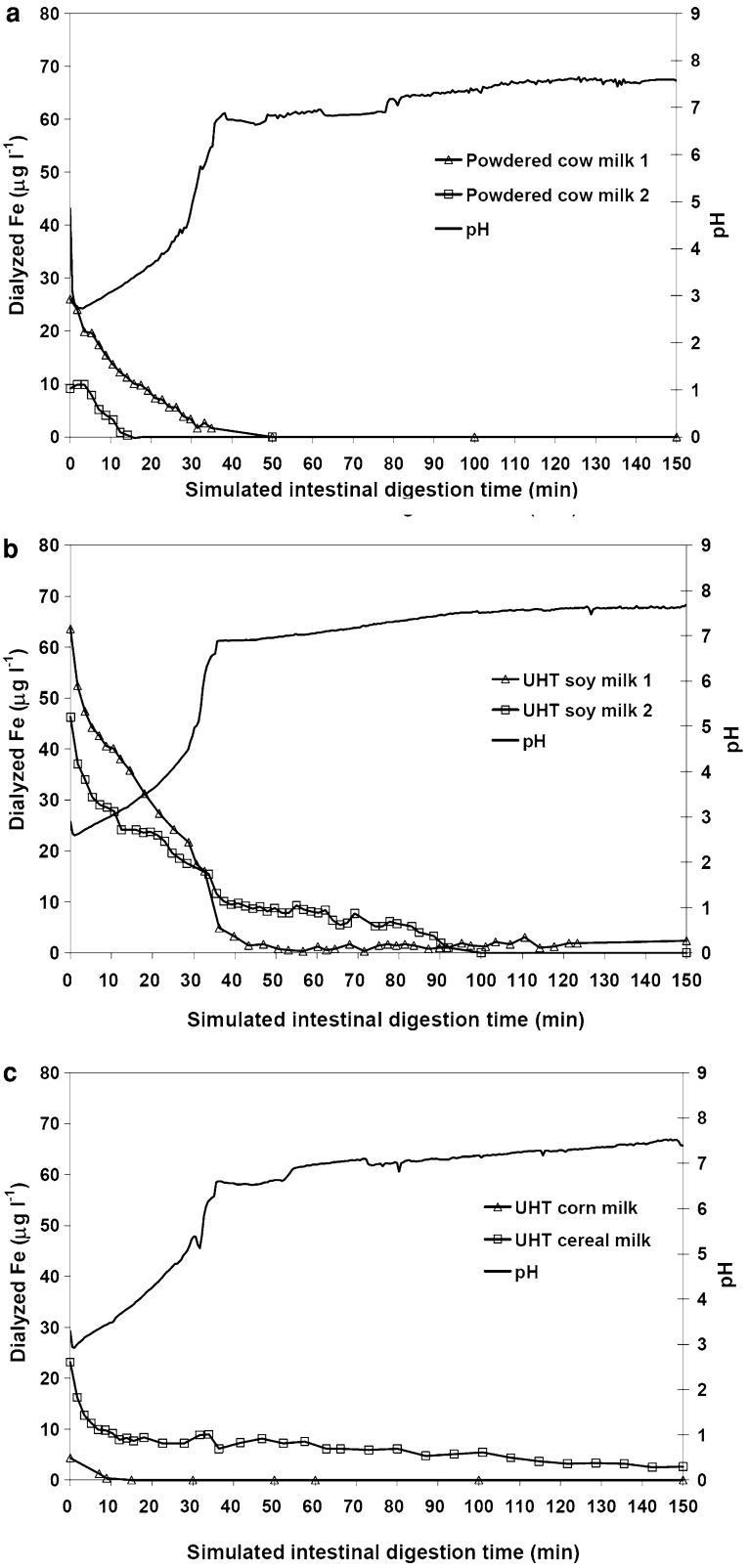

Fig. 3 Dialysis profiles of iron and pH change during continuous dialysis of **a** powdered cow's milk, **b** UHT soymilk and **c** UHT corn milk and UHT cereal milk by means of the CFD–ETAAS–pH system. The dialysis flow rate was 1 mL min^{-1}

soybeans may inhibit iron absorption. The iron dialyzability of soymilk was therefore possibly affected by both inhibitor (calcium and phytate) and enhancer (vitamins A and C).

For UHT cereal milk, iron can be gradually dialyzed until the end of 2.5 h intestinal digestion at which time dialyzed iron from UHT corn milk was too low to be detectable (Fig. 3c). The total iron content of UHT corn

milk was the lowest among the different kinds of milk studied.

The results for iron dialyzability obtained in this study show that dialysis profiles and degrees of dialyzability are different for different kinds of milk. Obviously, dialysis profile is affected by components in the digested meals and this, in turn, results in different degrees of dialyzability. The dialysis profile can be a useful tool for investigation of the effects of food components on dialyzability to provide a better understanding of dialyzability of minerals.

Iron dialyzability for different milk samples

Dialyzability was calculated by summation of dialyzed amounts of iron during intestinal digestion. The results from determination of the iron dialyzability of different kinds of milk by an in-vitro method based on CFD are shown in Table 2. The total iron content was found to vary from 0.8 to 17.1 mg L^{-1}, being highest for iron-fortified powdered cow milk 1 and lowest for UHT corn milk. The iron dialyzability was found to be 1.7% for fortified powdered cow milk 1 and not determinable for powdered cow milk 2 and UHT corn milk, because levels of dialyzable iron were undetectable. The iron dialyzability was 20.4, 24.9, and 37.7% for UHT cereal milk, UHT soymilk 1, and UHT soymilk 2, respectively. The iron dialyzability was higher for UHT soymilk (24.9–37.7%) than for powdered cow milk.

The iron dialyzability of some milk samples (cow milk 1, soymilk 1, and cereal milk) was also determined by the equilibrium dialysis method; the results are presented in the last two columns of Table 2. The iron dialyzability determined by two methods was not significantly different at a confidence level of 95% when tested by the *t*-test method.

Method validation by analytical recovery study

Because no reference material with bioavailability data is available, validation of the proposed method can be achieved only by studying analytical recoveries of the mineral of interest. A milk sample was subjected to the proposed analytical procedure to determine the dialyzable iron in the dialysate and the non-dialyzable iron in the retentate. The non-dialyzable iron in the retentate was determined by transferring the food suspension in the dialysis tubing into a beaker (100 mL) and rinsing the dialysis tubing with 0.01 M EDTA (2×3 mL) and with 2% HNO_3 (2×10 mL), into the same beaker, before subsequent digestion and iron determination. The total iron content of the samples were also determined after total digestion of the milk samples. The results are given in Table 3. It can be seen that dialyzed and non-dialyzed amounts differ slightly between replicates, probably because of inhomogeneity of the sample being used. Recoveries were between 77.9 and 90.5% with an average of 83.6%. This is thought to be partly because of incomplete removal of iron from the dialysis bag to determine the retained fraction despite repeated washing. This error will not, however, affect the percentage dialyzability results.

Conclusions

A dynamic in-vitro simulated gastrointestinal digestion method for determination of iron dialyzability was developed by connecting a simple CFD system to ETAAS and pH measurement. The system can be used for simultaneous monitoring of dialyzed metal concentration and dialysate pH during dialysis. The CFD–ETAAS–pH system was shown to be a practical and inexpensive tool for studies of dialyzability and

Table 2 Total content, amount dialyzed, and dialyzability of iron for different kinds of milk as determined by on-line CFD-ETAAS and equilibrium dialysis methods ($n = 3$)

Sample	Total iron (mg L^{-1})	Dialyzed iron			
		CFD		Equilibrium dialysis	
		mg L^{-1}	Dialyzability (%)	mg L^{-1}	Dialyzability (%)
Powdered cow milk 1 (calcium and iron fortified)	17.1 ± 0.7	0.28 ± 0.04	1.7 ± 0.3	0.19 ± 0.03	1.1 ± 0.2
Powdered cow milk 2 (calcium fortified)	1.1 ± 0.1	< 0.09 (not detectable)	–	ND	ND
UHT soymilk 1 (high iron, vitamins B, D, E, and soy protein)	5.1 ± 0.0	1.27 ± 0.08	24.9 ± 1.6	1.18 ± 0.15	23.2 ± 3.2
UHT soymilk 2 (high calcium, soy protein, and vitamins A, C and E)	3.0 ± 0.3	1.13 ± 0.07	37.7 ± 2.4	ND	ND
UHT corn milk (high vitamins A and E)	0.80 ± 0.10	< 0.05 (not detectable)	–	ND	ND
UHT cereal milk (high calcium, vitamin B1, B2, E, and soy protein)	4.1 ± 0.3	0.84 ± 0.01	20.4 ± 0.4	0.81 ± 0.03	19.8 ± 0.6

ND for not determined

Table 3 Analytical recovery of iron from powdered milk sample (three individual replicates are shown)

Sample	Dialyzed		Non-dialyzed		Recovery (%)
	Amount (mg kg^{-1})	Dialyzability (%)	Amount (mg kg^{-1})	Remaining (%)	
Powdered milk-based formula	3.0	4.8	45.3	73.1	77.9
	2.1	3.4	54.0	87.1	90.5
	3.1	5.1	48.0	77.4	82.4
Average	2.7 ± 0.6	4.4 ± 0.9	49.1 ± 4.5	79.2 ± 7.2	83.6 ± 6.4

Total iron 62.0 ± 1.0 mg kg^{-1}

bioavailability. Information about mineral dialyzability can be useful for nutritional evaluation of foods and for study of the effect of food components on mineral bioavailability. Knowledge of nutrient bioavailability is useful for managing mineral intake and for reduction of the health risk from mineral deficiencies.

Acknowledgements The authors are grateful for financial support from the Thailand Research Fund and the Postgraduate Education and Research Program in Chemistry, Higher Education Development Project, Ministry of Education.

References

1. Smolin LA, Grosvenor MB (1994) Nutrition science and applications. Saunders College Publishing, PA, USA
2. Scalbert A, Morand C, Manach C, Remesy C (2002) Biomed Pharmacother 56:276–282
3. Glahn RP, Wortley GM (2002) J Agric Food Chem 50:390–395
4. Lynch SR (1997) Nutr Rev 55:102–110
5. Hurrell RF (1997) Eur J Clin Nutr 51:S4–S8
6. Garcìa-Casal MN, Layrisse M, Peña-Rosas JP, Ramírez J, Leets I, Matus P (2003) Nutr Res 23:451–463
7. Tuntawiroon M, Sritongkul N, Brune M, Rossander-Hulten L, Pleehachinda R, Suwanik R, Hallberg L (1991) Am J Clin Nutr 53:554–557
8. Uicich R, Pizarro F, Almeida C, Díaz M, Boccio J, Zubillaga M, Carmuega E, O'Donnell A (1999) Nutr Res 19:893–897
9. Atkinson SA, Shah JK, Webber CE, Gibsom IL, Gibson RS (1993) J Nutr 123:1586–1593
10. House WA (1999) Field Crop Res 60:115–141
11. Wienk KJH, Marx JJM, Beynen AC (1999) Eur J Nutr 38:51–75
12. Van Campen DR, Glahn RP (1999) Field Crop Res 60:93–113
13. Reddy MR, Hurrell RF, Cook JD (2000) Am J Clin Nutr 71:937–943
14. Narasinga Rao BS, Prabhavathi T (1978) Am J Clin Nutr 31:169–175
15. Lock S, Bender AE (1980) Brit J Nutr 43:413–420
16. Miller DD, Schricker BR, Rasmussen RR, Van Campen D (1981) Am J Clin Nutr 34:2248–2256
17. Schricker BR, Miller DD, Rasmussen RR, Van Campen D (1981) Am J Clin Nutr 34:2257–2263
18. Wolters MGE, Schreuder HAW, Van Den Heuvel G, Van Lonkhuijsen HJ, Hermus RJJ, Voragen AGJ (1993) Br J Nutr 69:849–861
19. Shen LH, Luten J, Robberecht H, Bindels J, Deelstra H (1994) Lebensm Unters Forsch 199:442–445
20. Minekus M, Marteau P, Havenaar R, Huis in't Veld JHJ (1995) ATLA 23:197–209
21. Chaiwanon P, Puwastien P, Nitithamyong A, Sirichakwal PP (2000) J Food Comp Anal 13:319–327
22. Chen B, Beckett R (2001) Analyst 126:1588–1593
23. Ekmekcioglu C (2002) Food Chem 76:225–230
24. Hallberg L, Brune M, Erlandsson M, Sandberg AS, Rossander-Hulten L (1991) Am J Clin Nutr 53:112–119

Available online at www.sciencedirect.com
ScienceDirect
Talanta 71 (2007) 1710–1719
Talanta
www.elsevier.com/locate/talanta

A multisyringe flow-through sequential extraction system for on-line monitoring of orthophosphate in soils and sediments

Janya Buanuam [a], Manuel Miró [b,*], Elo Harald Hansen [c], Juwadee Shiowatana [a], José Manuel Estela [b], Víctor Cerdà [b]

[a] *Department of Chemistry, Faculty of Science, Mahidol University, Rama VI Road, Bangkok 10400, Thailand*
[b] *Department of Chemistry, Faculty of Sciences, University of the Balearic Islands, Carretera de Valldemossa km. 7.5, E-07122 Palma de Mallorca, Illes Balears, Spain*
[c] *Department of Chemistry, Technical University of Denmark, Kemitorvet, Building 207, DK-2800 Kgs. Lyngby, Denmark*

Received 16 May 2006; received in revised form 29 July 2006; accepted 1 August 2006
Available online 15 September 2006

Abstract

A fully automated flow-through microcolumn fractionation system with on-line post-extraction derivatization is proposed for monitoring of orthophosphate in solid samples of environmental relevance. The system integrates dynamic sequential extraction using 1.0 mol l^{-1} NH_4Cl, 0.1 mol l^{-1} NaOH and 0.5 mol l^{-1} HCl as extractants according to the Hieltjes–Lijklema (HL) scheme for fractionation of phosphorus associated with different geological phases, and on-line processing of the extracts via the Molybdenum Blue (MB) reaction by exploiting multisyringe flow injection as the interface between the solid containing microcolumn and the flow-through detector. The proposed flow assembly, capitalizing on the features of the multicommutation concept, implies several advantages as compared to fractionation analysis in the batch mode in terms of saving of extractants and MB reagents, shortening of the operational times from days to hours, highly temporal resolution of the leaching process and the capability for immediate decision for stopping or proceeding with the ongoing extraction. Very importantly, accurate determination of the various orthophosphate pools is ensured by minimization of the hydrolysis of extracted organic phosphorus and condensed inorganic phosphates within the time frame of the assay. The potential of the novel system for accommodation of the harmonized protocol from the Standards, Measurement and Testing (SMT) Program of the Commission of the European Communities for inorganic phosphorus fractionation was also addressed. Under the optimized conditions, the lowest detectable concentration at the 3σ level was $\leq$0.02 mg P l^{-1} for both the HL and SMT schemes regardless of the extracting media. The repeatability of the MB assay was better than 2.5% and the dynamic linear range extended up to 7.0 mg P l^{-1} in NH_4Cl and NaOH media and 15 mg P l^{-1} whenever HCl is utilized as extractant for both the HL and SMT protocols.

Keywords: Multisyringe flow injection; Microcolumn sequential extraction; Orthophosphate; Soil; Sediment

1. Introduction

Assessment of the bioavailability of macronutrients and trace elements in environmentally significant solid substrates is a key issue for ecology and environmental management. It is now widely accepted that the accessibility of the various elements for biota uptake depends strongly on their specific chemical forms and binding sites. A commonly used technique for identification of the phase associations of elements in solid phases is based on the application of sequential extractions [1–5]. These methods involve the rational use of a series of moderately selective reagents for releasing of targeted species from particular mineralogical fractions into the liquid phase under simulated natural and/or anthropogenic modifications of the environmental conditions. Sequential extraction procedures have been traditionally performed in a batchwise fashion. Yet, in the last decade, it has been realized that the conventional, manual procedures cannot mimic environmental scenarios accurately because naturally occurring processes are always dynamic, rather than static as they are identified by the traditional equilibrium-based approaches.

Recent trends have been focused on the development of alternative methods aimed at mimicking environmental events more correctly than their classical extraction counterparts [6]. Several

* Corresponding author. Tel.: +34 971 259576; fax: +34 971 173426.
E-mail address: manuel.miro@uib.es (M. Miró).

0039-9140/$ – see front matter © 2006 Elsevier B.V. All rights reserved.
doi:10.1016/j.talanta.2006.08.007

attempts have been made on the characterization and evaluation of dynamic (non-steady-state) partitioning methods, mostly exploiting continuous-flow or flow injection systems, where fresh portions of leaching agents are continuously provided to small containers or columns containing the solid material [7–18]. Dynamic approaches should be regarded as appealing avenues for fractionation assays not only because they alleviate the shortcomings of batch procedures including analyte re-adsorption and limited information on the size of actual available pools, but at the same time result also in improved precision and sample throughput. Furthermore, the overall leaching process may be monitored as a function of the exposure time, giving rise to a more realistic insight into the extractability of elements from different geological reservoirs. As a consequence of the development of flow-based extraction approaches, on-line leachate measurements are readily applicable, as deduced from current trends in the field [9,12–14,16,18,19]. However, most of the works capitalize on hyphenated analytical methods based on coupling of the miniaturizated column extraction manifold to continuously operating atomic spectrometers, such as flame atomic absorption spectrometry, inductively coupled plasma-mass spectrometry or inductively coupled plasma-atomic emission spectrometry, whereby the on-line generated extracts are directly injected into the detection system without any further treatment [9,13,14,16,18,19].

As a result of the precise fluidic control via syringe pumps, the second generation of flow injection (FI), namely, sequential injection (SI) analysis [20] has opened for new avenues in miniaturisation of sample processing including fractionation of solid samples [21]. While most FI-procedures employ continuous, uni-directional pumping of solutions, SI is based on exploiting programmable, bi-directional discontinuous flow as coordinated and controlled by a computer. Despite the well-recognized advantages of SI-microcolumn extraction as compared to its FI counterpart in terms of ruggedness, reagent consumption, precise handling of extracts and selection of the fractionation mode [6,22,23], automated post-column derivatization, which may be indispensable for macronutrient monitoring, is inherently hindered in SI due to the requirements of aspiration of the overall solutions into a holding coil [24].

To circumvent the above drawbacks, a hybrid flowing stream approach, the so-called multisyringe flow injection (MSFI) analysis [25–27], is here proposed as the interface between the microcolumn system and detector for on-line microfluidic manipulation of leachates and reagents. To the best of our knowledge, MSFI, which compiles the advantageous features of FI and SI systems, has not been exploited for dynamic fractionation assays so far.

The hyphenated MSFI-microcolumn set-up has been assembled for automated flow-through partitioning and accurate determination of the content of bioavailable forms of orthophosphate in soils and sediments utilizing the Molybdenum Blue method for extract processing. Although environmental solids contain both organic and inorganic forms of phosphorus [28,29], the latter are most relevant as a consequence of the well-known contribution to euthrophication [30]. In the terrestrial environment, phosphorus is an essential nutrient to support the plant growth; yet, direct uptake of organic forms is regarded to be unlikely. For the very same reason, it is essential that the analytical approach used ensures that distinction between readily available inorganic phosphorus and organic bound phosphate reliably can be accomplished.

In this communication, the potential of the MSFI set-up for accommodation of two sequential extraction schemes involving different operationally defined extracting conditions is assessed. In this context, the Hieltjes–Lijklema (HL) procedure [31] and the harmonized protocol from the Standards, Measurement and Testing (SMT) program of the European Commission [32] were selected and conducted in a dynamic fashion. Careful optimization of the chemical variables for the derivatization reactions is regarded to be crucial for appropriate performance of the analyzer due to the extreme pH conditions of the extracts obtained on-line in the various partitioning steps, not only to attain the desired selectivity, especially in regard to the presence of silicon, but also ensure the distinction between orthophosphate and organic-bound phosphorus.

2. Experimental

2.1. Instrumentation

The flow manifold devised for dynamic microcolumn fractionation and on-line spectrophotometric determination of orthophosphate is shown in Fig. 1. It comprises a 5000-step syringe pump (SP) (Crison Instruments, Alella, Barcelona, Spain) for handling of the leaching reagents and performance of fractionation analysis; a 10-port multiposition selection valve (SV, Valco Instruments, Houston, TX) for selection of the appropriate extractant, and a multisyringe piston pump (MSP, MicroBu 2030, Crison Instruments) for on-line post-column derivatization of the extracts. The automatic SP is furnished with a 5 ml syringe (Hamilton, Switzerland) and a three-way solenoid valve at its head (SP1), which allows connection with the manifold or the carrier (water) reservoir. The central port of the SV is connected to SP via a holding coil (HC; used to house the selected extractant), which consists of a 1.42 m long PTFE tubing (1.5 mm i.d.), with an inner volume of 2.5 ml.

The MSP is equipped with four syringes (S1-S4) of 5, 2.5, 2.5 and 2.5 ml, respectively, whose pistons are connected in block to the same stepper motor. The solenoid commutation valves (V1–V4) (N-Research, Caldwell, NJ) placed at the head of the syringes permit the connection of the liquid drivers with the manifold (On) or with reagent reservoir (Off) regardless of the motion of the piston pump. This module also incorporates two additional discrete three-way solenoid valves (V5 and V6) for effecting soil extraction and on-line extract analysis under optimum experimental conditions.

All the connections including the extract loop and knotted reactors (KR) are made from PTFE tubing of 0.87 mm i.d. The length of the extractant loop, KR1 and KR2 are 42, 65 and 51 cm, respectively, corresponding to ca. 250, 385 and 300 μl, respectively.

A diode-array spectrophotometer (Hewlett-Packard HP8452A) equipped with a flow-through cell (18 μl inner

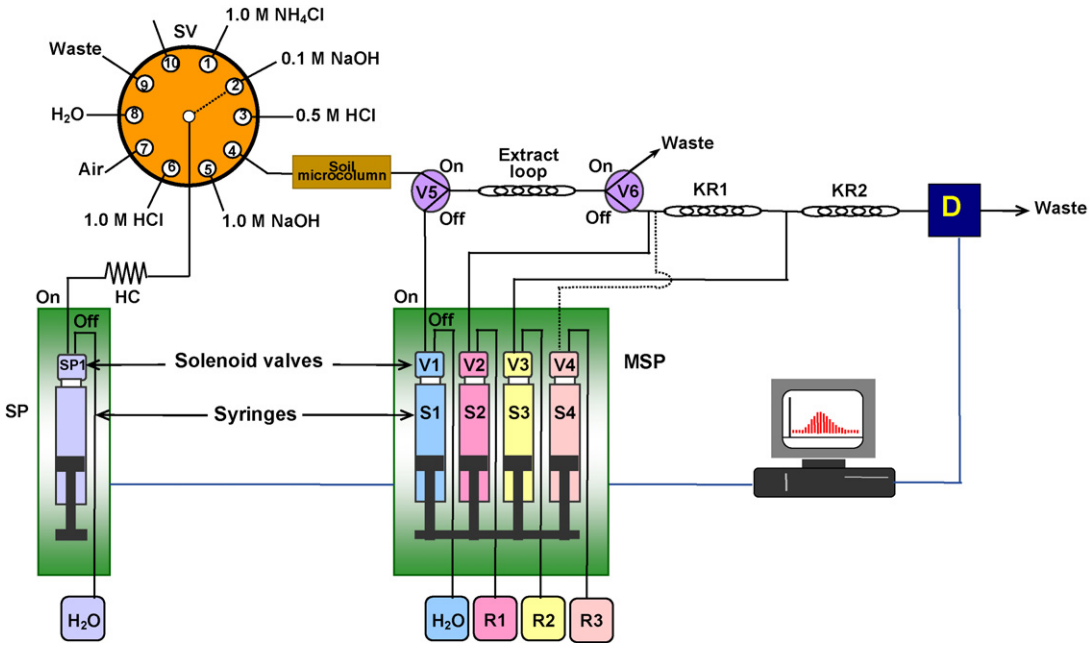

Fig. 1. Schematic diagram of the hybrid flow-through microcolumn extraction/MSFI system for automated fractionation and on-line determination of orthophosphate. R1: 6 g l^{-1} ammonium molydate + 0.125% (w/v) oxalic acid in 0.3 M H_2SO_4 (for HL scheme) or 6 g l^{-1} ammonium molydate + 0.25% (w/v) oxalic acid in 1.0 M H_2SO_4 (for NaOH-P in SMT); R2: 0.15 g l^{-1} $SnCl_2$ + 0.94 g l^{-1} $N_2H_4{\cdot}H_2SO_4$ in 0.25 M H_2SO_4; R3: 6 g l^{-1} ammonium molybdate in water (for HCl-P in SMT). SP: syringe pump; MSP: multisyringe pump; SV: selection valve, V: solenoid valve, KR: knotted reactor, D: detector.

volume, 1 cm optical path) is used as a detector. The analytical and reference wavelengths for monitoring of the Molybdenum Blue (MB) complex and minimization of Schlieren effects, respectively, are set at 690 and 530 nm. The transient spectrophotometric signals are acquired via an HP–IB interface at a frequency of 1.00 Hz. Instrumental control and data acquisition are performed using the software package AutoAnalysis 5.0 (Sciware, Spain).

2.2. Flow-through microcolumn assembly

The design of the extraction microcolumn has been described in detail in a previous work [22]. Made of PEEK, it comprises a central dual-conical shaped sample container for facilitating fluidized-bed like mixing conditions. The entire unit is assembled with the aid of filter supports and caps at both ends. The membrane filters (Fluoropore™, Millipore, 13 mm diameter with 0.45 and 1.0 μm pore sizes for sediment and soil samples, respectively) used at both ends of the extraction microcolumn allowed solutions and leachates to flow freely through but retained the particulate matter. Solid amounts up to 300 mg can be automatically processed without clogging effects as reported elsewhere [19].

2.3. Reagents, solutions and samples

All chemicals were of analytical-reagent grade and used as received. Solutions were prepared with double distilled water. A stock standard solution of orthophosphate (100 mg P l^{-1}) was prepared from KH_2PO_4 (Merck). Working solutions were prepared by stepwise dilution of the stock phosphorus solution. A stock standard solution of silicon (10 g Si l^{-1}) was prepared from $Na_2SiO_3{\cdot}5H_2O$, and diluted standards were used for the investigation of the effect of silicate on the analytical readouts.

The chemical extractants used in both the HL and SMT sequential extraction schemes are summarized in Table 1 along with the geological phosphorus fractions released.

The reagent utilized in the HL scheme (R1) for post-column formation of molybdophosphoric acid was composed of 6 g l^{-1} ammonium molybdate (Panreac) in 0.3 M H_2SO_4 (Merck) containing 0.125% (w/v) oxalic acid (Probus). For the determination of HCl and NaOH extractable phosphorus in the SMT scheme, a solution of 6 g l^{-1} ammonium molybdate was prepared in water (R3) and in 1.0 M H_2SO_4 containing 0.25% (w/v) oxalic acid (R1), respectively. A solution containing 0.15 g l^{-1} $SnCl_2$ (Scharlau) and 0.94 g l^{-1} hydrazine sulphate (Sigma) in 0.25 M H_2SO_4 (R2) was employed for on-line reduction of the molyb-

Table 1
Leaching reagents and corresponding phosphorus fractions in two extraction procedures

Procedure	Step I	Step II	Step III
Hieltjes–Lijklema	1.0 M NH_4Cl, pH 7 (Labile P)	0.1 M NaOH (Fe and Al-bound P)	0.5 M HCl (Ca-bound P)
SMT	1.0 M NaOH (Fe and Al-bound P)	1.0 M HCl (Ca-bound P)	

dophosphoric acid to the blue-coloured MB complex regardless of the fractionation scheme and extraction medium.

Two certified reference materials, namely SRM 2704 and SRM 2711, from the National Institute of Standards and Technology (NIST) were used for traceability studies. The SRM 2704 is a sediment collected from the Buffalo River in the area of the Ohio Street Bridge, NY, with a particle size distribution of 38–150 μm while the SRM 2711 is a pasture soil collected in the till layer of a wheat field (Montana, MT) with particle size <74 μm. The conical microcolumn was packed, in both cases, with 50 mg solid samples, the estimated free column volume being 250 μl.

2.4. Dissolution of solid residues and samples

Residues leftover after the sequential extraction schemes, and extracts collected downstream following post-column derivatization, were digested for quantitation of fixed and total released phosphorus, respectively. The microwave digestion procedure used can be regarded as a modified version of the EPA Method 3051 [33], named microwave-assisted acid digestion for sediments, sludges, soils, and oils. Hence, digestions were performed in a closed-vessel microwave system (Milestone, model MLS-1200 Mega, Italy) using 1.0 ml of concentrated HNO_3 (65%, Scharlau) and 3.0 ml of concentrated HCl (30%, Scharlau). The microwave digestion program consists of five steps each lasting 5 min. The power program applied is detailed as follows: 250 W/400 W/650 W/250 W/0 W. After cooling, if needed, the digests were filtered through 0.45 μm cellulose acetate filters (Minisartfilters, Sartorius, Göttinger). The clear digests were made up to 50 ml and the content of orthophosphate was determined by spectrophotometry using a batchwise standard addition method.

The pseudo-total (aqua regia) phosphorus content in the NIST 2711 was determined using the microwave digestion conditions detailed above.

2.5. General procedure for flow-through sequential extraction

The programmable flow-through fractionation assays were conducted with the aid of SP and SV. In the HL scheme, firstly, the HC was flushed with carrier (water), whereupon a 100 μl air plug from port 7 of SV and 2.0 ml of 1.0 M NH_4Cl from port 1 were consecutively aspirated into HC. Afterward, V5 and V6 were turned 'On' and SP was set to dispense 250 μl of 1.0 M NH_4Cl (which matches the free column volume) from HC through the microcolumn at a flow rate of 3.0 ml min^{-1}, allowing dynamic extraction to take place. The resulting leachate was stored into the extract loop and subsequently swept into the MSFI network for post-column derivatization and on-line determination of orthophosphate using a multicommutation protocol. The program was initially designed for eight cycle runs (equivalent to 2.0 ml of extractant volume) but the operational sequence proceeds until quantitative stripping of labile phosphorus forms.

Prior to continuing with the ensuing HL extraction step, a washing protocol is implemented by aspiration of 100 μl of air and 2.0 ml of H_2O from port 7 and 8, respectively, into HC, and using the same procedure described above for flow-through extraction. Thereafter, the next extractant (viz., 0.1 M NaOH or 0.5 M HCl) is aspirated repeatedly from the respective valve port and delivered to the soil containing microcolumn until completion of the phosphorus extraction.

For the SMT protocol, the dynamic fractionation was performed using an identical operational sequence with 1.0 M NaOH and 1.0 M HCl as leaching reagents.

2.6. Multicommutation protocol for on-line post-column derivatization

Two different multicommutation flow modalities for on-line injection of MB reagents, the so-called merging zones and sandwich-based approaches, were assayed. In both cases, switching of solenoid valves was effected during a single forward displacement of the piston bar of the MSFI pump. Both operational procedures are thoroughly described in the following:

2.6.1. Merging zones mode

As the name implies, the multicommutation protocol was programmed to merge the extract with the two reagent zones for development of the MB reaction as detailed in Table 2. After collection of the leachate in the extract loop, V1 and V2 were switched to 'On' while V5 and V6 were synchronously switched to 'Off'. As a result, the orthophosphate zone merged with a well-defined plug of ammonium molybdate to yield the heteropolyacid species in KR1. Subsequently, V3 was activated to 'On', whereby the reaction zone reaching the next confluence point overlapped with the reducing $SnCl_2$ segment to form the blue-coloured MB complex in KR2. The interdispersed zones were finally delivered downstream to the flow-through diode-array spectrophotometer by the carrier contained in S1, and the blue complex was monitored at 690 nm. Whenever the analysis

Table 2
Multicommuted merging zone protocol for on-line post-column derivatization

Multicommutation step	Solenoid valve position					Reagent (μl)		Carrier (μl)	Total flow rate (ml min^{-1})
	V1	V2	V3	V4	V5	R1	R2		
Merging of the extract and R1	On	On	Off	Off	Off	80	–	160	6.75
Delivery of the reaction zone to KR2	On	Off	Off	Off	Off	–	–	160	4.50
Merging of the reaction zone with R2	On	Off	On	Off	Off	–	120	240	6.75
Delivery of the MB zone to detector	On	Off	Off	Off	Off	–	–	2600	4.50

Table 3
Multicommuted sandwich-type protocol for on-line post-column derivatization

Multicommutation step	Solenoid valve position					Reagent (μl)		Carrier (μl) (S1)	Total flow rate (ml min^{-1})
	V1	V2	V3	V4	V5	R1	R2		
Fronting zone of R1	Off	On	Off	Off	Off	25	–	–	2.25
Simultaneous delivery of extract and R1	On	On	Off	Off	Off	80	–	160	6.75
Delivery of the rear end of extract into MSFI network	On	Off	Off	Off	Off	–	–	90	4.50
Tailing zone of R1	Off	On	Off	Off	Off	40	–	–	2.25
Injection of R2	On	Off	On	Off	Off	–	160	320	6.75
Delivery of the MB zone to detector	On	Off	Off	Off	Off	–	–	2440	4.50

was completed, all valves were returned to their original position for starting the following fractionation assay.

2.6.2. Sandwich-based mode

The multicommutation protocol involves the injection of two zones of molybdate which are stacked at each end of the leachate plug. The automated MSFI-multicommuted protocol using a sandwiched-based injection is summarized in Table 3. The method started when V2 was activated to 'On' and S2 was set to dispense 25 μl of molybdate into KR1. Thereafter, the combined extract/reagent zone was dispensed downstream. A second plug of molybdate (namely, 40 μl) was injected at the rear end of the leachate for sandwiching of the phosphorus containing segment. The reduction of molybdophosphoric acid to the Molybdenum Blue complex was performed in a merging zone fashion. To this end, 160 μl of $SnCl_2$ were injected at the front end of the interdispersed zone, and the transient signal of the MB complex was recorded by the detector.

3. Results and discussion

3.1. Configuration of the flow network for post-column phosphorus derivatization

3.1.1. Implementation of the HL sequential extraction scheme

In this three-step partitioning scheme, 1.0 M NH_4Cl, 0.1 M NaOH and 0.5 M HCl are used as leaching reagents for consecutive extraction of phosphorus pools associated with different geological phases. The flow system was devised aimed at monitoring the orthophosphate, released on-line, via the MB method. Preliminary experiments were carried out for optimization of the MSFI configuration attending the variable chemical composition of the extracts, the volume of which was maintained at 250 μl. Two different reagent injection modalities, namely, the merging zones and the sandwich-type approaches, were assayed as described under Experimental. The merging zones was finally selected over the sandwich mode because the axial interdispersion between segments is not favored in a knotted coil [34,35], thus rendering double peak profiles.

The effect of MB reagent volumes (viz., ammonium molybdate and tin(II) chloride) on the analytical readouts was investigated taking into consideration the different sizes of the various syringes. The analytical sensitivity improved by 75% when increasing the size of the molybdate plugs from 40 to 80 μl, and remained constant up to 130 μl. This might be attributed to the compensation of the better radial mixing of the reagent and extract plugs with the higher dilution of the extract for volumes above 80 μl. Reagent volumes above 130 μl are unnecessary for the present design because they lead to undue dilution. Similar trends were obtained for the optimization of tin(II)chloride volume. To prevent excessive consumption of reagents, the multicommutation protocol was programmed to merely inject 80 μl ammonium molybdate and 120 μl tin(II) chloride per assay.

The influence of the flow rate on the on-line MB derivatization reaction was evaluated over the range from 3.0 to 5.0 ml min^{-1} (for S1) for the three extractant media of the HL scheme. The higher the flow rate the lower was the yield for MB formation, which is not surprising considering the relative slow reaction rate of the derivatization reaction. In fact, the peak height dropped by 20% when increasing the flow rate from 3.0 to 4.5 ml min^{-1}. Yet, the higher the flow rate the lower is the yield of the competitive reaction for generation of the interfering molybdosilicate species and the better is the analytical throughput. Taking into account the variable sensitivity of the MB method in the various leachate solutions (see below) and the stripping of silicate from solid substrates in alkaline medium, the flow rate was fixed to 4.5 ml min^{-1} for processing of the extracts obtained in the first two steps of the HL method. Regarding the apatite-phosphate fraction, it should be born in mind that the kinetics of formation of molybdophosphoric acid are not favoured in the acidic leachate medium. Therefore, a flow rate of 3.0 ml min^{-1}, that can be programmed automatically, was utilized for monitoring of the orthophosphate released in the last step of the HL scheme.

3.1.2. Implementation of the SMT sequential extraction scheme

Within the framework of the Standards, Measurement and Testing Programme of the European Commission, a batch extraction protocol for fractionation of phosphorus in environmental solids was harmonized in order to improve the reproducibility among laboratories [32]. The so-called SMT protocol was originally designed to obtain five phosphorus fractions, namely, total phosphorus (TP), inorganic phosphorus (IP), organic phosphorus (OP), apatite phosphorus (Ca-bound P) and non-apatite phosphorus (Al and Fe-bound P). It should be taken into account that some of the SMT partitioning steps are performed in a single rather than sequential manner and that the calcination of the solid residue as demanded for the TP and OP assays cannot be effected in an on-line fashion. Consequently,

the potential implementation of the SMT fractionation assays related to the measurement of the inorganic (apatite + non-apatite) phosphorus fractions was ascertained. These two fractions are regarded as the most relevant ones for assessing the readily available phosphorus for plant uptake.

The SMT protocol is characterized for endorsing more aggressive leachants as compared with the HL scheme. The immediate consequence is that the optimal MSFI operational conditions for the HL fractionation as detailed above cannot be extrapolated directly to the SMT partitioning. The use of 1.0 M rather than 0.1 M NaOH for leaching of phosphorus associated to hydrous oxides of Al and Fe (non-apatite phosphorus) facilitates the concomitant release of large amounts of silicate. Actually, a 20% increase in the analytical signals was detected whenever the molybdate reagent for HL containing 0.125% (w/v) oxalic acid in 0.3 M H_2SO_4 was utilized for analyzing a 1.0 mg P l^{-1} standard containing 200 mg Si l^{-1} in 1.0 M NaOH. It is known that the interference of silicate on the orthophosphate MB determination can be minimized by increasing both the acidity of the reaction medium and the concentration of the masking organic acid [36–39]. The effect of the concentration of sulphuric acid was thus evaluated from 0.3 to 1.5 M while that of oxalic acid from 0.125 to 0.25% (w/v). Yet, since the acidity has opposite effects on the selectivity and sensitivity of the molybdophosphate formation [36–38], the molybdate reagent was finally prepared in a 1.0 M H_2SO_4 medium containing 0.25% (w/v) oxalic acid. Under these experimental conditions, silicate was tolerated up to 400 mg Si l^{-1} at the 10% interference level.

As to the SMT apatite fraction, the method's sensitivity using the HL reagent decreased dramatically as a result of the slow development of the reaction for molybdophosphoric acid formation under strong acidic conditions. Therefore, the heteropolyacid forming reagent was prepared in distilled water and the reaction flow rate was affixed at 3.0 ml min^{-1}. No appreciable increase of blank signals was detected, thus indicating that the acidity of the extractant suffices for preventing the self-reduction of molybdate. No oxalic acid was here added because of the negligible stripping of silicate from solids at low pH [40].

Although different reagents are needed for monitoring of the inorganic phosphorus in the HL and SMT extracts, a single MSFI assembly was arranged with no need for neither manual manipulations of reagents and leachates nor the changing of the composition of the carrier solutions for the various assays as demanded in previous flow systems for analyzing phosphorus containing soil solutions [40,41]. These facts emphasize the flexibility of MSFI for automated performance of derivatization reactions regardless of the variable chemical composition of the extracts in both fractionation schemes.

Fig. 2 illustrates the extraction patterns as obtained by on-line MSFI analysis of minute volumes of leachate (namely, 250 μl) for SRM 2704 and SRM 2711 following microcolumn extraction using both the HL and the SMT schemes. The extractograms give rise to valuable knowledge on: (i) the extraction kinetics, (ii) the content of phosphorus in available pools, (iii) the efficiency of the leachants and (iv) the actual extractant volumes for quantitative release of orthophosphate. The SMT extractograms show sharp leaching profiles while those of HL depict a gradual stripping of the nutrient species as a result of the milder leachants used. This is especially noticeable in the HCl extraction step in SRM 2704 where the amount of calcium bound phosphate leached in the first 2.0 ml in SMT is twofold higher to that of HL for the same extractant volume.

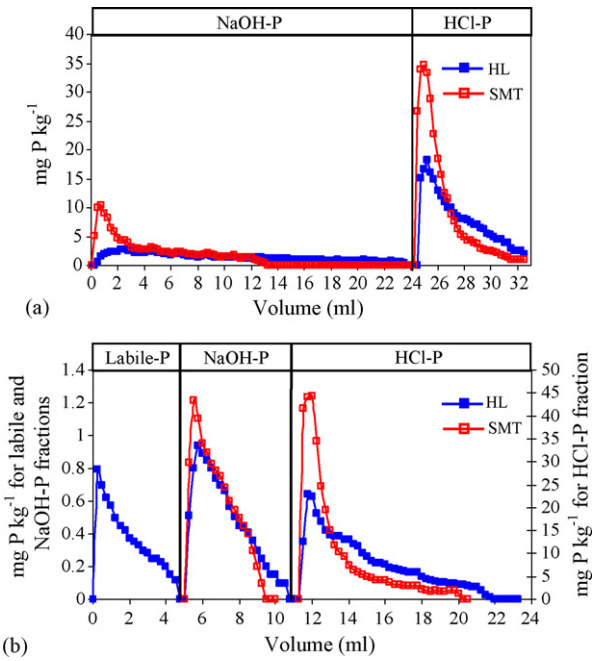

Fig. 2. Comparison of the on-line MSFI extraction profiles of orthophosphate in (a) SRM 2704 and (b) SRM 2711 as obtained by the application of HL and SMT protocols in a dynamic fashion. The labile phosphorus in 1.0 M NH_4Cl was <LOD for SRM 2704. The concentration of orthophosphate is given as mg P kg^{-1} sample.

The analytical results for SRM 2704 and SRM 2711 also evidence that different types of samples, in this case, agricultural soil and river sediment, behave differently under the same extraction conditions (see extraction patterns for the Al and Fe-bound phosphate in Fig. 2). This is attributed to the particular phosphorus soil phase associations existing in each kind of solid, thus, revealing the difficulty for setting a universal extraction protocol for dynamic fractionation of macronutrients.

3.2. Analytical performance of the MSFI analyzer

Under the optimized chemical and physical variables, the dynamic linear range of the multicommutated MB method was established over the range 0.05–7.0 mg P l^{-1} for the NH_4Cl and NaOH extraction media in the HL scheme, and 0.35–15 mg P l^{-1} for the 0.5 M HCl medium. For the NaOH and HCl steps in SMT, the regression lines extended from 0.1 to 7.0 and from 0.5 to 15 mg P l^{-1}, respectively. The limit of detection (LOD) assessed from three times the standard deviation of either the blank or a 50 μg P l^{-1} standard solution were 0.01, 0.01 and 0.02 mg P l^{-1} for NH_4Cl, NaOH and HCl steps in HL, respectively. In SMT, LODs of 0.02 and 0.01 mg P l^{-1} for 1.0 M NaOH and 1.0 M HCl were, respectively, obtained. Repeatability was estimated from 10 consecutive injections of a 1.0 mg P l^{-1} standard solution in each extracting medium. Relative standard deviations (R.S.D.)

Table 4
Comparison of the extraction/determination parameters for the HL scheme in SRM 2711 for three different procedures applied to phosphorus fractionation and extract analysis

Parameters	MSFIA (this work)		SI-MCE/FIA [42]		Batch [31]	
	Amount (mg)	Volume (μl)	Amount (mg)	Volume (μl)	Amount (mg)	Volume (μl)
1. Reagent consumption per extract analysis						
Ammonium molybdate	0.5	80	7.2	600	6.0	150
Reducing agent[a]	0.02	120	0.2	600	5.3	300
Masking agent[b]	0.1	80	2.4	1000	0.1	300
2. Extractant volume (ml)						
NH_4Cl fraction	4.5		25		2×50	
NaOH fraction	6		30		50	
HCl fraction	11		30		50	
3. Analysis time per extract (min)	0.77		0.74		20	
4. Operational time for overall fractionation and extract analysis per sample (h)	2.8		2.7		45.3	

[a] Tin(II) chloride was used as a reducing reagent for MSFIA and SI-MCE/FIA, while ascorbic acid was employed for batchwise analysis.
[b] Oxalic acid was employed as a masking agent for MSFIA, and tartaric acid for the SI-MCE/FIA and batch approaches.

of 1.0, 0.9 and 2.4% were obtained for the NH_4Cl, NaOH and HCl solutions in HL, respectively, and 1.0 and 2.2% for the NaOH and HCl media in SMT, respectively.

In Table 4, the analytical performance of the on-line MSFI analyzer for HL fractionation and orthophosphate determination is critically compared with that of the batchwise method [31] and an SI-microcolumn extraction (SI-MCE) system with further off-line analysis of the extracts by flow injection analysis [42]. A distinguishing feature of the MSFI-multicommutation set-up with respect to the FI and batch systems is the minimum consumption of reagents. Thus, in the proposed system, the consumption of MB chemicals is reduced more than 15-fold as regards to former methods. This is a consequence of the time-based injection of well-defined volumes of solutions at the precise instant for development of the reactions as effected via activation of the solenoid valves. Whenever not needed, the MB reagents are delivered to their respective reservoirs in lieu of being propelled downstream as occurs in continuous, forward-flow assemblies. Therefore, discontinuous-flow based MSFI analyzers might be viewed as environmental-friendly chemical processors.

The slightly higher operational time in MSFIA versus SI-MCE/FIA for fractionation/determination of orthophosphate has its origin in the different number of extracts analysed, that is, 86 extracts in the proposed on-line system as compared with merely 27 using the former FI set-up. Yet, the potential of the flow-through hyphenated MSFI system for handling of minute fractions of extract, that is $\leq$250 μl versus $\geq$5000 μl for methods involving fraction collection, ensures a unrivaled temporal resolution that yields a detailed insight into the leaching kinetics of phosphorus from the different soil/sediment compartments, as illustrated in Fig. 3. Hence, the content of inorganic phosphorus in readily mobilisable reservoirs can be more accurately estimated. At the same time, the sample mass to extractant volume ratio for each sequential extraction step can be calculated with improved accuracy, thereby avoiding the usage of any surplus of reagent for quantitative leaching of phosphorus in the various geological phases. According to Fig. 3 and data presented in Table 4, the leachant volumes used in the MSFI on-line fractionation system are three to four times lower to those required whenever off-line measurements are applied.

3.3. Accuracy of the proposed flow-through microcolumn extraction-multisyringe flow injection system for orthophosphate fractionation

The SRM 2704 river sediment and SRM 2711 Montana soil were utilized to evaluate the reliability and accuracy of the developed flow-through microcolumn hyphenated method. The amount of extractable orthophosphate in both standard reference materials resulting from the application of dynamic partitioning is listed in Tables 5 and 6 along with the certified total phosphorus content and the pseudo-total (aqua regia) phosphorus concentrations. The amount of extractable phosphorus for both solid substrates determined on-line by summation of all fractions plus residue is much lower than the certified values, while

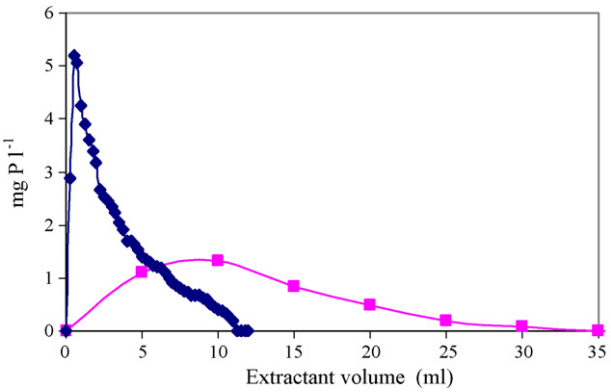

Fig. 3. Comparison of orthophosphate extractograms for the HCl step in the HL scheme for SRM 2711 as obtained by using off-line MB detection (5 ml per subfraction) and on-line MSFI spectrophotometric analysis (250 μl per subfraction).

Table 5
Comparison of extractable amounts of phosphorus in SRM 2711 (mg kg^{-1}) as obtained by using the Hieltjes–Lijklema and SMT sequential extraction schemes with on-line and off-line MB detection modes

Fractions	Hieltjes–Lijklema			SMT	
	On-line (MSFIA)	Off-line[a] (MWD)	Off-line[b] (SI-MCE) [42]	On-line (MSFIA)	Off-line[a] (MWD)
(1) Labile P	7 ± 1	36 ± 2	45 ± 5		
(2) Al and Fe-bound P	13.1 ± 0.4	84 ± 6	93 ± 10	11 ± 1	105 ± 2
(3) Ca-bound P	324 ± 45	370 ± 25	373 ± 18	365 ± 9	384 ± 9
(4) Residue	215 ± 14	215 ± 14	288 ± 43	202 ± 9	202 ± 9
Summation (1 + 2 + 3 + 4)	559 ± 47	705 ± 29	799 ± 48	578 ± 13	690 ± 13

Results are expressed as the mean of five fractionation assays ± S.D.; pseudo-total P: 700 ± 30 mg P kg^{-1}; certified value: 860 ± 70 mg P kg^{-1}; MWD: microwave digestion; SI-MCE: sequential injection-microcolumn extraction.
[a] The concentration of orthophosphate in the extracts is determined by batchwise MB standard addition.
[b] The concentration of orthophosphate in the extracts is determined by FIA-MB.

a good agreement, with maximum deviations of 8%, is obtained between the summation of fractions for SRM 2704 and SRM 2711 following acidic microwave digestion of the extracts collected downstream (after on-line detection) and the endorsed and pseudo-total concentrations, respectively.

According to the MB chemistry, only dissolved orthophosphate can react with MB reagents for generation of the reduced blue-coloured complex. Therefore, the on-line MSFI extraction system with spectrophotometric monitoring detects merely the extractable, reactive inorganic phosphorus. However, in the off-line assays, the extracts that may contain other phosphorus compounds, such as organic phosphorus and condensed inorganic phosphates (see below), can be degraded under microwave digestion into orthophosphate, thus providing information on the total phosphorus released. As a result, the total phosphorus content after appropriate processing of the MSFI extracts is not significantly different at the 0.05 significance level to the certified or pseudo-total phosphorus concentrations in both SRM materials, as shown in Tables 5 and 6.

3.4. Comparison of on-line and off-line modes for phosphorus determination in soil/sediment extracts

The phosphorus fractionation results using the on-line hyphenated MSFI assembly for SRM 2711 were contrasted with those previously obtained by sequential injection microcolumn extraction (SI-MCE) and fraction collection prior to off-line FI analysis [42]. As shown in Table 5, the extractable phosphorus monitored spectrophotometrically is severely affected by the mode of extract processing. It should be stressed that even though the HL and SMT schemes were originally designed for inorganic phosphorus fractionation, soil organic phosphorus can be concurrently released by the extracting reagents themselves. In fact, the most commonly accepted schemes for soil organic phosphorus fractionation [43,44] involve alkaline and acid extractions with 0.1–0.5 M NaOH and >0.1 M HCl, respectively, thus matching the chemical conditions for HL and SMT extractions. NaOH creates electrostatic repulsions by increasing the negative charge of both organic and mineral components [45] while HCl dissolves salts of some organic phosphate esters that are relatively insoluble in alkaline solution [43].

Furthermore, several organic phosphates are instable in alkaline and acid conditions, and therefore might be hydrolyzed under the fractionation conditions to free phosphate, thus leading to the overestimation of the content of readily accessible orthophosphate. The effects of alkaline and acid hydrolysis for a wide range of soil organic phosphorus compounds have been found to be markedly influenced by the nature of the phosphorus species [44,46,47]. The extraction of fast hydrolysable phosphorus forms (e.g., phosphatidyl choline) may hence explain the discrepancy in Table 5 between the on-line and off-line (SI-MCE) data for NaOH and HCl extracts in the HL scheme. Regarding the NH_4Cl extracts in HL, the contribution from organic phosphorus hydrolysis should here be negligible because organic substances cannot be leached under mild extraction media. Yet, common sources of readily hydrolysable phosphorusin soils, that might

Table 6
Comparison of extractable amounts of phosphorus in SRM 2704 (mg kg^{-1}) as obtained by using the Hieltjes–Lijklema and SMT sequential extraction schemes with on-line and off-line MB detection modes

Fractions	Hieltjes–Lijklema		SMT	
	On-line (MSFIA)	Off-line[a] (MWD)	On-line (MSFIA)	Off-line[a] (MWD)
(1) Labile P	<LOD	<LOD		
(2) Al and Fe-bound P	114 ± 14	103 ± 6	164 ± 18	177 ± 14
(3) Ca-bound P	310 ± 43	595 ± 17	288 ± 18	664 ± 21
(4) Residue	232 ± 26	232 ± 26	171 ± 5	171 ± 5
Summation (1 + 2 + 3 + 4)	656 ± 52	930 ± 32	623 ± 26	1012 ± 26

Results are expressed as the mean of five fractionation assays ± S.D.; certified value: 998 ± 28 mg P kg^{-1}; LOD: limit of detection.
[a] The concentration of orthophosphate in the extracts is determined by batchwise MB standard addition.

be released in the first extraction step of HL, are the condensed inorganic phosphates (e.g., pyrophosphate and polyphosphates) [44].

It should be noted that the hydrolysis of organic phosphorus and condensed inorganic phosphates in off-line based fractionation analysis might occur not only during the timeframe of the extraction but to a significant extent during the residence period prior to actual phosphorus determination. As opposed to batch partitioning and dynamic methods involving off-line or at-line analysis of phosphorus containing fractions, the novel multisyringe flow approach leads to a substantial shortening of the assay protocol, thus minimizing the potential decomposition of hydrolyzable phosphorus compounds. Each microvolume of extract leaving the microcolumn is readily treated on-line with MB reagents, while the released organic species in the batchwise method and SI-MCE system with off-line analysis remain in intimate contact with the extracting reagent for >15 and 3 h, respectively. Therefore, the flow-through MSFI fractionation analyzer with MB detection should be regarded as a unique tool for accurate monitoring of mobilisable orthophosphate in environmental solid substrates, even though organic phosphorus may be leached with the extracting reagents.

4. Conclusion

Multisyringe flow injection analysis has been presented as an appealing analytical tool for on-line processing of the extracts generated in flow-through dynamic fractionation assays. Prominent features of the assembled analytical set-up involving multicommutated post-column injection of reagents are the considerable saving of chemicals, the high temporal resolution of the leaching processes, the accurate evaluation of sample mass to leachant volume ratios, and the improved reliability, robustness and automation with respect to methods with off-line analysis of extracts.

The intrinsic versatility of the MSFI analyzer has been exploited for the accommodation in a single set-up of two well-accepted schemes for fractionation of inorganic phosphorus, i.e., the HL and SMT protocols, even though the chemical composition of the extracts resulting from both schemes is significantly different. As a consequence of the most aggressive extractants utilized in the SMT protocol, higher leachable contents and sharper extraction profiles were encountered as compared to the HL scheme. However, SMT does not give information on the labile inorganic phosphorus, which is regarded to be the readily available fraction for plant uptake. Furthermore, the extreme chemical conditions adopted in this scheme are unlikely to mimic the changes in the chemical properties of the solid occurring under environmental scenarios.

The flow-through microcolumn system hyphenated with spectrophotometric detection has been also proven unique for accurate monitoring of available orthophosphate in the extracts due to the minimization of the potential hydrolysis of extracted organic and condensed phosphorus into orthophosphate.

Further research is aimed at expanding the flexibility of the multisyringe flow injection analysis system for monitoring of ultratrace levels of pollutants, viz., heavy metals and metalloids, in solid substrates following dynamic fractionation and on-line solid-phase extraction for isolation and pre-concentration of the targeted species.

Acknowledgments

Janya Buanuam is grateful for financial support granted by the Royal Golden Jubilee Ph.D. Program of the Thailand Research Fund and to the Postgraduate Education and Research Program in Chemistry (PERCH) of the Higher Education Development Project of the Commission on Higher Education (Thailand). Manuel Miró is indebted to the Spanish Ministry of Education and Science for contract sponsorship through the *Ramón y Cajal* research program. The authors are grateful to the Spanish Ministry of Education and Science for financial support through projects CTQ2004-03256 and CTQ2004-01201. Special thanks are also due to Anders Sølby (DTU workshop) for construction of the extraction microcolumn.

References

[1] F.M.G. Tack, M.G. Verloo, Intern. J. Environ. Anal. Chem. 59 (1995) 225.
[2] G. Rauret, Talanta 46 (1998) 449.
[3] A.V. Filgueiras, I. Lavilla, C. Bendicho, J. Environ. Monit. 4 (2002) 823.
[4] C. Gleyzes, S. Tellier, M. Astruc, Trends Anal. Chem. 21 (2002) 451.
[5] J. Hlavay, T. Prohaska, M. Weisz, W.W. Wenzel, G.J. Stingeder, Pure Appl. Chem. 76 (2004) 415.
[6] M. Miró, E.H. Hansen, R. Chomchoei, W. Frenzel, Trends Anal. Chem. 24 (2005) 759.
[7] W. Tiyapongpattana, P. Pongsakul, J. Shiowatana, D. Nacapricha, Talanta 62 (2004) 765.
[8] J. Shiowatana, N. Tantidanai, S. Nookabkaew, D. Nacapricha, J. Environ. Qual. 30 (2001) 1195.
[9] D. Beauchemin, K. Kyser, D. Chipley, Anal. Chem. 74 (2002) 3924.
[10] P.S. Fedotov, A.G. Zavarzina, B.Ya. Spivakov, R. Wennrich, J. Mattusch, K. de P.C. Titze, V.V. Demin, J. Environ. Monit. 4 (2002) 318.
[11] H. Kurosaki, S.M. Loyland-Asbury, J.D. Navratil, S.B. Clark, Environ. Sci. Technol. 36 (2002) 4880.
[12] L.-M. Dong, X.-P. Yan, Talanta 65 (2005) 627.
[13] M. Jimoh, W. Frenzel, V. Müller, H. Stephanowitz, E. Hoffmann, Anal. Chem. 76 (2004) 1197.
[14] M. Jimoh, W. Frenzel, V. Müller, Anal. Bioanal. Chem. 381 (2005) 438.
[15] J. Shiowatana, N. Tantidanai, S. Nookabkaew, D. Nacapricha, Environ. Int. 26 (2001) 38.
[16] M. Schreiber, M. Otto, P.S. Fedotov, R. Wennrich, Chemosphere 61 (2005) 107.
[17] P.S. Fedotov, R. Wennrich, H.-J. Stärk, B.Ya. Spivakov, J. Environ. Monit. 7 (2005) 22.
[18] P.S. Fedotov, E.Yu. Savonina, R. Wennrich, B.Ya. Spivakov, Analyst 131 (2006) 509.
[19] R. Chomchoei, M. Miró, E.H. Hansen, J. Shiowatana, Anal. Chem. 77 (2005) 2720.
[20] C.E. Lenehan, N.W. Barnett, S.W. Lewis, Analyst 127 (2002) 997.
[21] M. Miró, E.H. Hansen, Anal. Bioanal. Chem. 382 (2005) 878.
[22] R. Chomchoei, E.H. Hansen, J. Shiowatana, Anal. Chim. Acta 526 (2004) 117.
[23] R. Chomchoei, M. Miró, E.H. Hansen, J. Shiowatana, Anal. Chim. Acta 536 (2005) 183.
[24] M. Miró, E.H. Hansen, Trends Anal. Chem. 25 (2006) 267.
[25] M.A. Segundo, L.M. Magalhaes, Anal. Sci. 22 (2006) 3.
[26] B. Horstkotte, O. Elsholz, V. Cerdà, J. Flow Injection Anal. 22 (2005) 99.
[27] M. Miró, V. Cerdà, J.M. Estela, Trends Anal. Chem. 21 (2002) 199.
[28] A. Barbanti, M.C. Bergamini, F. Frascari, S. Miserocchi, G. Rosso, J. Environ. Qual. 23 (1994) 1093.

[29] P. Pardo, J.F. López-Sánchez, G. Rauret, Anal. Bioanal. Chem. 376 (2003) 248.
[30] B.Ya. Spivakov, T.A. Maryutina, H. Muntau, Pure Appl. Chem. 71 (1999) 2161.
[31] A.H.M. Hieltjes, L. Lijklema, J. Environ. Qual. 3 (1980) 405.
[32] V. Ruban, J.F. López-Sánchez, P. Pardo, G. Rauret, H. Muntau, Ph. Quevauviller, J. Environ. Monit. 1 (1999) 51.
[33] US-EPA method 3051, Microwave Assisted Acid Digestion of Sediments, Sludges, Soils, and Oils, Code of Federal Regulations, 1991, Title 40, Part 136, Paragraph 33.
[34] B. Kalberg, G.E. Pacey, Flow Injection Analysis: A Practical Guide, Techniques and Instrumentation in Analytical Chemistry, vol. 10, Elsevier, 1989, p. 49.
[35] J. Ruzicka, E.H. Hansen, Flow Injection Analysis, 2nd ed., Wiley/Interscience, New York, 1988, pp. 105–106.
[36] T. Fujiwara, K. Kurahashi, T. Kumamaru, H. Sakai, Appl. Organometall. Chem. 10 (1996) 675.
[37] J.-Z. Zhang, C.J. Fisher, P.B. Ortner, Talanta 49 (1999) 293.
[38] S.-C. Pai, C.-C. Yang, J.P. Riley, Anal. Chim. Acta 229 (1990) 115.
[39] C.X. Galhardo, J.C. Masini, Anal. Chim. Acta 417 (2000) 191.
[40] W. Tiyapongpattana, Application of Continuous Flow Technique for Sequential Extraction and for Determination of Phosphorus in Soil and Sediment, Master thesis, Mahidol University, Bangkok, Thailand, 2002.
[41] N. Amornthammarong, P. Anujaravat, K. Sereenonchai, P. Chisuwan, P. Sastranurak, P. Wilairat, D. Nacapricha, Talanta 68 (2005) 480.
[42] J. Buanuam, M. Miró, E.H. Hansen, J. Shiowatana, Anal. Chim. Acta 570 (2006) 224.
[43] G. Anderson, in: A.D. McLaren, G.H. Peterson (Eds.), Soil Biochemistry, vol. 1, Marcel Dekker, New York, 1967, pp. 67–90.
[44] B.L. Turner, B.J. Cade-Menun, L.M. Condron, S. Newman, Talanta 66 (2005) 294.
[45] E.W. Russell, Soil Conditions and Plant Growth, 11th ed., Longman Scientific & Technical, Harlow, UK, 1988.
[46] M.I. Makarov, L. Haumaier, W. Zech, Soil Biol. Biochem. 34 (2002) 1467.
[47] B.L. Turner, N. Mahieu, L.M. Condron, Soil Sci. Soc. Am. J. 67 (2003) 497.

Anal Bioanal Chem (2006) 386: 363–369
DOI 10.1007/s00216-006-0633-9

ORIGINAL PAPER

Nattikarn Kaewkhomdee · Chatvalee Kalambaheti · Somrudee Predapitakkun · Atitaya Siripinyanond · Juwadee Shiowatana

Iron fractionation for corrosion products from natural gas pipelines by continuous-flow sequential extraction

Received: 29 April 2006 / Revised: 13 June 2006 / Accepted: 16 June 2006 / Published online: 28 July 2006

Abstract The forms and quantities of iron species in corrosion product samples from natural gas pipelines were examined, using a continuous-flow sequential extraction system. Sequential extraction consists of four steps that dissolve water soluble iron ($FeSO_4$), acid soluble iron ($FeCO_3$), reducible iron (Fe-(oxyhydr)oxides) and oxidisable iron (FeS_2) fractions, respectively. Selectivity of extracting reagents for particular iron species was evaluated by determination of co-extracted anions, using ion chromatography, and evolved CO_2, using indirect flame atomic absorption spectrometer (FAAS). Iron was found predominantly in the reducible fraction (61–99%), indicating that Fe-(oxyhydr)oxides are the major constituents of the corrosion products.

Keywords Corrosion product · Iron fractionation · Sequential extraction

Introduction

Steel pipelines are widely used in the petroleum and natural gas industries, and the deterioration due to corrosion is a well-known problem. The cost of corrosion and corrosion protection in the United States of America is estimated to be in excess of 276,000 million dollars per year [1]. In natural gas pipelines, iron corrosion is an extremely complex process, because a large number of parameters are involved. Firstly, gas contaminants are primary causes of corrosion. The most common gases are O_2, CO_2 and H_2S [2, 3]. O_2 is not normally present in natural gas but can pass through leaks. It can cause corrosion problems, even at very low concentrations. CO_2 and H_2S are weakly acidic gases and become corrosive when dissolved in water. The corrosion products from O_2, CO_2 and H_2S contaminants are Fe-(oxyhydr)oxides, $FeCO_3$ and Fe-sulphide, respectively. Fe-sulphide may be present as FeS or FeS_2, depending on the corroding condition [3]. Secondly, microbiologically influenced corrosion (MIC) can occur from sulphate-reducing bacteria (SRB) [4]. SRB consume sulphate ion (SO_4^{2-}) and produce CO_2 and H_2S, which, on the other hand, can also enter the corrosion processes from organic fermentation. Finally, water plays a very significant role in corrosion.

The corrosion mechanism can be indicated by the anion side of the corrosion products or the iron compounds. The analysis and identification of corrosion products can assist the engineer to solve a corrosion problem by giving information that may help in understanding (1) the nature and type of corrosive attack, (2) the metal or metal phase that has been attacked in an alloy, (3) the environmental conditions that contribute to the corrosion.

Corrosion products are generally investigated by surface characterisation techniques such as X-ray diffraction (XRD) [2, 5–11], X-ray photoelectron spectroscopy (XPS) [6, 11, 12], Mössbauer spectroscopy [6, 8], Raman spectroscopy [3, 10] and scanning electron microscopy (SEM) combined with energy dispersive spectrometry (EDS) [2, 7, 10]. These techniques have been used complementarily to allow complete characterisation of the corrosion products. One method alone often has limitations; for example, identification by XRD can be very difficult when the crystallinity is very low (this is often the case for corrosion products). Detection limits of XRD and SEM-EDS are poor, and results obtained from XRD are sometimes difficult to interpret. The disadvantages of XPS are the need of high vacuum, poor resolution and low sensitivity, while Raman spectroscopy has low selectivity.

The sequential extraction technique has been widely used to fractionate metals in a solid sample according to their leachability. A succession of chemical reagents was employed

N. Kaewkhomdee · A. Siripinyanond · J. Shiowatana (✉)
Department of Chemistry, Faculty of Science,
Mahidol University, Rama VI Road,
Bangkok, 10400, Thailand
e-mail: scysw@mahidol.ac.th
Tel.: +66-2201-5122
Fax: +66-2354-7151

C. Kalambaheti · S. Predapitakkun
Analytical and Petroleum Research Department,
PTT Research and Technology Institute,
PTT Public Company Limited,
Ayutthaya 13170, Thailand

to extract, sequentially, various targeted phases in the sample. The results are useful for obtaining information about origin, mode of occurrence, bioavailability, potential mobility and transport of elements in natural environments [13–16].

In our previous work [17, 18], a continuous-flow sequential extraction system was developed for simplicity, rapidity, less risk of contamination and improved accuracy of the traditional sequential extraction technique. The dynamic extraction system also provides kinetics data for detailed investigation [19].

The objective of this study was to apply the dynamic extraction system to determine the fractional distribution of iron in corrosion products. An important problem with sequential extraction techniques is the selection of suitable extractants (types, concentrations, pHs and temperatures) to obtain a good selectivity of sequential extraction of sulphate, carbonate, (oxyhydr)oxides and sulphide phases of corrosion products. Ideally, the extraction schemes are designed to dissolve specifically one mineralogical phase at a time. The lack of selectivity of extractants used in some extraction schemes for soils, which leads to errors in fractionation data, has been reported [15, 16, 20, 21].

For the selectivity of an extraction scheme for iron, Heron et al. [22] reported an extraction scheme to study the fractionation of iron in contaminated aquifer sediments. These results were used to quantify the iron species associated with the sediment samples. The scheme was applied to standard iron, and the selectivity was confirmed by SEM and XRD. Poulton and Canfield [23] developed an extraction scheme for fractionation of iron in modern and ancient sediments. The selectivity of the extraction scheme was tested on standard iron compounds and their mixtures. Each scheme used a variety of extractants, and the results were highly dependent on the extraction scheme used. Criteria for selection of an extraction scheme included (1) nature of sample such as pH and organic content and (2) ability for defining the desired phase of metals. In this work, the modified sequential extraction scheme of the Standard, Measurement and Testing Program (SM&T) (formerly BCR) [15] was used to selectively extract, water soluble iron ($FeSO_4$), acid soluble iron ($FeCO_3$), reducible iron (Fe-(oxyhydr)oxides) and oxidisable iron (Fe-sulphide) fractions using a dynamic continuous-flow extraction system coupled with appropriate detection techniques. The selectivity of extractants for iron fractionation in corrosion products was examined by simultaneous determinations of iron and co-extracted anions. Being leached at the same time as observed in the extractograms obtained indicates chemical association of the ions. The dynamic extraction system was finally applied to study the forms and quantities of iron species in corrosion products.

Experimental

Chemicals and apparatus

All chemicals were of analytical grade. Milli-Q water was used throughout. Standard iron solution (1,000 mg l^{-1}) was purchased from Merck (Darmstadt, Germany). The working standards were prepared when required. $FeSO_4 \cdot 7H_2O$, Fe_2O_3 and FeS_2, purchased from M&B (Dagenham, UK), Sigma (Missouri, USA) and Fisher (Loughborough, UK), respectively, were dried at 100 °C to constant weight and kept in a desiccator until required. Plastic containers and glassware were cleaned and soaked in 10% (v/v) HNO_3 for at least 24 h and rinsed three times with Milli-Q water.

A flame atomic absorption spectrometer (Perkin-Elmer Model 3100, Connecticut, USA) equipped with a deuterium background corrector was used for the determination of iron in the extracts. Absorbance measurements were made at 248.3 nm.

Corrosion product samples

Corrosion product samples were collected from natural gas pipelines. All samples were washed with methanol and petroleum benzene, dried and ground in an agate mortar to obtain homogeneity. The ground samples were stored in a desiccator until required.

Continuous-flow extraction system

Extraction chamber

The continuous-flow extraction system employed in this work has been previously described (Fig. 1a) [17, 18]. The extraction chamber was designed to allow containment and stirring of a weighed sample. Extractants could flow sequentially through the chamber and dissolve the targeted phases. The chamber and its cover were constructed from borosilicate glass to have a capacity of approximately 10 ml. The outlet of the chamber was furnished with a Whatman (Maidstone, UK) glass microfibre filter (GF/B, 47 mm diameter, 1 μm particle retention) to allow dissolved matter to flow through. Extractant was pumped through the chamber by a peristaltic pump [Micro tube pump, MP-3N, EYELA (Tokyo Rikakikai Co. Ltd)] at approximately 4 ml min^{-1} using Tygon tubing of 2.25 mm inner diameter. Heating of the extractant, when required, was carried out by passing the extractant through a glass heating coil approximately 120 cm in length, which was placed in a water bath before the extraction chamber.

Extraction procedure

A weighed sample (0.25 g) was transferred to a clean extraction chamber, together with a magnetic bar. A glass microfibre filter was then placed on the outlet, followed by a silicone rubber gasket, and the chamber cover was securely clamped in position. The chamber was connected to the extractant reservoir and the collector vial by Tygon tubing and placed on a magnetic stirrer. The magnetic stirrer and peristaltic pump were switched on to start the extraction. The extracting reagents were continuously

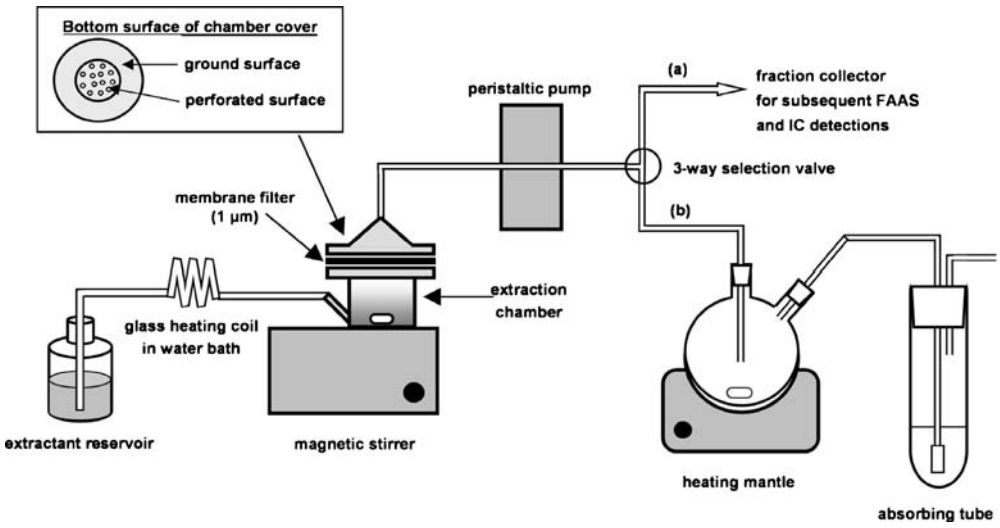

Fig. 1 Diagram of a continuous-flow sequential extraction system connected to (**a**) the fraction collector used in phases I, III and IV; (**b**) a unit used in phase II for collecting extract in the round-bottomed flask and CO_2 in the absorbing tube

moved through the chamber to effect a dynamic extraction process. The extract passed through the membrane filter, and collection of subfractions (60 ml volume intervals) was repeated until all four leaching steps had been completed.

Extraction scheme

The modified sequential extraction scheme of the Standard, Measurement and Testing Program (SM&T) (formerly BCR) [15] for iron was carried out on the following solutions:

Step I
: water, 70 °C (water soluble fraction)
Step II
: 0.11 mol l^{-1} CH_3COOH (acid soluble fraction)
Step III
: 0.1 mol l^{-1} $C_6H_8O_6$/ 0.2 mol l^{-1} $(NH_4)_2C_2O_4{\cdot}H_2O$ adjusted to pH 3.3 with HNO_3, 100 °C (reducible fraction)
Step IV
: 8: 3 v/v (30% H_2O_2: 0.02 mol l^{-1} HNO_3), 85 °C (oxidisable fraction)

Total dissolution of residue corrosion product samples and iron compounds

Residues from the extraction after steps I–IV or corrosion product samples (0.25 g) were digested with aqua regia (1:3 v/v mixture of concentrated HNO_3 and HCl) until the solutions were clear. After being cooled, the digested solutions were made up to volume in volumetric flasks. Iron compounds, i.e. $FeSO_4{\cdot}7H_2O$, Fe_2O_3 and FeS_2, were dissolved in pure hot water, concentrated HCl, and aqua regia, respectively. The dissolved solutions were diluted with pure water to the desired dilution factors.

Iron in extracts and digests were determined by flame atomic absorption spectrometer (FAAS) using external calibration.

Selectivity of extractants

For the selectivity study of extractants for the water soluble and oxidisable phases, the ion chromatographic equipment, consisting of a Waters Model 510 HPLC pump, an Alltech guard column and an Allsep Anion column (4.6 mm inner diameter), was used for sulphate separation. Detection was performed by a Waters Model 430 conductivity detector to monitor sulphate concentrations. Data were recorded with a Shimadzu Model C-R6A integrating recorder. An eluent of 4 mmol l^{-1} potassium hydrogen phthalate (KHP) was degassed ultrasonically before being used. For all samples, a 100 μl sample loop was used. The detection signal was recorded as peak height.

For the selectivity study of extractant for the acid soluble phase, the outlet tube of the extraction chamber was connected to a 250 ml two-necked round-bottomed flask, which was placed on a heating mantle. The other neck of the round-bottomed flask was connected to a Pyrex absorption tube, 25±200 mm, containing an absorbing solution (Fig. 1b). We evaluated the trapping efficiency of the absorbing solution by using successive absorbing tubes and found that only one absorbing tube was adequate to trap all the CO_2(g) evolved.

For this study the corrosion product sample was first treated with water to dissolve water soluble iron; the extracts were collected in fraction collectors. Then CH_3COOH at various concentrations (0.05 mol l^{-1}, 0.11 mol l^{-1}, 0.25 mol l^{-1}, 0.35 mol l^{-1} and 0.50 mol l^{-1}) was allowed to flow to leach the acid soluble iron. For this step the extract was collected in a two-necked round-bottomed flask, which was gently heated to purge the CO_2 quantitatively into an absorbing solution containing 2.5 mmol l^{-1} calcium hydroxide. The absorbing solution was centrifuged, and the amount of calcium in the supernatant was determined.

The amount of precipitated calcium carbonate ($CaCO_3$) was then calculated, and carbonate was determined. The concentrations of iron in the extracts and calcium were determined by FAAS.

In the reducible fraction the selectivity of extractant was not determined. Depending on the environmental conditions and oxidation pathways, different Fe-(oxyhydr)oxides can form [24], and, therefore, determination of the co-extracted anions is difficult. Therefore, the iron species of this phase is not specified in this paper. For the extractant used, ascorbic acid/oxalate solution was selected because of its reducing property and its high iron complexing capacity. This extractant has been widely used to dissolve metals in the reducible phase in many sequential extraction schemes [15].

Results and discussion

Typical extractogram of sequential extraction

With a continuous-flow extraction system, not only iron concentrations can be obtained, but also kinetics information of dissolution of various iron species from the sample can be observed in an extractogram (a graph of the metal concentration in a subfraction versus the corresponding subfraction number). A typical extractogram showing four iron species in corrosion product samples is given in Fig. 2. It also illustrates that the extractants are efficient in leaching the iron completely in each phase, because the iron concentration in the extract decreases to the baseline level before changing over to the next extractant. The extracted iron of each phase was determined by summation of the amounts in subfractions of the particular step. Overlaid extractograms of various species give additional information on their chemical association, as will be presented later in this manuscript.

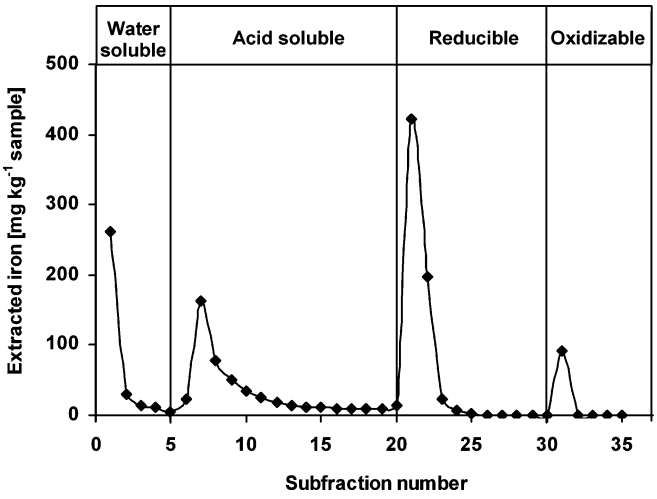

Fig. 2 Extractogram of iron for corrosion product sample as obtained by a continuous-flow sequential extraction system. Signals of water soluble, acid soluble and oxidisable phases were magnified ten times for clarity

Recovery of extraction of iron species

The efficiency of the four extractants employed in the modified SM&T extraction scheme for iron fractionation was primarily studied on pure iron compounds ($FeSO_4 \cdot 7H_2O$, Fe_2O_3 and FeS_2). The iron compounds and their mixture were subjected to total dissolution and sequential extraction followed by FAAS detection. Table 1 shows a very good selectivity of each extraction step, with less than 1% being extracted in other steps. Therefore, this extraction scheme showed satisfactory results for the possibility of studying iron species in real samples of corrosion products. Due to the complex nature of real samples, they may not behave similarly to the mixture of pure iron compounds. Therefore, the selectivity of the extractants for real samples was also investigated.

Selectivity of extractants

A number of sequential extraction schemes have been used for the elemental fractionation of soils and sediments. The accuracy of these schemes depends on many factors, especially the selectivity of the extractants used. In this work we performed a study of time-resolved extraction profiles of elements of concern to evaluate their co-elution, which, in turn, indicates chemical association. Ion chromatography was used to determine the sulphate concentration in the extracts of the water soluble and oxidisable steps. For the acid soluble extraction step, co-extracted carbonate was monitored. Carbonate ion generated in this step is not stable in the acidic medium. Therefore, the evolved CO_2 was trapped in a gas absorbing unit containing an absorbing solution with subsequent indirect FAAS measurement. Concentrations of iron, together with those of co-extracted anions, were plotted to confirm the association of iron with particular anions. Co-extraction and stoichiometric relationships of extracted iron and co-extracted anions were used to demonstrate the selectivity of extractant of each step.

Water soluble and oxidisable phases

In water soluble phase, iron sulphate ($FeSO_4$) was the main iron species in the samples. The selectivity of water for $FeSO_4$ was obvious from the solubility data of various forms of iron compounds likely to be present in the corrosion products, because $FeCO_3$, Fe-(oxyhydr)oxides and Fe-sulphide are not soluble in water. Nevertheless, this was confirmed by chromatographic determination of co-extracted sulphate in extracts. For the oxidisable extraction step, Fe-sulphides were oxidised by HNO_3/H_2O_2 to obtain ferric and sulphate ions (Eq. 1). Therefore, sulphate was also determined in this leaching step.

$$FeS_2(s)+7/2O_2+H_2O(aq) \rightarrow Fe^{3+}(aq)+2SO_4^{2-}(aq)+2H^+ \quad (1)$$

Table 1 Extraction recovery of iron from iron compounds in a four-step continuous-flow sequential extraction system (n=3) (*ND* not detectable)

Iron compound	Total iron [mg Fe]	Extracted iron [mg Fe]					Percentage of Fe recovered
		Water soluble phase	Acid soluble phase	Reducible phase	Oxidisable phase	Sum	
$FeSO_4 \cdot 7H_2O$	251±6	247±4	ND	ND	ND	247±4	98
Fe_2O_3	999±15	ND	ND	998±33	ND	998±33	100
FeS_2	258±8	ND	ND	2.0±0.1	245±8	247±8	96
$FeSO_4 \cdot 7H_2O^+$ Fe_2O_3+FeS_2	1,503±17	244±5	ND	991±20	245±7	1,480±28	98

At the selected experimental ion chromatographic conditions, carbonate, chloride, nitrate, oxalate, sulphate and thiosulphate can also be detected. Carbonate was eluted at void peak, while chloride, nitrate, oxalate, sulphate and thiosulphate can be detected at 5 min, 6 min, 7 min, 9 min and 12 min, respectively. The sulphate peak showed a well-defined resolved peak with no interfering anion peak. The calibration graph was rectilinear for 5-100 mg l^{-1} of sulphate, with a good linear regression (R^2=0.9998).

As can be seen in Fig. 3, no sulphate was detected in the extracts of acid soluble and reducible phases, and good correlation between the molar ratio of iron and sulphate in the water soluble (1:1) and oxidisable (1:2) steps confirmed the selectivity of water and 30% H_2O_2 in 0.02 mol l^{-1} HNO_3 for $FeSO_4$ and Fe-sulphide, respectively. In addition, the molar ratio of iron and sulphate in oxidisable phase from the extractograms was close to 2 indicating that FeS_2 was predominant in this phase. The extractograms demonstrated the usefulness of continuous-flow sequential extraction for chemical association studies. This type of study is not possible with a batch extraction, which gives only a single concentration of element for each step and does not provide a time-dependent extraction profile.

Acid soluble phase

CH_3COOH at various concentrations has been used to release metals associated with the carbonate fraction in soils [15, 16]. The efficiency of acid concentration in the extraction of this phase depends on several parameters, such as the nature and grain size of the sample and carbonate content. The effects on extractability of increasing the CH_3COOH concentration from 0.05 mol l^{-1} to 0.50 mol l^{-1} were investigated for corrosion products. Figure 4 shows that the amounts of extractable iron in the acid soluble phase depend on the concentration of CH_3COOH used. An increase in acid concentration causes a considerable increase in extractability. Low acid concentration was insufficient for the complete solubility of this carbonate phase, while higher concentration showed an improved efficiency of leaching but may cause partial dissolution of Fe-(oxyhydr)oxides, resulting in increased amounts of extractable iron. This could be a major source of overestimation of iron in the acid soluble step. Determination of co-extracted carbonate ion in the extracts by ion chromatography was not possible because the carbonate ion is not stable in the acidic medium. For this reason, the continuous-flow sequential extraction module was connected to a gas absorbing unit to monitor co-extracted carbonate ion for the study of selectivity of

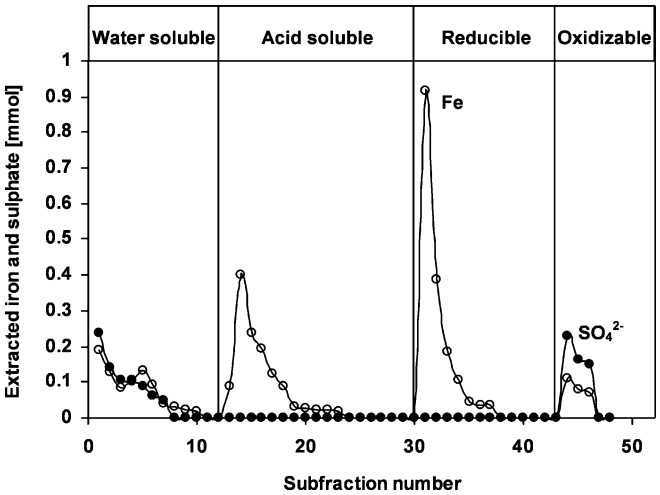

Fig. 3 Extractograms of iron (*open circles*) and sulphate (*closed circles*) for a corrosion product sample

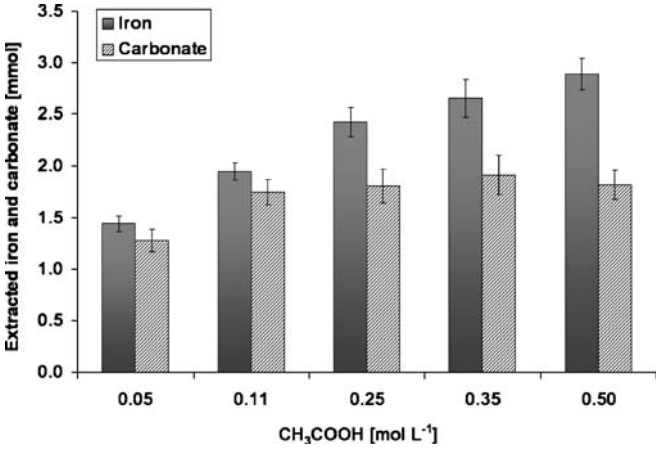

Fig. 4 Effect of the CH_3COOH concentrations on the extracted iron and carbonate (n=3)